

Forming the structure and properties of hybrid coatings on reversible rotating extrusion dies

K. Lukaszkwicz*

Institute of Engineering Materials and Biomaterials, Silesian University of Technology, ul. Konarskiego 18a, 44-100 Gliwice, Poland

* Corresponding e-mail address: krzysztof.lukaszkwicz@polsl.pl

Received 23.10.2012; published in revised form 01.12.2012

Manufacturing and processing

ABSTRACT

Purpose: The purpose of this monograph was to develop the methodology of formation, classification of properties and analysis of the structure of the surface layers, particularly the zone connecting the core and the coating and between the single layers created on the working surfaces of dies for the plastic formation on non-ferrous metals, with particular consideration to the specific nature of the extrusion process with reversibly rotating die (the KOBO method).

Design/methodology/approach: Nanocrystalline structure layers production technology was developed, which included nanocomposite and low-friction layers with desired usable properties ensuring increased durability, abrasive and adhesion wear strength. The production process of dual-layer coatings, such as hard nitride layer - low friction DLC layer, was carried out in the continuous mode, on a device furnished with technologies of lateral, rotating cathodes and central rotating cathode, within one technological process. The developed coatings were tested under the working conditions for the elements coated with them (tools – dies), in order to establish the anticipated responses and properties during their use.

Findings: The numerous interdisciplinary tests and analyses carried out in the scope of material science, production technology and computer techniques as well as the results obtained provided foundation for the formation of structure and tribological properties of the dies by controlled process conditions. The required final quality and durability of the tools for plastic metal formation in the extrusion process was obtained, which has been proven under operating conditions.

Practical implications: Economically efficient process improvement, increased production efficiency and quality and products reliability through increased durability and unfailling operation time of tools for plastic formation of non-ferrous metals and improved usable properties shall guarantee measurable economic effects to the manufacturers and users of the products. Moreover, it will enhance their competitiveness both on the domestic and overseas markets.

Originality/value: The Author's original approach was the development of a dual-layer coating within one process. Such coatings consists of the internal hard PVD layer providing the appropriate hardness, strength, low thermal conductivity and restricting the impact of external factors on the wear process of the dies used for non-ferrous metals extrusion and the external low-friction layer providing good tribological properties, which, in combination with the appropriate formation of the transition zone between the base material and coating, and between the single layers in the coating, providing adhesion sufficiently high, enabled increased operating durability of the dies, and this has been proved in this paper.

Keywords: PVD and CVD surface layers; Extrusion with reversibly rotating die; Computational materials science; Microstructure; Mechanical properties; Functional properties

Reference to this paper should be given in the following way:

K. Lukaszkwicz, Forming the structure and properties of hybrid coatings on reversible rotating extrusion dies, Journal of Achievements in Materials and Manufacturing Engineering 55/2 (2012) 159-224.

1. Introduction

One of the primary challenges lying ahead of the modern knowledge- and innovation-based economy is the necessity to reduce material and energy consumption, as a prerequisite for sustainable development and the reasonable management of natural resources. The objectives are feasible, in most of the cases, by employing innovative materials treatment methods or by replacing the traditionally used materials with the new-generation materials featuring improved functional and strength properties. By combining skilfully numerous technological operations, including the surface layer modification technology, the intended outcome can be achieved, i.e. a material having properties necessary for the optimum performance of the tool or construction being designed. The functional properties of many products depend not only on the possibility of transmitting mechanical loads through the entire active section of an element made of the material applied or on its physiochemical properties, but very often on the structure and properties of surface layers [1-3].

Rapid advancements in many state-of-art industries, including plastic working, have depended mostly on the capabilities of surface engineering [4-6]. Extrusion is a very popular process in plastic working, especially for non-ferrous metals and their alloys, as it enables to produce tubes, bars, wires and shaped sections with complicated shapes, while maintaining a high accuracy of dimensions [7-9]. The key user of such products is the aviation and automotive sector, medical sector, window and furniture production industry, as well as transportation, electronic industry and power sector. The elements obtained in plastic formation processes, including by way of extrusion, should be characterised, in particular, by the expected mechanical properties, high accuracy of dimensions, a clean and smooth surface, as well as an acceptable price. The working surfaces of extrusion dies working in difficult operating conditions are exposed to severe mechanical and thermal loads, intensive wear or to the exposure of a corrosive environment [10-12].

Knowledge concerning improvements in the service life of tools becomes especially vital when higher extrusion efficiency is taken into consideration at the same time. A relatively short life of dies used is a negative characteristic of the process which should be considered against its advantages. The durability of dies is substantially affecting the level of product manufacturing costs and product quality. It is estimated that instrumentation costs represent more than ten per cent (even up to 40%) of a unit production cost. Hence the endeavours to improve the durability of extrusion equipment used, notably by applying surface engineering technology, are a continuous trend.

Progress in the manufacture and improvement of service life of tools used in modern industries is mainly achieved because the techniques of depositing thin coatings made of hard ceramic materials resistant to wear are becoming more and more widespread. A wide selection of the currently available types of coatings and deposition technologies derives from a growing demand, in the recent years, for the state-of-art material surface modification and protection methods.

From among a myriad of techniques enhancing the strength of materials, CVD (Chemical Vapour Deposition) and PVD (Physical Vapour Deposition) methods are playing an important role in industrial practise.

Many new coating materials have emerged due to dynamic development seen in surface structure and properties formation for parts of machines and tools, including monolayer, multilayer, multicomponent, graded, nanocrystalline and nanocomposite and adaptation coatings [13-17]. An innovative approach in surface treatment is represented by the application of hybrid technologies offering a broad spectrum of types of the associated processes permitting to fabricate a whole array of materials with their unique properties, for precisely defined applications, unachievable with the standard surface treatment methods [18-20].

Surface engineering has for a dozen or so years been an object of interest of the scientific circles from which the Author originates. The research pursued at the Institute of Engineering Materials and Biomaterials is concerned with possible modifications of engineering materials' surface by the deposition of coatings with the CVD and PVD technique [21-25], and also by using hybrid technologies [26-28], laser technologies [29-32] and formation of surface layers with the powder metallurgy methods [33,34]. Issues relating to tool materials have also been a vital area of the Team's scientific focus for several dozen years [35-38]. The subject of the investigations undertaken under the work is, therefore, a natural direction of development of the research areas pursued by the Institute.

The paper reviews the methods of extrusion and destruction of dies caused by a group of factors influencing their degradation, most of all temperature, friction, abrasive wear and adhesion wear. The main focus was put on a possibility of surface modification of tools for the plastic working of non-ferrous metals as a result of depositing hard nanocrystalline coatings fabricated with the Physical Vapour Deposition (PVD) method with an additional thin low-friction layer obtained with the Chemical Vapour Deposition (CVD) method significantly improving resistance to abrasive and adhesion wear of tools for plastic working of metals.

2. State-of-the-art review

2.1. Overview of the extrusion process and working conditions and of typical dies' wear mechanism

Plastic working is one of those industries undergoing most intensive growth. The dynamic development of theory and manufacturing technologies has been seen in this field. It is now commonly thought that the most economical method of plastic working is extrusion whereupon a cylinder-shaped charge placed in a container is flowing out through a die opening under the influence of pressure exerted by a tool, usually a displacement pump connected to a press punch (Fig. 1). The shape of the product flowing out from the die is formed by the die opening [39-41].

Extrusion has certain characteristics that distinguish this method from other plastic working methods, including [39]:

- products with an advantageous structure and good properties can be produced;
- empty products or full products with complicated shapes can be manufactured in a single operation;

- very high degrees of deformation in a single operation can be accomplished (cross section can be changed by over 90%);
- a beneficial state of strains in form of triaxial uneven pressing exists allowing for the formation of materials with small plasticity.

Originally, extrusion, due to very high pressures, was used mainly for the formation of products made of materials characterised by a low yield point. As the extrusion technology had evolved by preheating a charge material and tools, and by using special lubricants, it became possible to extrude steel and other metals with a high melting point, both by cold and hot extrusion. At present, extrusion is the basic method of manufacturing tubes, bars and shaped sections and machine parts made of steel and non-ferrous metals and their alloys.

Two basic methods of extrusion are known depending on the direction of metal flow: direct and indirect extrusion. So-called side extrusion is also in use where metal is flowing perpendicular to the motion of punch direction. An analysis of metal flow, in particular in a deformation zone, is an important issue during extrusion, as it conditions the structure, properties and quality of finished products. Special attention should be drawn to knowledge regarding the possibility of controlling the flow of metal, as it is necessary to reduce material deformation inhomogeneity. The decisive factors influencing a flow method of the extruded metal is a degree of friction on the contact point of an ingot with a container, degree of deformation, extrusion speed and the geometry and kinetics of tools (die) [39].

It is essential in material engineering to produce materials with a nanocrystalline structure ensuring favourable mechanical and functional properties of products. Numerous methods have been developed for metals leading to a strong refinement of grains as a consequence of intensive plastic deformation. The methods are jointly referred to as Severe Plastic Deformation (SPD) as a large number of defects is produced in a material as a result of plastic deformation and such defects, during spatial reorganisation and relative conversion, enable to refine a grain to the nanometric range. Of the numerous Severe Plastic Deformation methods, the ones used most often include [3,42,43]:

- Equal Channel Angular Extrusion (ECAE);
- Cyclic-Extrusion Compression (CEC);
- High-Pressure Torsion (HPT);
- Accumulative Roll-Bonding (ARB);

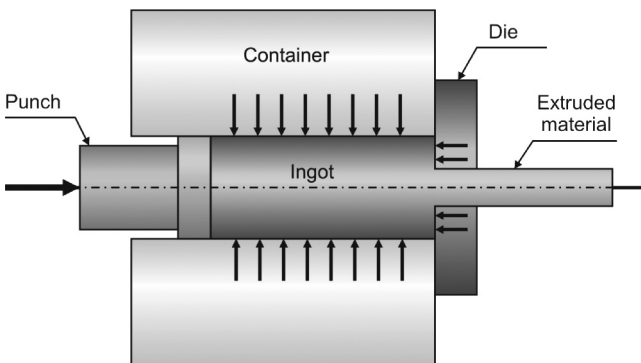


Fig. 1. Extrusion process diagram and principles [40]

- Repetitive Corrugation and Straightening (RCS);
- Hydrostatic Extrusion (HE);
- KOBO method.

The severe plastic deformation methods, except for ARB, HE and KOBO extrusion, have not been applied industrially, yet, due to inconveniences related to limitation of dimensions of the so manufactured products. Constructional and material solutions are continued to be sought for tools forming according to high pressures applied and the related need to evacuate large amounts of heat produced in deformation. By applying the ARB, HE methods, and especially the KOBO method having, apart from the values of an experimental test, the features of an industrial process, enable to produce materials with a nanocrystalline structure, however, further studies are needed and optimisation of process conditions [3, 7].

One of the most innovative methods of plastic working is the KOBO technology the idea of which is based on a cyclic change of a metal deformation path by introducing an additional, reverse, cyclically changing influence of working tools on metal (Fig. 2) and enables both, forging [44, 45], rolling [46, 47], drawing [7, 48], and extrusion [49, 50].

References [7, 49-56] indicate that most of experimental data on the progress of deformation with the KOBO method and on strength properties of the products obtained is relating to extrusion.

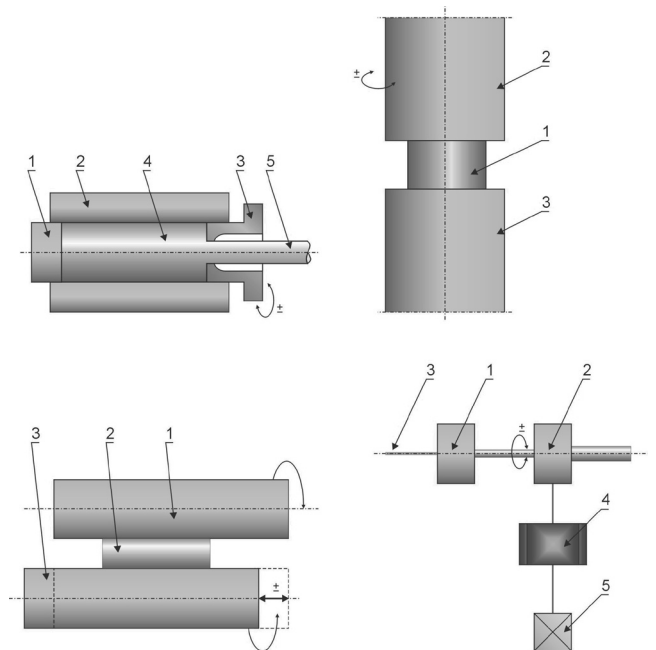


Fig 2. Schematic examples of technical solutions of metal materials deformation processes with the KOBO method [56]: a) extrusion (1 - punch, 2 - container, 3 - die rotating on both sides, 4 - metallic charge, 5 - product); b) forging (1 - metallic charge, 2 - punch rotating on both sides, 3 - die/anvil); c) rolling (1 - metallic charge, 2 - upper roll, 3 - lower roll transferred cyclically, axially); d) drawing (1 - fixed drawing die, 2 - drawing die rotating on both sides, 3 - metallic charge, 4 - transmission gears, 5 - motor)

It can be concluded on the basis of such data that a behaviour of metals subjected to KOBO method extrusion is conditioned only to a small extent by a temperature, while the dominant factor is the kinetics of the process carried out ensured with a high frequency of the strain path as a result of cyclic metal torsion, with high deformation speed and a small degree of processing ratio. This is associated with an activation of a low-energy deformation mechanism based on viscoplastic flow conditioned by very intensive creation and migration of spot defects. A plastic deformation of metal in the KOBO method is presented as a viscous fluid flow process, although it invariably remains in a solid state.

A substantial reduction in deformation work can be achieved by plastic working with the KOBO method, along with a reduction in process temperature and elimination of interannealing with the conventional extrusion methods. The KOBO methods provides an opportunity to fabricate functional products efficiently and with low energy intensiveness and in an environmentally-friendly manner, enables to perform cold plastic working, i.e. without preheating a material of hard-deformable alloys and to process their internal structure in a stable manner and to manufacture products with a complex geometry. Its advantages are especially important for structure refinement to nanometric dimensions and to generate extraordinarily advantageous mechanical properties [7,57].

The experience gathered so far in laboratory investigations as well as in industrial conditions (in a Rolling Mill in the Czech Republic, Będzin Steel Mill, Metal Processing Department of IMN, Gliwice) shows that although a substantial reduction can be attained in the process temperature, extrusion force and the resulting reduction of deformation work, nevertheless, an improved life of tools, especially of working surfaces of dies, as a result of KOBO-method extrusion is still an open issue, considering additional parameters of a die's motion - angle of rotation on both sides and frequency of such changes and a tendency of the extruded material to stick to the tool.

The quality of extruded products is defined by a set of the following characteristics: surface smoothness, dimensional tolerance, grain size, mechanical properties - with most of them being conditioned mainly by the correct progress of the process, suitable selection and shape of the die and its usable properties that change over the operating time [39].

Extrusion is characterised by a necessity to use very high pressure presses and, therefore, tools have to be used, most of all dies, with complicated shapes and a very high manufacture cost, operating in extremely disadvantageous conditions of mechanical and thermal loads.

From a tool user's prospective, a tool's resistance to damages is most important apart from durability. Tribological wear of working surfaces of dies in case of extrusion depends on multiple factors, such as temperature, extrusion speed, die shape and geometry, calibrating part length, surface condition, cyclic temperature changes due to contact with hot metal, as well as properties of the pressed metal and steel the die is made of. Tribological wear occurring in extrusion, particularly at a higher temperature, is very complex and usually encompasses the processes of friction, abrasive wear, abrasive-adhesion wear, adhesion wear, thermal wear and deformation. They do not occur individually in the majority of cases, and - by creating hybrid mechanisms - affect the tool surface aggregately [58,59].

During extrusion, the occurring movement of the plasticised metal with relatively small hardness on the working surface of the die with its much higher hardness causes a friction effect in the contact zone of the deformed material with the tool surface, which largely influences the extrusion force as well as this how the extruded metal is flowing. Usually, friction occurring during extrusion is of a semi-fluid or semi-dry character, because lubricants are used. Dry friction occurs if no lubricants are used the energy of which used for plastic deformation work and to overcome adhesion and cohesion force is nearly totally converted to heat causing temperature to rise. Only its small portion can be stored in the tool's surface layer as a result of deformation. The friction occurring between a die's working surface and the extruded material largely influences its durability, progress of plastic deformation, deformation inhomogeneity, which in turn is decisive for a final product's functional properties. Very important are the friction forces existing in a die calibration eye where biggest interferences occur in the flow of the extruded material caused by a suddenly changing section and the resulting growing speed of metal flow. Excessive friction resistance in a die eye causing inhomogeneous material flow is an undesired phenomenon [60-62].

The effects of friction forces are disadvantageous, hence the main issue in the extrusion process is to reduce the existing friction resistance by using suitable lubricants and lubrication methods [63]. Friction can be lowered by selecting low-adhesion materials, e.g. ceramics or by producing DLC, MoS₂, WS₂ type coatings on the tool surface. The coatings, having a very low friction coefficient, are referred to as self-lubricating or low-friction coatings [6,64].

As some metals and their alloys, especially aluminium, copper, titanium and platinum are strongly susceptible to adhering to steel surfaces of dies, a service life of dies is considerably shortened stemming from adhesion or abrasive-adhesion wear. As a result of high pressures, local joints and adhesions between contacting surfaces lead to the displacement of the material particles within the material volume, and not directly on the surface during their relative movement. A material loss in a die's working section is possible as a result of detaching the joints. Materials' susceptibility to tacking increases at a higher temperature, and surface seizing is observed in exceptionally severe working conditions caused by a sudden increase in the resistance of sliding friction, which may result from the system's lost thermal and mechanical balance [58,61,65,66].

In contact with a metal being extruded which is heated to a high temperature, the die surfaces, apart from intensive wear, are also subjected to corrosive activity of the treated material and to cyclic temperature changes as it is necessary to replace an ingot in a recipient [67].

The majority of metals have an unlimited ability to plastic deformations during extrusion, as a result of three-axial compression with high values of stresses. Any limitations in the use of extrusion are imposed due to tool strength and durability [68]. Dies are the parts most susceptible to wear and having at the same time biggest influence on dimensional accuracy and a product surface quality. Materials ensuring appropriate durability in working temperature, resistance to corrosive activity of the extruded metal, abrasion at increased temperature and to thermal fatigue should be used for the manufacture of dies working in

difficult conditions. The main groups of materials meeting such requirements are high-alloy hot-work tool steels [69,70].

The chemical composition and structure of modern hot-work tool steels is a result of experimental studies pursued for decades. While efforts were made to improve dies' life, the content of alloy elements in steels was being modified [71] or the impact of factors causing physical tool destruction was being limited by using appropriate die lubricants effectively lowering the friction, as well as isolating dies from direct contact between the extruded material and tool material [72].

A turning point for improving the operating properties of dies was the introduction of their surface modification methods, in particular through thermochemical treatment [73,74], low-temperature physical vapour deposition (PVD) of surface layers [75-77], or using hybrid technologies being a combination of the aforementioned methods [78-80]. Its limitations should, however, be pointed out when underlining an incontestable value of this approach, linked to the fact that nitrided layers produced on dies do not ensure suitably long service life and results repeatability. It also becomes a general issue that adhesion of the extruded material to the die cannot be prevented [81-84].

2.2. Importance of nanocrystalline antiwear coatings

The research topics referring to the fabrication of antiwear coatings represent one of the most essential directions of surface engineering development, guaranteeing the production of coatings with high functional properties for mechanical properties and resistance to tribological wear.

New operational features for the commonly used tools are very often obtained by deposition of simple monolayer, single-component coatings with PVD methods due to the low range of the process temperature. Their mechanical and operational properties are not satisfactory in many cases, however.

The will to develop increasingly harder coating materials emerged due to a relationship known between hardness and resistance to abrasive wear. Progress in the production of surface layers with the PVD and CVD method allows to produce multilayer coatings [85-87], functional graded coatings [88, 89] and adaptation coatings [90] exhibiting high mechanical and functional properties and capable of maintaining a low friction coefficient in multiple working environments, while maintaining high hardness and enhanced resistance.

When choosing a coating material, one encounters a barrier resulting from the fact that many properties expected from an "ideal" coating, i.e. high hardness and wear resistance combined with high strength and good ductility cannot be achieved at the same time. The requirements concerning the properties of different areas of a layer often collide, which additionally makes it difficult to choose layer materials [91-94].

The application of nanocrystalline coatings, especially nanocomposite coatings with as desired application properties as possible, is often regarded as a solution for this problem [4,95-101]. Similar to conventional polycrystalline materials, according to the Hall-Petch relationship, as the grain size decreases so increases coating hardness. This effect is especially important for decreasing grains to a critical value of about 10 nm (Fig. 3) [102].

Coatings with the same structure exhibit very high hardness (40-80 GPa) [103-105], stability in high temperature [17,106], corrosive resistance [107,108], as well as high abrasive and erosive wear resistance [109,110]. For a structure with a grain size smaller than the critical value, a material's hardness decreases as a new deformation mechanism emerges, i.e. the reverse Hall-Petch relationship (Fig. 3).

The main idea of obtaining the high hardness of coatings with a nanocomposite structure is to limit possibilities to produce and move dislocations within the grain and emergence of a new deformation mechanism linked to the movement of grain boundaries. Such coatings' structure consists of highly durable crystalline phases and a size of ~10 nm, deposited in a soft amorphous matrix ensuring high ductility, where they are spaced every 1-3 nm (Fig. 4).

According to a model proposed by Veprek [111-113], the high hardness of nanocomposite coatings stems from the fact that dislocation movement is eliminated on small grains and spaces between them, causing deformation. When the size of grains is reduced to nanometres, a dislocation activity as a source of material ductility is eliminated. This type of coatings is characterised by a large quantity of grain boundaries with a crystalline/amorphous phase separation surface limiting the formation and development of cracks. This mechanism explains brittle cracking resistance of coatings [114]. On the other hand, their good ductility derives from diffusion possibilities and slip along grain boundaries [115-116].

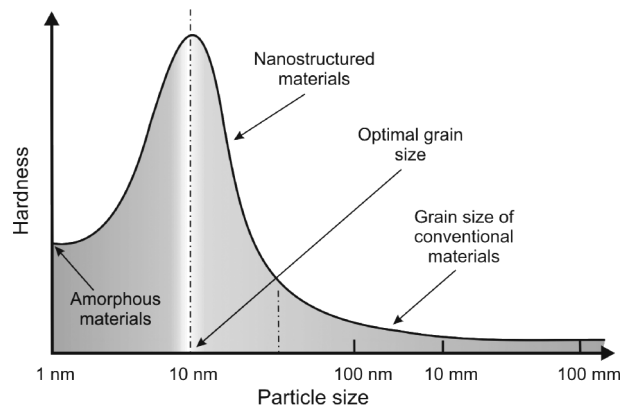


Fig. 3. Diagram of materials hardness in the function of grain size [102]

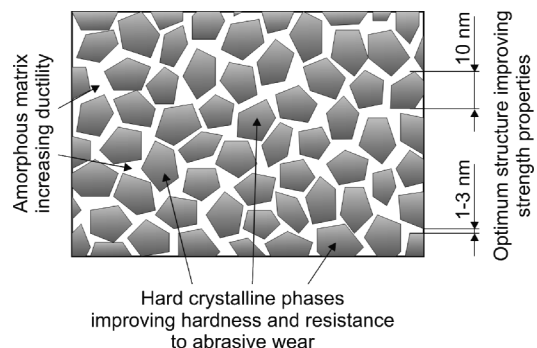


Fig. 4. Schematic diagram of nanocomposite coating

The literature presents three concepts of producing hard, durable, ductile nanocomposite coatings resistant to dynamic loads and with good substrate adhesion by:

- applying a graded transient layer between a substrate material and a crystalline/amorphous proper layer improving adhesion and limiting stresses (a combination of graded functional and nanocomposite coatings) [117];
- producing a structure consisting of hard, crystalline phases with the size of 3-10 nm in an amorphous matrix limiting a dislocation activity, stopping or changing the direction of dissipation of cracks and maintaining high hardness [118];
- producing a structure with a large quantity of grain boundaries ensures ductility by slide along grain boundaries and by nanocracks along the phase separation boundary crystalline grain/amorphous matrix [119].

Frequently, to enhance the hardness of nanocrystalline coatings, they are annealed at the right temperature, usually in a nitride atmosphere. Crystallisation occurs as a result of this heat treatment procedure and mechanical properties are improved [120].

There are many systems of nanocrystalline grains of (nc-) transition metal nitrides (TiN, TiAlN, CrN, BN, VN, ZrN, W₂N, etc.), carbides (TiC, VC, WC, etc.), borides (TiB₂, TiB, CrB₂, etc.), oxides (Al₂O₃, TiO₂, B₂O₃, SiO₂, etc.) or sulphides (TiSi₂, CrSi₂, ZrSi₂, etc.) arranged in an amorphous matrix (a-) (Si₃N₄, BN, C), such as: nc-TiN/a-Si₃N₄, nc-TiN/a-Si₃N₄/a-nc-TiSi₂, nc-CrN/a-Si₃N₄, nc-W₂N/a-Si₃N₄, nc-TiAlN/a-Si₃N₄, nc-TiN/a-BN, nc-TiC/a-C, nc-WC/a-C [102,121,122].

Low-friction diamond-like layers of the DLC type (Diamond-Like Carbon) or molybdenum disulfide MoS₂ [123-125] play a very important role in a reduction of friction resistance, especially in technical dry friction conditions.

DLC layers exhibit particularly advantageous tribological properties. In general, coatings produced with various methods carry such a term in the literature, as well as those with differentiated chemical and phase composition representing a mixture of amorphous and fine-crystalline carbon with sp¹ hybridisation (linear), sp² (trigonal) typical for graphite and sp³ (tetragonal) typical for diamond [126]. Carbon atoms with sp¹ hybridisation occur only in small amounts, whereas a ratio of sp³/sp² phase fraction is determining the properties and is one of the criteria of carbon coatings' classification. A low friction coefficient and good electrical conductivity is ensured for coatings by sp² phase, whereas sp³ phase fraction is decisive for high hardness, resistance to tribological wear and chemical volume [58].

The most general division concerns layers, in formation of which take part a-C:H hydrogen atoms (amorphous hydrogenated carbon), ta-C:H (tetrahedral hydrogenated carbon) and layers free of ta-C hydrogen (tetrahedral carbon), a-C (amorphous carbon). The properties of DLC layers are conditioned by the fraction of individual phases characterised by various types of bonds between atoms with different hybridisation and a hydrogen concentration (Fig. 5). The modification of diamond-like carbon layers with atoms of non-metallic or metallic a-C:H:X, ta-C:X elements (where X - Si, N, O, Ti, W, Cr) influences an improvement in their mechanical properties, mainly hardness [127,128].

Advantageous tribological properties of frictional contacts with a fraction of diamond-like DLC layers, in particular for a-C

and a-C:H, are related mainly with the slide phenomena occurring in the transient phase, fulfilling the role of grease, produced in the friction contact zone as a consequence of DLC layer graphitisation and oxidation processes [129,130].

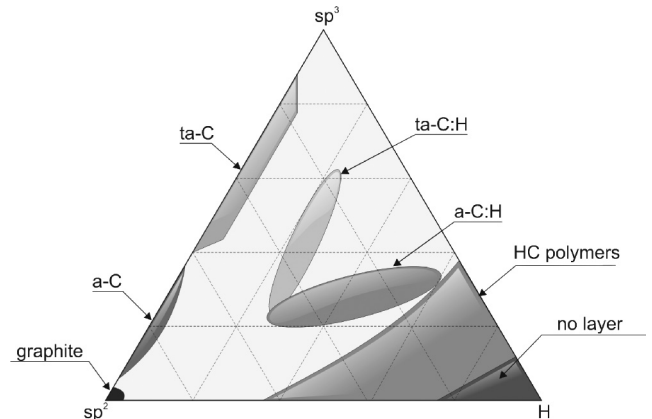


Fig. 5. Triple phase balance system classifying carbon layers depending on hydrogen concentration and fraction of [123] type bonds

Perfect and, owing to a variety of production techniques, differentiated properties of DLC layers have contributed to the intensive development of studies into their industrial applications.

As products working in heavy duty conditions are commonly used, it is necessary to intensify research efforts into selection of an appropriate material, production technology and deposition of wear resistant coatings onto them. A concept of fabricating products with optimum properties within the core zone and in the surface layer is possible by exploiting a potential offered by state-of-the-art production technologies, e.g. powder metallurgy and modern hybrid coatings deposition technologies, in particular PVD and CVD methods for nanocrystalline coatings and low-friction layers.

3. Genesis, thesis, purpose and scope of the paper

3.1. Genesis of the paper

Plastic working is a widely popularised technology for producing elements with complex shapes. Extrusion (Fig. 6) is one of five key plastic working processes used in the metal processing industry, with its share estimated at approx. 28%. It is now commonly asserted that extrusion is the most economical method of metal plastic working processes, and the anticipated outlooks for the sector are buoyant.

The fast wear of dies' working surfaces during extrusion is technologically and economically significant, as it deteriorates dimensional accuracy and the final product's surface quality. There are many enterprises operating in Poland using extrusion technologies for producing various types of profiles and shaped

sections of non-ferrous metals, and the number of new dies used in such processes per annum can be estimated at several thousand pieces. According to market figures, a production volume for extruded shaped sections is estimated at 100,000 T, which requires the use of about 4000 dies with an estimated cost of 40 mPLN. Savings of 5-8 mPLN can be realised by increasing the life of dies by 10%. It is also note-worthy that Europe's consumption of aluminium profiles only accounts for 1.2 million tonnes. The above analysis as well as high requirements for surface smoothness and a dimensional tolerance of products manufactured using the extrusion technology are determining a quest for innovative solutions in the field of surface engineering, improving life and service quality of forming dies.

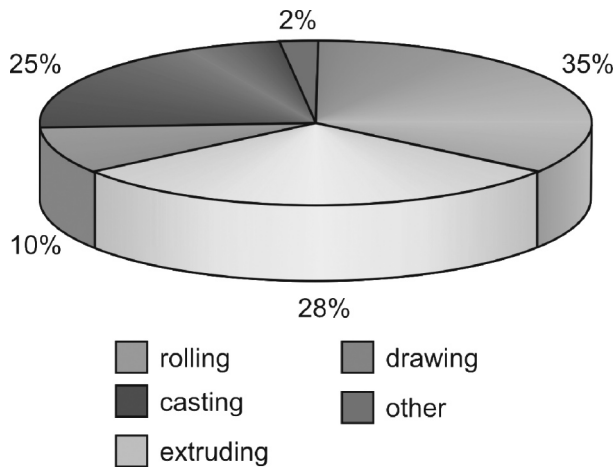


Fig. 6. Share of individual plastic working methods in the production of aluminium semi-products (acc. to Aluminium Technology Roadmap 2006)

The most effective method of extending the life of many products is to produce coatings on their surface, especially with a nanocrystalline structure with physical vapour deposition or chemical vapour deposition methods. Mechanical and operational properties of coatings can be influenced by selecting appropriately the chemical composition of a surface layer and by optimising its deposition process conditions [131-134]. An analysis of state of the problem in the field of surface engineering and the directions of its development (Fig. 7) indicate that development trends will be maintained in Poland and in the world [43,57,121,135,136].

The outcomes of the FORSURF project [58,137,138] undertaken by the Institute of Engineering Materials and Biomaterials under the framework of foresight research also reveal that nanostructural surface layers technologies, including also the selected PVD and CVD methods (Figs. 8-10) will represent the development directions of the most beneficial technological solutions for surface layers structure and properties formation of products and parts thereof in the nearest 20 years. It should also be highlighted that strategic development prospects for physical vapour deposition technologies (PVD), considered as very optimistic, are also true for cathode arc evaporation (CAD) methods, and plasma-assisted vapour deposition methods (PACVD/PECVD) (Figs. 11-13) have the best strategic positions in the group of chemical vapour deposition (CVD) methods.

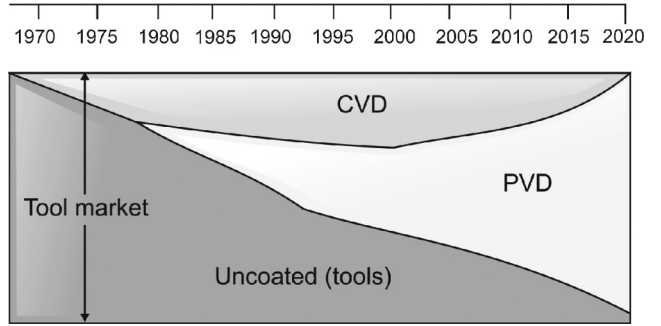


Fig. 7. Development of PVD and CVD technology with an example of materials used for tools (acc. to Oerlikon Balzers)

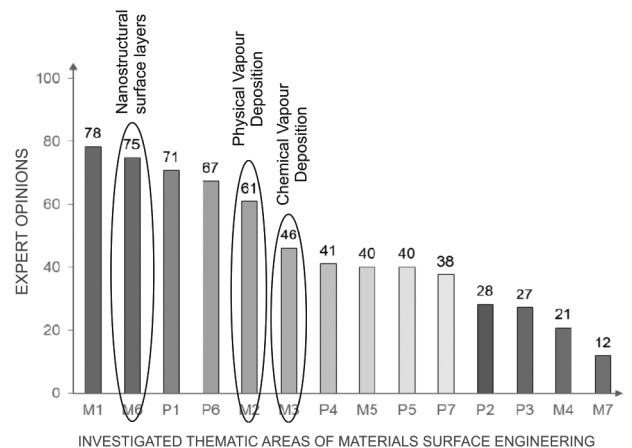


Fig. 8. Results of heuristic research concerning the possible practical applications of the analysed groups of technologies in industry in the nearest 20 years [138]

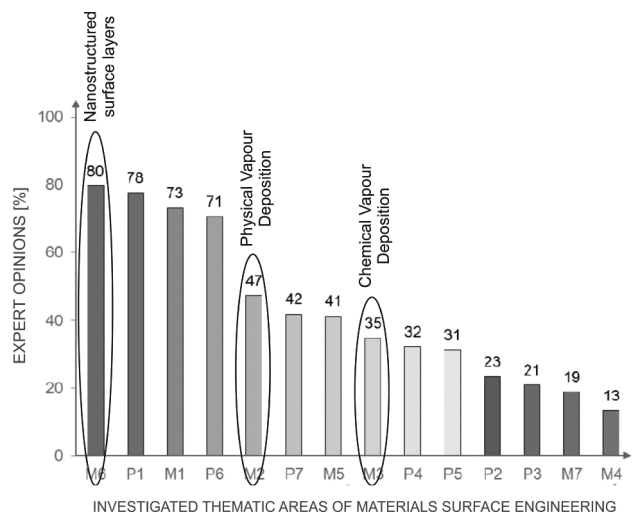


Fig. 9. Results of heuristic research evaluating which groups of the analysed technologies will be subject to greatest attention in scientific and research works in the nearest 20 years [138]

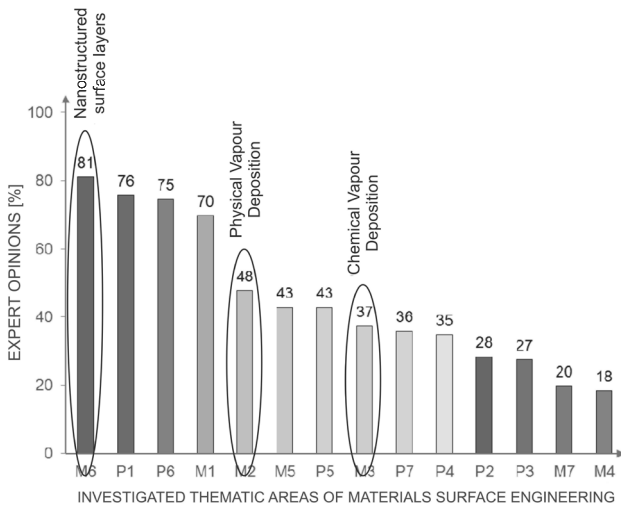


Fig. 10. Results of heuristic research evaluating which groups of the analysed technologies are essential and their importance in the nearest 20 years should be growing [138]

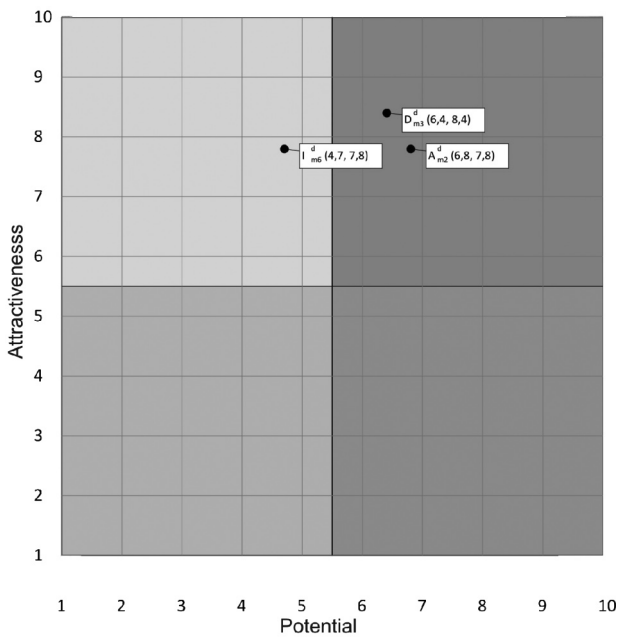


Fig. 11. Dendrological matrix of technology value: (A_{m2}^d) cathode arc evaporation (CAD), (D_{m3}^d) Plasma Assisted Chemical Vapour Deposition(PACVD/PECVD), (I_{m6}^d) nanocrystalline coatings deposition [138]

One of the crucial objectives set by the contemporary industry is to ensure the reliability and high quality of extruded products and to strive for a reduction of manufacturing costs. For this reason, a search for new solutions and gathering the new knowledge in the field of extended life of tools by producing

nanocrystalline layers on their surface with physical and/or chemical vapour deposition technologies is an important element of such efforts and deserves attention.

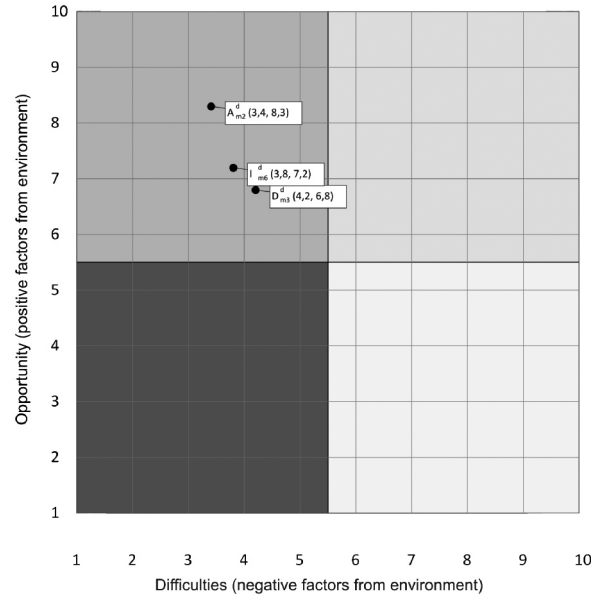


Fig. 12. Meteorological matrix of environment influence for the following technologies: (A_{m2}^d) cathode arc evaporation (CAD), (D_{m3}^d) Plasma Assisted Chemical Vapour Deposition (PACVD/PECVD), (I_{m6}^d) nanocrystalline coatings deposition [138]

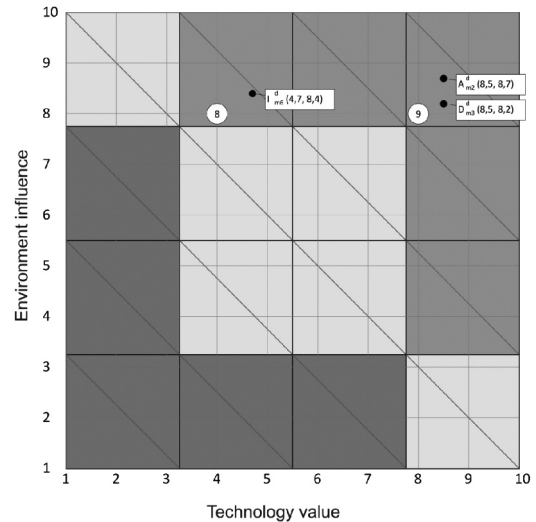


Fig. 13. Matrix of strategies for technologies: (A_{m2}^d) cathode arc evaporation (CAD), (D_{m3}^d) Plasma Assisted Chemical Vapour Deposition(PACVD/PECVD), (I_{m6}^d) nanocrystalline coatings deposition [138]

3.2. Thesis, purpose and scope of the paper

A study review of the literature points out that the existing methods of modifying the surface of dies used for extrusion, in particular by nitriding or hybrid treatment consisting of nitriding and deposition of TiN, Ti(C,N) or CrN coatings produced with physical vapour deposition methods in order to obtain a multi-layer structure of the "nitrided layer/PVD coating" type, despite improving process efficiency, have not solved all the issues related to a long-term improvement of quality of surface of the products manufactured and sometimes of dies' performance, or the issue of sticking the extruded material to the tool. This necessitates a search for alternative methods of dies' surface improvement eliminating the above performance-related shortcomings. The state-of-the-art review in the field of coatings fabricated with physical and chemical vapour deposition methods shows that the existing technological opportunities related to optimisation and appropriate selection of surface layers have not been fully materialised so far.

The literature study performed and the results of own research pursued up till now allow formulating the following thesis of the paper: the required functional characteristics of dies for plastic working of metals in the extrusion process are a result of correct structure formation, mechanical and tribological properties of hard nanocrystalline coatings with a thin low-friction layer (synergic interaction of constituent layers in the operational process) with taking into account the specificity of the extrusion process with cyclic die rotation.

Therefore the necessity to implement cognitive and applicational research programmes taking into consideration the concepts of surface engineering and plastic working of metals.

The underlying purpose of the research was to indicate that the thesis of the paper is formulated correctly. The achievement of the purpose was associated with developing a methodology of formation, properties classification and an analysis of surface layers' structure (synergically interacting surface layers), in particular of a bonding zone between a core and a coating, as well as between individual layers produced on the working surfaces of dies for the plastic working of non-ferrous metals, with particular regard to the specificity extruding with a reversely rotating die.

Appropriate research tasks had to be implemented in order to verify the thesis adopted. This is shown in the established management algorithm encompassing the scope of necessary technological operations and research ensuring the required functional features of extrusion dies (Fig. 14). To find an answer to the research question emerging from the thesis, a shape of a die used in the extrusion method with a reversely rotating die (KOBO) was used in the first place for a numerical simulation of an extrusion process due to extremely hard working conditions.

The following had to be done to solve the problem under the work followed:

- to establish, with computer methods, models of spatial distributions of internal stresses and displacements of the investigated layers in relation to operational conditions;
- to develop a manufacturing technology of layers with a nanocrystalline structure, including a nanocomposite structure and low-friction layers with desired functional properties ensuring improved durability, resistance to abrasive and adhesion wear;

- to examine the developed coatings in working conditions of elements coated with them (tools - dies) to identify the anticipated behaviours and properties in operation;
- to carry out the tests of mechanical properties and the structure of the layers produced and a character of bonding between the coating and surface of the coated substrate material, as well as between individual layers produced on dies' working surfaces.

4. Research material and methodology

4.1. Research material

A material for the research consisted of specimens dimensioned $\phi 30 \times 5$ mm and extrusion dies used in the KOBO

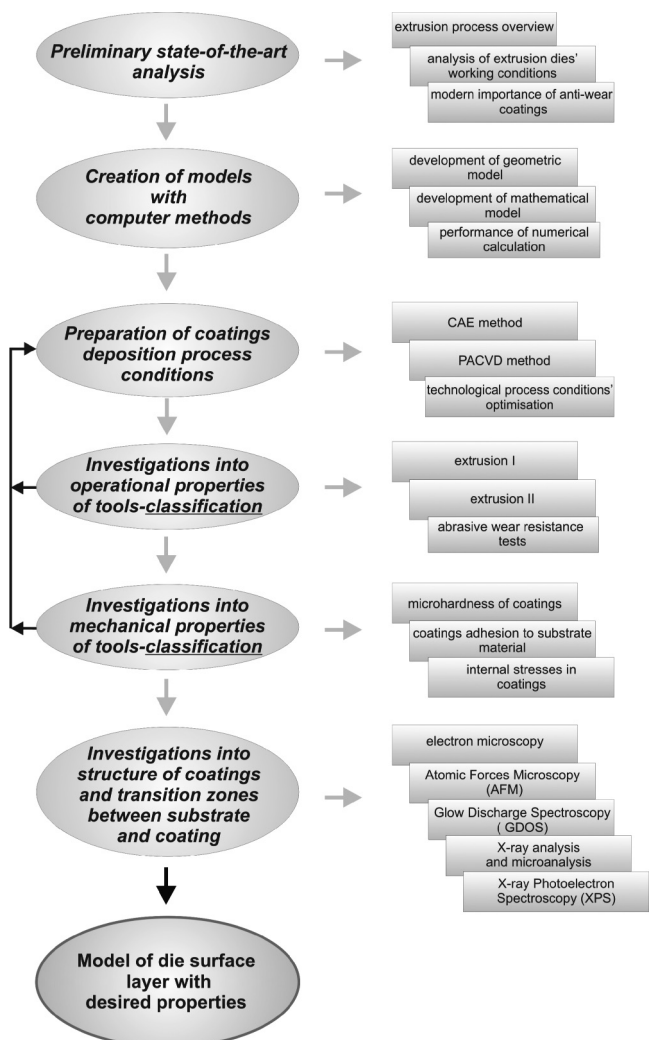


Fig 14. Scope of the work and research

method made of hot-work X40CrMoV5-1 tool steel with chemical composition given in Table 1 coated with hard nanocrystalline and low-friction layers produced with the PVD and CVD technique.

Steel after melting in an electric vacuum furnace at a pressure of 1 Pa was poured into ingots and subjected to preliminary forging into rods with the diameter of 75 mm and 3 m long which were next soft annealed to ensure good workability and uniform distribution of carbides in the die. Specimens were made by machining and the specimens next underwent standard heat treatment including quenching and double tempering. Austenitisation was carried out in a vacuum furnace at 1020°C for 30 minute with two 30-minute isothermal intervals made while heating at 640 and 840°C. The specimens were tempered twice after quenching, each time for 2 hours, at 560 and 510°C. The specimens after heat treatment were sand blasted and worked mechanically with a magnetic grinder, with special heed paid to prevent from creating cracks.

Prior to the coatings production process, the specimens were ground and polished to obtain the roughness of $Ra \leq 0.03 \mu\text{m}$, and then washed in organic solvents and alkali detergent solutions, including the use of ultrasound aid. The so prepared specimens were placed into a work chamber of a coating deposition device.

The production process of hybrid two-layer coatings of the hard nitride layer - low-friction layer DLC type was performed continuously with a $\pi 300$ device by PLATIT[®] fitted with LARC[®] (Lateral Rotating Cathodes) cathodes and a CERC[®] (Central Rotating Cathode) cathode (Fig. 15) in a single technological process.

Table 1. Chemical composition of hot-work X40CrMoV5-1 tool steel

Mass concentration of elements								
C	Mn	Si	P	S	Cr	W	Mo	V
0.398	0.36	1.03	0.016	0.003	5.05	0.01	1.32	0.94

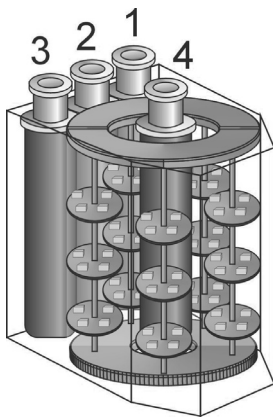


Fig. 15. Cathode configuration in a $\pi 300$ device by PLATIT[®] for coating deposition with the arc method with LARC[®] and CERC[®] technology: 1-Ti, 2-AiSi, 3-Cr, 4-Al

In the first stage, hard nanocrystalline nitride TiAlSiN, CrAlSiN, AlTiCrN, CrN layers were produced with a PVD technique with the arc method. To obtain the high adhesion of coatings, the substrate surface was ion-etched and a chromium-based metallic transition layer was applied. In the second stage,

low-friction DLC layers were produced after decreasing the temperature with the PACVD method. To obtain the high adhesion of a low-friction layer, a chromium- and/or titanium based metallic transition layer was applied with the arc method, and next a DLC a-C:H:Si and a-C:H layer with the PACVD method.

An MoS₂ layer was produced in a reactive magnetron sputtering process with a PL200 device by PLATIT[®].

Variable process conditions were applied:

- substrate polarisation potential;
- current intensity in cathode;
- gas flow rate;
- pressure in the device chamber.

In order to achieve appropriate properties, the technological conditions of coating deposition were agreed based on microhardness and tribological resistance tests (for low-friction layers).

Fig. 16. shows a configuration of layers in coatings produced on extrusion dies

The assumed shape of dies for testing coatings' properties in operational conditions - extrusion with the KOBO method - is shown in Figs. 17 and 18.

Selected coatings	AlTiCrN + DLC	TiAlSiN + DLC	CrN + DLC	CrAlSiN + DLC	CrAlSiN + MoS ₂
DLCor MoS ₂ low-friction layer	a-C:H:Si / a-C:H	a-C:H:Si / a-C:H	a-C:H:Si / a-C:H	a-C:H:Si / a-C:H	MoS ₂
2nd adhesive layer	Cr/CrN				Mo
Hard nitride layer	AlTiCrN	TiAlSiN	CrN	CrAlSiN	
1nd adhesive layer	Cr/CrN				
Surface cleaning	Ion etching				
	Surface pre-cleaning				
Substrate material	X40CrMoV5-1				

Fig. 16. Configuration of layers in coatings produced on extrusion dies

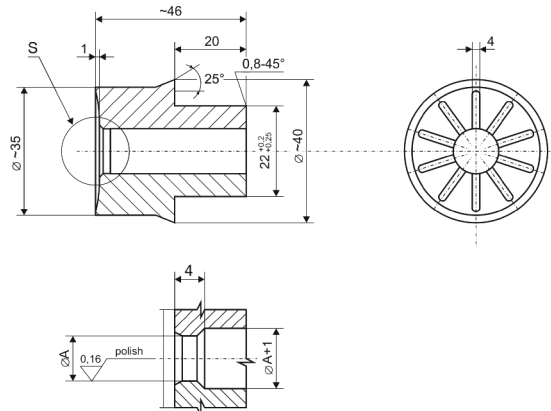


Fig. 17. Dimensions of a die for extrusion in the KOBO process

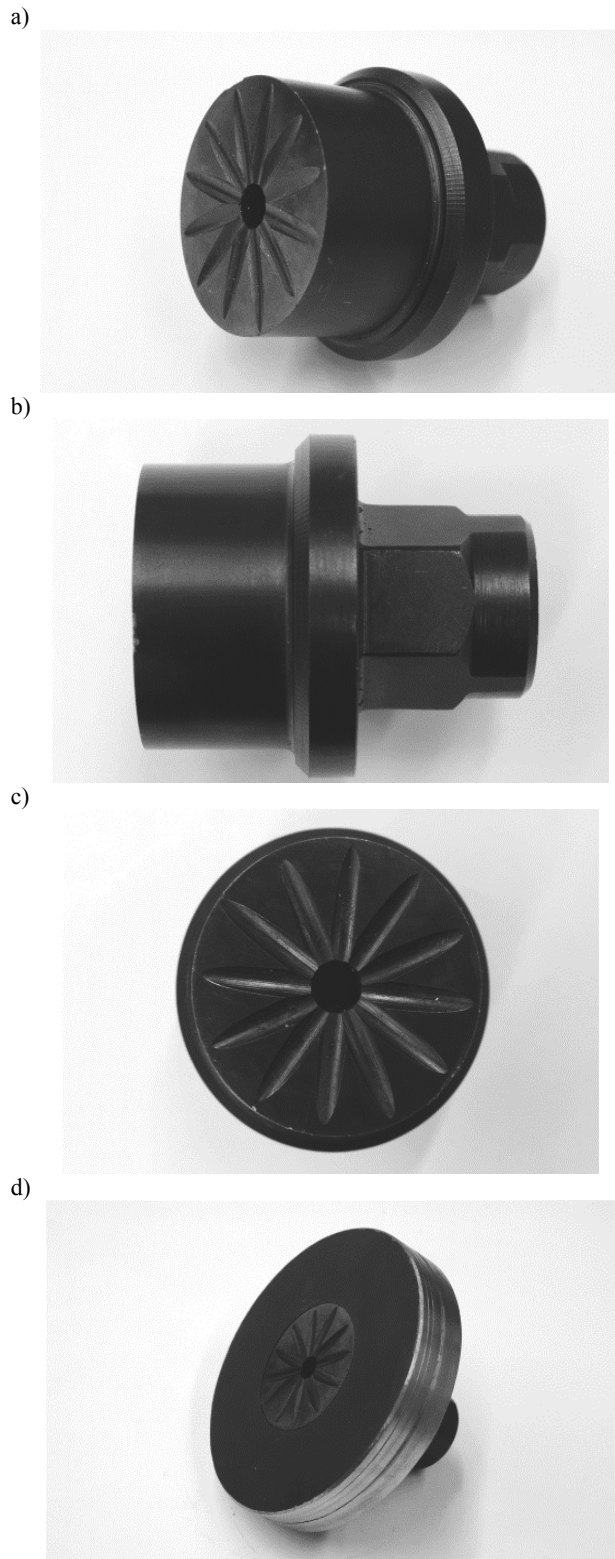


Fig 18. KOBO method extrusion dies: a) general view; b) side view, c) front view, d) view after placing in disc

4.2. Research methods and modelling of properties

The purpose of a numerical analysis was to determine a distribution of stresses and strains occurring in a die and of the layers produced on its surface during extrusion with a reversely rotating die. The following was prepared under the tests:

- a geometric model of a configuration of the elements taking part in extrusion;
- a discrete die configuration model - protection layers - extruded material;
- a numerical model of a die, protection layers and material deformed using the finite element method;
- numerical nonlinear calculations.

A die model used for extruding with the KOBO method was analysed (Fig. 17). A geometric model of an extruding unit (Fig. 19a) and a forming die (Fig. 19b) for calculations with the finite element method was prepared based on a CAD model by using the real dimensions of the elements.

The analysis was performed with ANSYS 12.1 software. 1/12 of the tool was modelled due to symmetry of geometry and a load. A model used for an MES analysis (Fig. 20) consisted of the following geometric elements: extruded material, low-friction layer, nitride layer, forming die. Such model geometry adopted resulted from the method of discretisation, type of finite elements and a need to reduce its number.

A mesh of elements was generated for the geometric models prepared for calculations with the finite element method. Due to the fact that the layers applied onto the working surface of dies have small thickness as compared to the tool dimensions, surface elements were used in model by using so-called the "shell over solid" method. Finite elements were used in the form of parametric SOLID elements with three degrees of freedom in a knot. The geometric model was subjected to discretisation with a SOLID 185 element for a substrate material (Fig. 21a). SHELL 181 elements for the coating (Fig. 21b) were used as a shell layer. The degree of freedom in a strength analysis are dislocations in solids and dislocations and rotations in surface elements.

The discrete models established are shown in Fig. 22. Contact with friction was defined between the solids. Axial pressure and angular motion were used as an excitation.

A die calculation model with coatings applied and the extruded material consists of 3829 nodes and 16214 elements.

Variable sizes of finite elements were used to avoid errors in stress calculations. Wherever larger stress gradients were expected, the mesh is more denser than in other areas where stresses should assume similar values. Smaller elements were hence used in layers that are better representing larger stress gradients, and elements in the material substrate increase as the coating is becoming more distant. The boundary conditions used for the analysis and a model load method resulted from the simplification made. As a repeating part of the die was used in the 1/12 model, the activity of the force of 70 kN was assumed. The material data used for the studies are listed in Tables. 2 and 3.

Non-linear properties of the extruded material presented as a stress-strain curve in Fig. 23 were used due to a non-linear character of the process. Frictional contact of 0.1 was assumed at the contact surface of the extruded material (hard workable EN AW-7075 [AlZn5,5MgCu] aluminium alloy) and a low-friction layer.

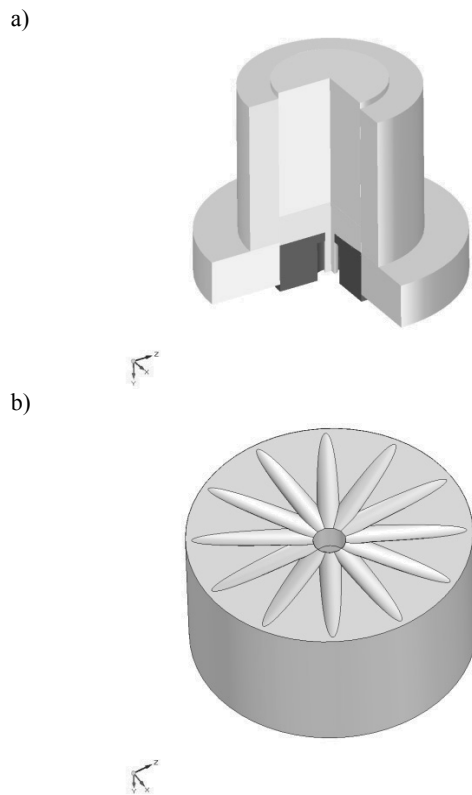


Fig. 19. CAD model: a) of elements taking part in extrusion, b) of a die

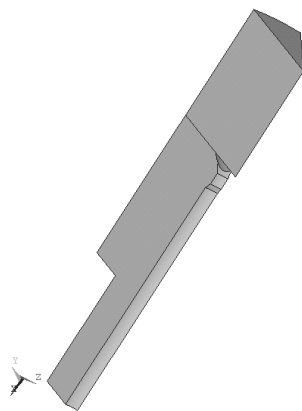


Fig. 20. Geometric model adopted for simulation tests

Service life tests of dies for plastic working of non-ferrous metals with coatings deposited thereon in working conditions - the extrusion of rods made of selected metals and non-ferrous metal alloys (aluminium with commercial purity of 99.5%, copper alloy with phosphorus Cu6,5P, aluminium alloy EN AW-7075) were carried out on a hydraulic press with a nominal pressure of 1 MN with the KOBO method (Fig. 24). The resistance of coatings to tribological wear and mechanical properties, dimensional accuracy and surface quality of the rods produced in extrusion

were taken into account in particular. In a classical extrusion method, a metal enclosed in a container is extruded through a die under the pressure exerted by a punch. The main difference between classical extrusion and the KOBO method is reverse die rotation. A separate driving system needs to be applied allowing to transmit a torque moment from a motor onto a work tool - a die (Fig. 24).

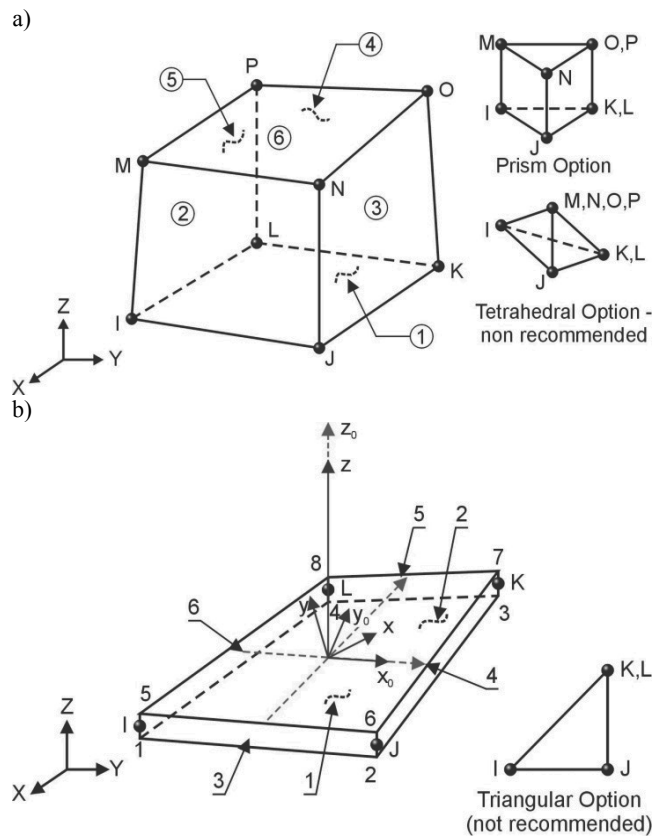


Fig. 21. Structural diagram of a) SOLID 185 element, b) SHELL 181 element

Table 2. Material data of die material

Element	Materials designation	Young modulus, GPa	Poisson coefficient
Coating	CrAlSiN	500	0.29
Low-friction layer	DLC	140	0.22
Die	Steel X40CrMoV5-1	210	0.30

Table 3. Material data of extruded material - EN AW-7075 aluminium alloy

Density, g/cm ³	2.8
Young modulus, GPa	70
Poisson coefficient	0.33

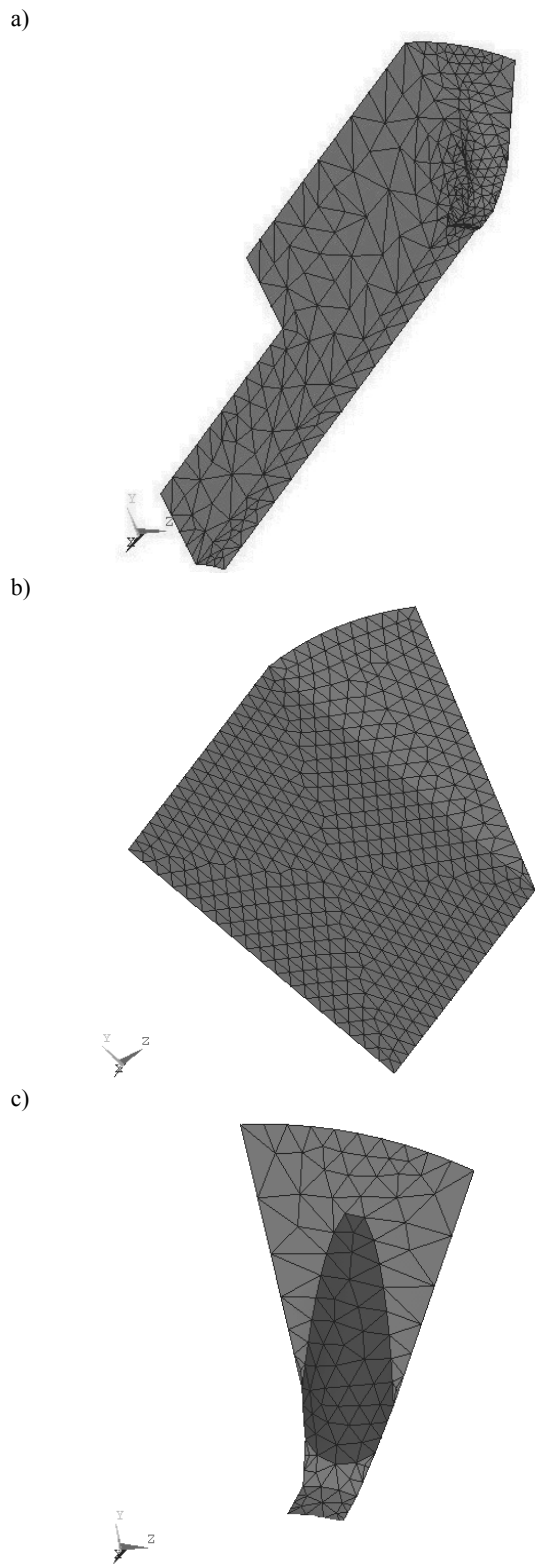


Fig. 22. Model of: a) die, b) extruded material, c) single layer for discretisation

The extrusion process implementation diagram with a reversely rotating die (KOBO method) is shown in Fig. 25.

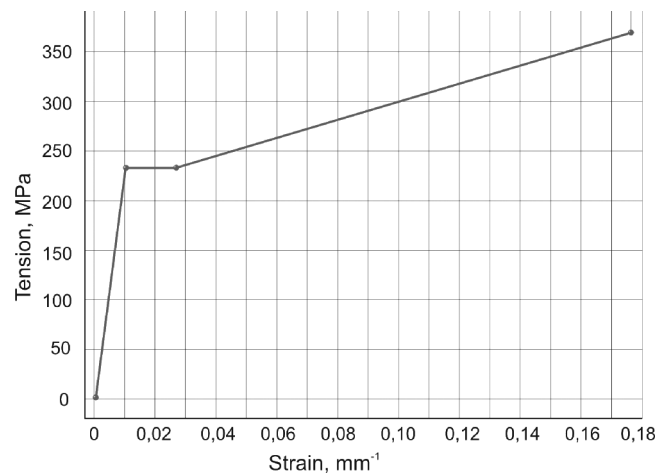


Fig. 23. Strain-stress curve for EN AW-7075 aluminium alloy

The mechanical properties of the extruded products (wires) were determined in a static tensile test. The tests were performed on a universal tensile testing machine Zwick/Roell Z050 at room temperature according to PN-EN-10002-1:2004.

The fractographic tests of coatings were made on transverse fractures in a scanning electron microscope SUPRA 35 by ZEISS, fitted with the EDS chemical composition analysis system. A side detector (SE) and InLens detector were used to produce SEM images, using secondary electrons detection with the accelerating voltage of 5-20 kV and maximum magnification of 30000 \times . The specimens with the cut notch were cooled in liquid nitride before breaking to eliminate a plastic deformation and ensure the brittle character of the fracture being created.

Diffraction investigations and coating structure investigations were conducted using a scanning-electron microscope (S/TEM) Titan 80-300 by FEI, equipped with an electron field gun XFEG with a Schottky emitter with increased brightness, an energy dispersion spectrometer EDS, an external energy filter for imaging EFTEM and for spectroscopy EELS, a system of three BF/ADF/HAADF detectors for scanning work mode. Observations were carried out within energy range of 80-300 kV in the classical model (TEM) with a spatial resolution below 0.10 nm and in the beam surface-scanning mode (STEM) with spatial resolution of up to 0.14 nm. An electron energy filter used allowed to obtain energy-filtered microstructure images (EFTEM) with greatly improve contrast and to perform a chemical micro- and nano-analysis with the Electron Energy-Loss Spectroscopy (EELS) method. With the high energy resolution of the system of approx. 0.8 eV, EELS spectroscopy allows to analyse chemical composition and identify chemical substances present in nanoareas. Microscope tests were performed on thin lamellas dimensioned about 20 \times 8 μ m that were next thinned to the final thickness of about 50-70 nm. Sampling was made on the cross-section of layers with an FIB Quanta 3D 200i device.

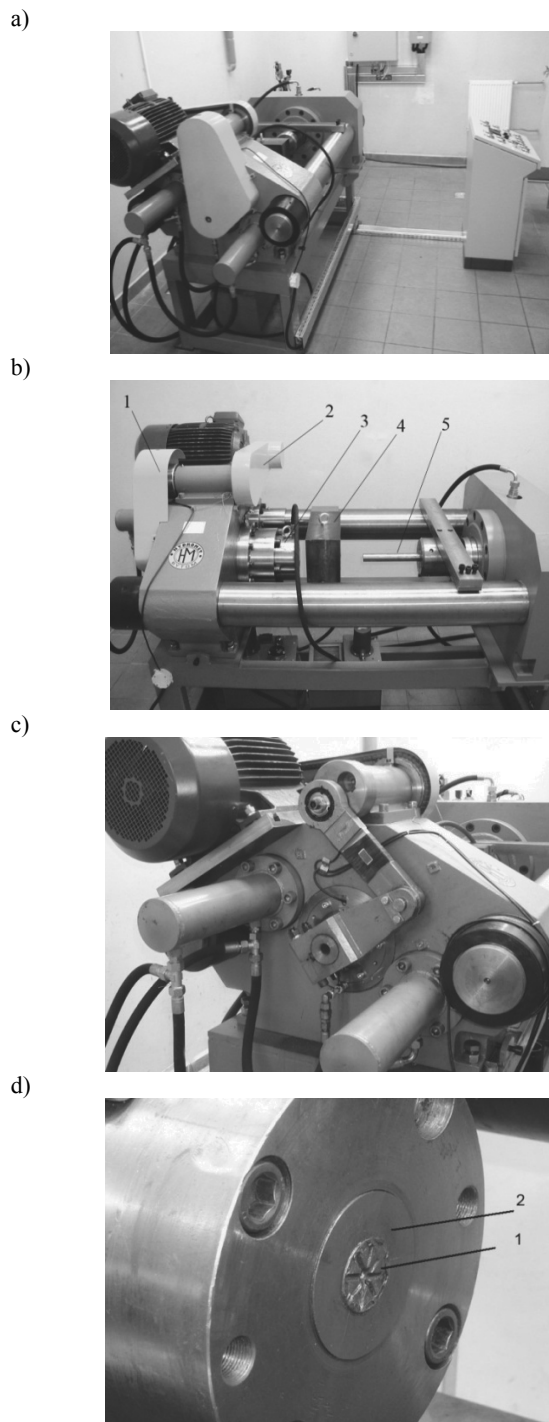


Fig. 24. Laboratory hydraulic press with pressure of 1 MN with a reversely rotating die system: a) general view of the press and control station; b) side view (1 - reversely rotating die system, 2 - die rotation system drive, 3 - die enclosure, 4 - recipient, 5 - punch); c) front view (with enclosure removed) on a frame enabling die rotation; d) work tool housing with a die (1) and disc (2)

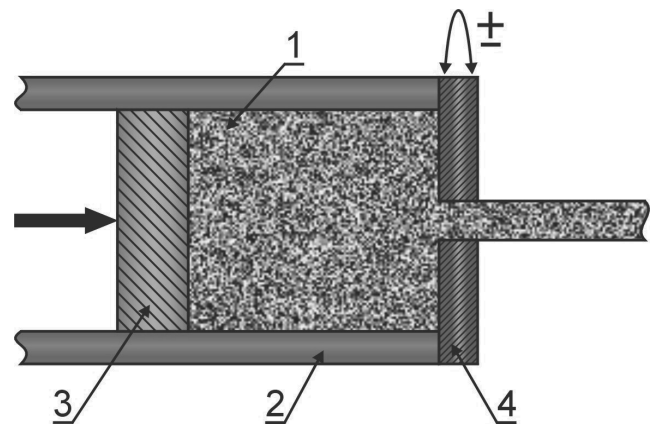


Fig. 25. Extrusion diagram with reversely rotating die (KOB0 method): 1 - extruded material, 2 - recipient, 3 - punch, 4 - reversely rotating die

Layers' surface topography tests and a fractional and multifraction analysis of the tested coatings was determined based on the measurements performed with an atomic force microscope (AFM) XE-100 by Park System. The areas of coatings dimensioned $10 \times 10 \mu\text{m}$, $5 \times 5 \mu\text{m}$ and $2 \times 2 \mu\text{m}$ were scanned during the measurement and $N=512 \times 512$ measurements of specimen height were made, where numbers refer, respectively, to the number of scanned lines and measuring points for each of them. Distance between lines and measuring points is constant and the same. The tests also enabled to determine the roughness of the layers' surface.

Changes in the concentration of chemical components of coatings were determined based on the following spectroscopy tests: X-ray Photoelectron Spectroscopy (XPS) and Auger Electron Spectroscopy (AES). Measurements were made using a multi-functional electron spectrometer PHI 5700/660 by Physical Electronics. The depth of the analysis made for the XPS technique is about several dozen nanometres, while this depth for the AES technique is several tenths nanometre. A crater with the diameter of more than ten micrometers using an ion gun was created to determine chemical composition of the coatings obtained, especially in transition areas between the substrate and the coatings applied. The specimen surface was etched with a collimated beam of ions Xe^+ with energy of 4 keV for about 12 hours. The crater formed was primarily analysed with a scanning electron microscope using secondary electrons. This enabled to distinguish characteristic areas for the substrate and for the coating. A definition of chemical classification of areas was determined by making measurements of Auger survey spectra within the kinetic energy range of 20 eV to 1800 eV. Linear profiles across the crater using the AES technique were made to determine the decomposition distribution of individual elements forming part of coatings. Information on changes in the concentration of chemical composition in transient areas within the scale of several dozens of millimetres was collected this way. The coatings obtained were also tested with the XPS technique. Photoemission spectra were obtained using monochromatic radiation $\text{Al K}\alpha$ with the energy of 1486.8 eV. A measurement of photoelectron spectrum was made within a wide range of binding energy of 0 eV to 1400 eV and exact measurements of core lines

of individual components from surface layers. Chemical composition was determined using MULTIPAK software.

Tests using a Raman spectrometer Jobin-Yvon (T64000) were made to estimate the ratio of sp² and sp³ bonds in the DLC layers produced. The source of excitation in the spectrometer was laser light with the wave length of 514.5 nm, and a detector was a cooled CCD camera with the resolution of at least 2 cm⁻¹. A laser beam was focussed on a specimen through a ×100 lens. The Raman spectra obtained were adjusted with Gaussian distribution curves.

Variations in the chemical concentration of the coating components in the perpendicular direction to the coating surface and concentration changes in the transient zone between the coating and the substrate material were evaluated based on tests with a GDOS-75 QDP glow discharge optical spectrometer by Leco Instruments.

X-ray tests of the analysed materials were carried out with an X'Pert PRO device by Panalytical, using the filtered radiation of a lamp with a cobalt tube with 40 kV voltage supply with 30 mA filament current intensity. An X-ray phase qualitative analysis of the examined layers was made with the Bragg - Brentano configuration with an Xceletor band detector and the grazing-incidence X-ray diffraction method for the primary X-ray beam using a parallel beam collimator before a proportional detector. The diffraction patterns were established for different incidence angles of the primary beam. 3 pole figures were measured for each of the analysed layer with the reflection method using an Euler's disc with the diameter of 187 mm with the specimen inclination angles of 0 to 75° in order to determine the distribution of normals for the selected plane and to determine Orientation Distribution Functions (ODFs) of coatings.

Stress measurements of the tested coatings were carried out with the sin²ψ or g-sin²ψ technique [139, 140] depending on the properties of the tested layers using X'Pert Stress Plus software.

The hardness tests of the deposited coatings were conducted with the Vickers method consisting of measuring the depth of indentation that usually does not exceed the tenths of a micrometer, and the set pressure does not exceed 0.05 N, which eliminates the impact of the substrate material on coating hardness. Hardness identified this way, called dynamic hardness, determines a material's strength properties, including not only a plastic strain, but also an elastic strain. The measurements were made in the loading and unloading mode, where the indenter is loaded with the set force, the load is maintained for certain time, and then it is unloaded. A precision measuring system allows to record the depth of the indentation formed during loading, as well as during indenter unloading. A hardness test with the Vickers method was performed with nano-indenting made with a Shimadzu DUH 202 nanohardness tester.

The adhesion of the coatings to the substrate material was evaluated with a scratch test used commonly for coatings produced in physical vapour deposition processes. The tests were made using a Revetest device by CSM using the following test conditions:

- pressing force range of 0-100 N;
- load increase rate (dL/dt) - 100 N/min;
- indenter movement rate (dx/dt) - 10 mm/min;
- acoustic emission detector sensitivity - 1.2.

The character of the damage formed was assessed based on observations with an MEF 4A microscope by Leica.

A classification established by Burnett and Rickerby was used to harmonise a vocabulary for the damages formed during coating adhesion tests [141].

A **friction coefficient and the wear of coatings** was determined in a test according to the ball-on-disk method. The tests were undertaken at room temperature with a T-01M device by ITE Radom under the following conditions:

- slide rate - 0.2 m/s (192 RPM);
 - normal load - 19.62 N;
 - friction radius - 10 mm;
 - counter-specimen - an Al₂O₃ ball with 10 mm diameter;
 - wear track - 1,000 m;
 - ambient temperature - 23°C (±1°C);
 - relative humidity - 30% (±5%);
- and at temperature increased with a high-temperature tribometer by CSM Instruments with the following conditions of the experiment:

- slide rate - 0.2 m/s (192 RPM);
- normal load - 5 N;
- wear radius - 5 mm;
- counter-specimen - an Al₂O₃ ball with 6 mm diameter;
- wear track - 500 m;
- ambient temperature - 400°C (±5°C);

The test were performed in compliance with ASTM G99-05 and ASTM G133-05. The wear tracks of the coatings were viewed with a confocal laser scanning microscope CLSM 5 Exciter by Zeiss with a light source of a 25 mW diode laser emitting radiation with a wavelength of 405 nm.

5. Overview of the research results

5.1. Results of numerical analysis

The distribution of stresses in a die was determined in the first stage, within a nitride and low-friction layer formed on its surface, as well as in the deformed material (EN AW-7075 aluminium alloy) during extrusion with the KOBO method with a reversely rotating die. A value of stresses reduced acc. to the Huber-Mises hypothesis in the places with the highest concentration of the analysed system elements was determined.

Pressure with a force distributed in form of pressure onto the die front surface occurs within 1 s. A simulation of extrusion with a reversely rotating die starts from the 2nd second. Rotation takes place as a result of the set dislocation, with its scaling done with the harmonic function ROT_x=COS(x). A simulation performed after the time of 1, 3, 4 and 5 s according to the extrusion conditions used, such as extrusion speed, frequency of a die's torsional motion and torsional angle have allowed to achieve a distribution of stresses within the die-coating-extruded material contact zone. Such stresses, in the form of a distribution of reduced stresses, are presented in Figs. 26-28, whereas Fig. 29 shows stresses occurring for the overall geometrical model of the system.

An analysis of the results obtained reveals that the maximum value of reduced stresses initiated with the activity of external forces during extrusion for an external low-friction layer is

700 MPa, while for a hard nitride layer - 2600 MPa. The maximum values of stresses for the both cases were situated at the edges of grooves made on the front die surface, the purpose of which is to increase deformation intensity (shearing, torsion) of the extruded material by transmitting a torque moment from a die onto the material.

The results of earlier works show [69,142,143] that the distribution of stresses in a die in extrusion processes as a result of external forces is conditioned by multiple factors, in particular an extrusion method, type of extrude material, extrusion force, ingot size, extrusion speed, etc. The values of stresses initiated with the activity of external forces for aluminium and other metals commonly undergoing plastic working are within the range of 600-1500 MPa. It is required for the correct influence of coatings that geometry and properties of the coated tool surface do not vary in operation.

The maximum value of reduced stresses for the analysed die made of hot-work X40CrMoV5-1 tool steel used in the EN AW-7075 alloy extrusion process with the KOBO methods spanned 100-1200 MPa. Similar to the analysed layers, the maximum values of stresses were situated at the peripheries of grooves made on its front surface. A yield strength value for typical grades of steels used for extruding dies shown in Table 4 indicates that a die material's plastic deformation up to the temperature of 300-400°C is impossible due to acceptable stress values initiated during extrusion, not exceeding a yield point value for steels used for dies.

Table 4.

Yield point for selected grades of hot-work tool steels in ambient and increased temperature (established according to the Böhler company's information materials and data excerpted from [144])

Type of steel	Yield point R_e , MPa				
	25°C	300°C	400°C	500°C	600°C
X38CrMoV5-1	1400	1200	1100	900	600
X40CrMoV5-1	1400	1200	1100	950	600
32CrMoV12-28	1370	1180	1080	950	650
X38CrMoV5-3	1400	1200	1150	980	630

A substantial plastic deformation occurs during cold extrusion with the KOBO method accompanied by a charge's temperature increase up to ca. 300°C which does not affect strength properties of the steel the die was made of, either. Nevertheless, a charge's temperature grows above 400°C during hot extrusion. However, a small heat conductivity coefficient of the external layers applied and their high oxidation resistance at increased temperature are effectively reducing the impact of external temperature on the die material.

If the die surface temperature in extruding reaches 500°C, a yield point value for steel is smaller than 1000 MPa, which may cause a plastic deformation of a die material.

A distribution of the model elements' dislocation after, respectively, 1, 3 and 5 s was also analysed. The values of the obtained dislocations are shown in Fig. 30.

5.2. Results of investigations into the service life of dies

Investigations into the service life of dies for plastic working of non-ferrous metals with coatings deposited on their surface were carried out during extrusion with a reversely rotating die (KOBO) due to extremely hard working conditions.

The research held to date into the extrusion of metals and alloys with the KOBO metal have been focussed on the phenomena connected with the process kinetics and mechanical properties. It has been evidenced that a material, while being extruded, behaves like a viscous fluid. The extrusion force is largely lowered if an additional, cyclic die rotation is applied. This is associated with the over-the-balance generation of spot defects as a result of intersecting dislocation [56,145].

The preliminary performance tests undertaken for dies coated with monolayer nitride nanocrystalline coatings produced with the PVD technique and two-layer coatings consisting of a nanocrystalline nitride layer with an additional low-friction layer, shown in Fig. 16, as well as studies into the kinetics of KOBO extrusion and into the impact of the type coatings and process conditions on mechanical properties of the products fabricated, have become reasons for selecting conditions of carrying out further detailed experiments.

It was found as a result of preliminary investigations that the life of dies coated with monolayer nanocrystalline coatings grows only to a small extent as compared to dies used currently in the extrusion process, worked conventionally as a result of thermal or thermochemical treatment. An extruded material's susceptibility to sticking to the die surface was a major problem for monolayer nitride coatings. However, the results attained for two-layer coatings (with an additionally deposited low-friction layer) have shown it is appropriate to conduct additional experiments, therefore, dies with the following layers applied were selected for further investigations:

- CrN+DLC,
- AlCrSiN+DLC,
- AlCrSiN+MoS₂,
- AlTiCrN+DLC.

An EN AW-7075 aluminium alloy was subjected to extruding because of its hard formability. Investigations for dies used traditionally in the extrusion process were additionally undertaken for comparative reasons, whose functional properties are enhanced in thermal treatment (quenching and high tempering) of thermochemical treatment (nitriding).

The first stage was EN AW-7075 aluminium alloy extrusion with constant die rotation frequency. The following process conditions were established:

- constant extrusion speed of $v=0.5$ mm/s;
- constant charge geometry of $\phi 40 \times 40$ mm;
- constant processing ratio of $\lambda=100$ - with $\phi 4$ mm product diameter;
- constant die rotation frequency of $f=5$ Hz;
- constant torsional angle $\gamma=\pm 8^\circ$;
- constant start charge and recipient temperature of 24°C;
- free product cooling in air;
- variable extrusion force.

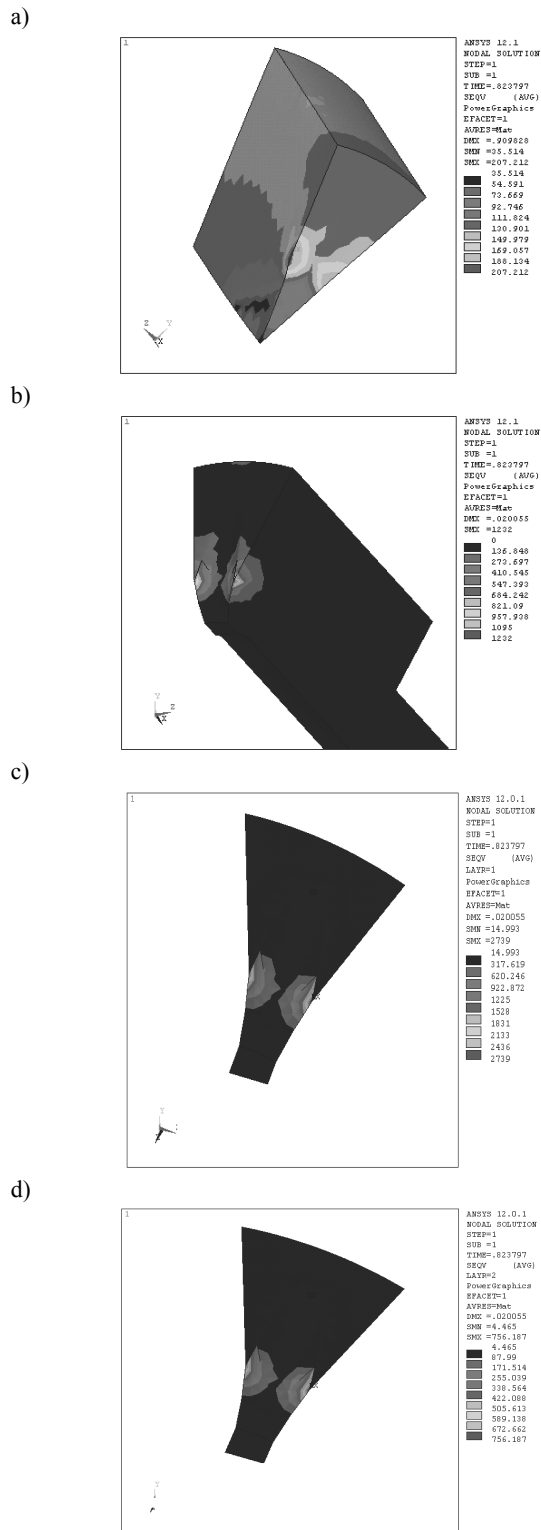


Fig. 26. Distribution of reduced stresses: a) in the extruded material, b) in a die, c) hard internal layer, d) external low-friction layer after 1 s of simulation

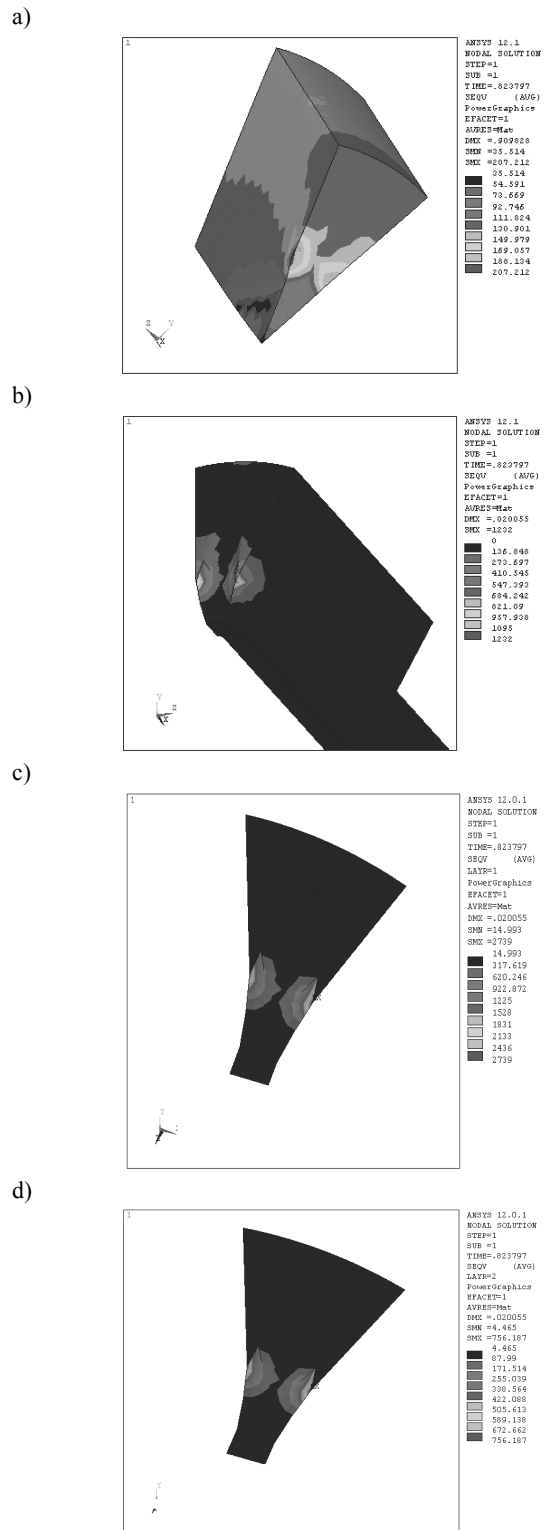


Fig. 27. Distribution of reduced stresses: a) in the extruded material, b) in a die, c) in a hard internal layer, d) in an external low-friction layer after 3 s of simulation

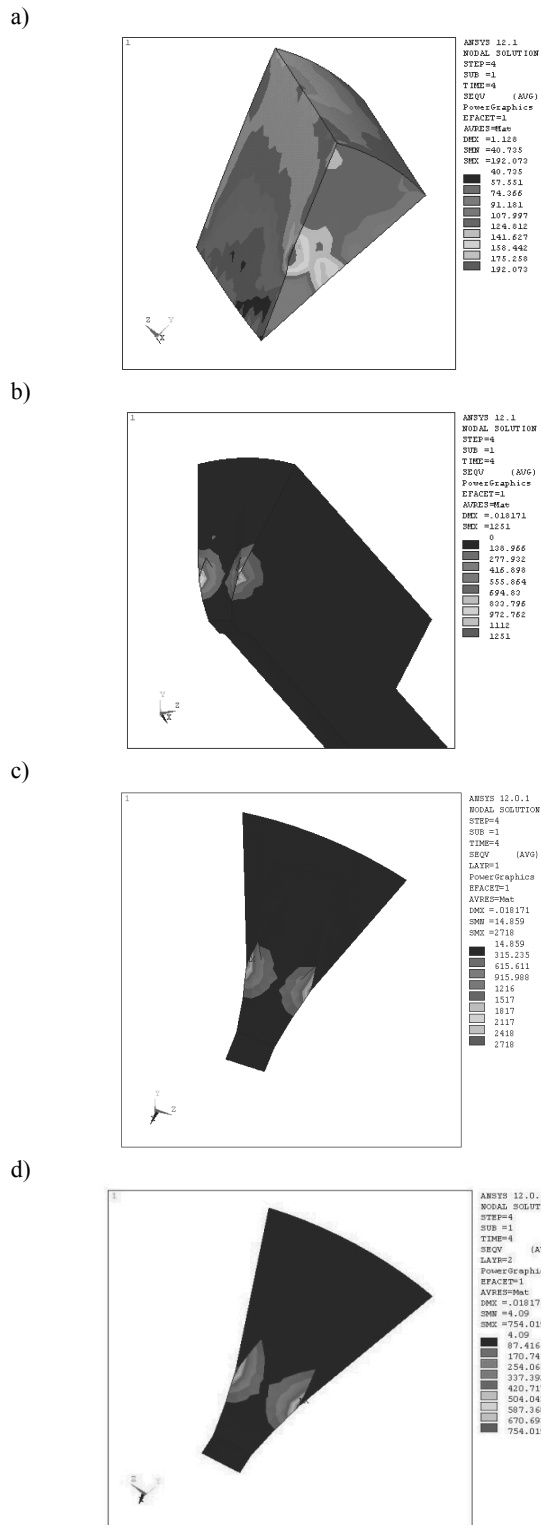


Fig. 28. Distribution of reduced stresses: a) in the extruded material, b) in a die, c) in a hard internal layer, d) in an external low-friction layer after 4 s of simulation

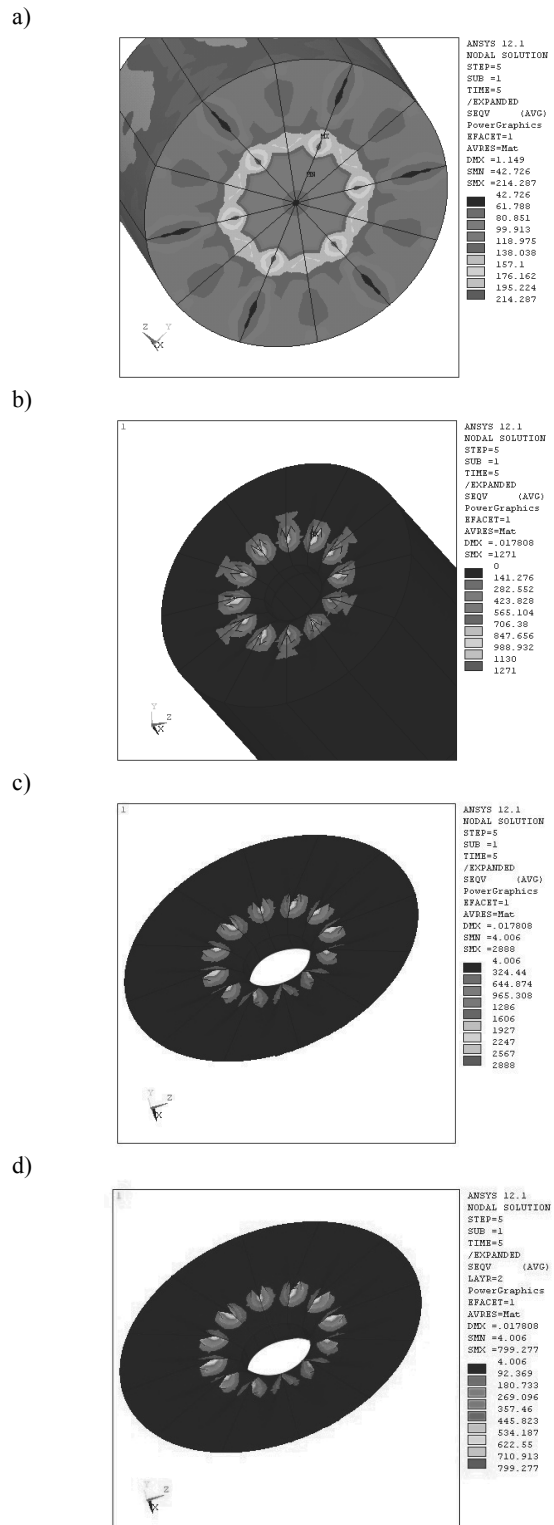


Fig. 29. Distribution of reduced stresses: a) in the extruded material, b) in a die, c) in a hard internal layer, d) in an external low-friction layer after 5 s of simulation

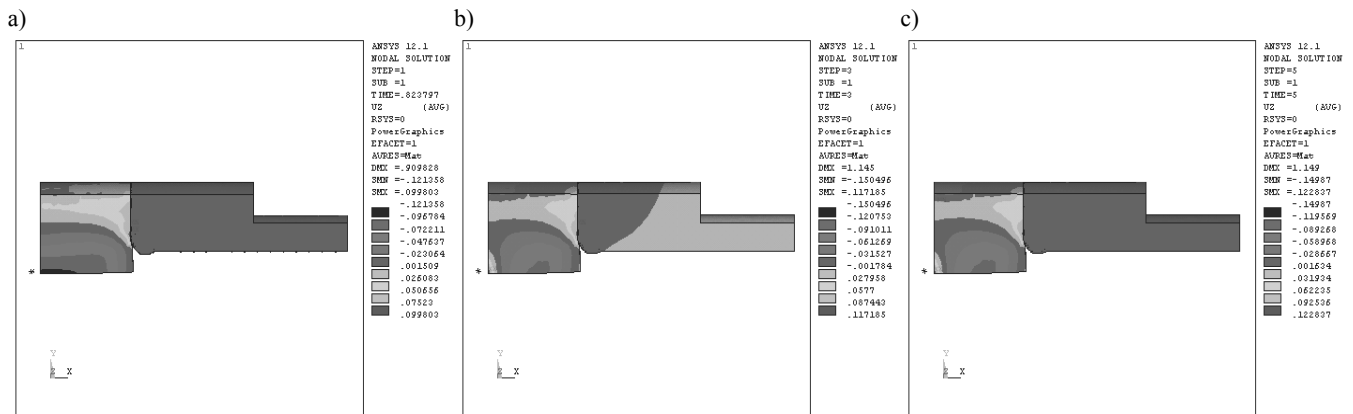


Fig. 30. Distribution of a model's elements dislocation after: a) 1 s, b) 3 s, c) 5 s of simulation

The purpose of selecting such parameters was to perform extrusion in extremely hard conditions. Such high extrusion speeds, processing ratios, especially when performing a process without material preheating, are not used industrially as well as in laboratory investigations. A fact is noteworthy that a press with the nominal pressure of 1 MN was used. The wear of coatings deposited onto the die surface was analysed at this stage and mechanical properties were measured of the wires produced in extrusion.

Extrusion in the second stage was performed with constant force in order to obtain homogenous mechanical properties for wires' length. The following process conditions were established:

- constant extrusion speed of $v=0.5$ mm/s;
- constant charge geometry of $\phi 40 \times 40$ mm;
- constant processing ratio of $\lambda=100$ - with $\phi 4$ mm product diameter;
- constant extrusion force of approx. 0.95 MN;
- constant torsional angle of $\gamma=\pm 8^\circ$;
- constant start charge and recipient temperature of 24°C ;
- free product cooling in air;
- variable die rotation frequency to maintain constant force.

The wear of coatings deposited onto the dies' surface was analysed after this stage and the wires produced underwent the tests of strength properties.

The third stage was held in extrusion conditions as for the first stage for a quantitative assessment of the dies' service life. Extrusion tests for a given die were interrupted according to the degree of wear of coatings and of a die and according to the quality of the product extruded. The wear of a die and a disc was assessed following the completion of extrusion.

The impact of temperature, speed and force of extrusion on the wear of coatings was evaluated in the fourth stage. The investigations to date consisted of extruding with set punch travel speed. The process can be carried out at the constant extrusion frequency and force by controlling a laboratory hydraulic press. Punch travel speed is a variable parameter in such case, however. For this reason, the tests were carried out with a constant force of 1 MN (i.e. with maximum nominal punch pressure) and constant frequency. Furthermore, dies with the eye diameter of 6 mm (processing ratio of $\lambda=44.4$) were used to increase speed

controllability. A lower processing ratio is connected with a lower extrusion force (lower plastic flow resistance); therefore it was decided to heighten the temperature. This factor is also substantially influencing the process progress. A recipient in the press used enables heating to 400°C and the same was used. Very high pressures are exerted on the die front surface at high extrusion speeds by decreasing a processing ratio and raising a temperature with a constant pressing force value and die rotation frequency, which translates into susceptibility to the wear of the coatings examined. The following process conditions were established:

- constant charge geometry of $\phi 40 \times 40$ mm;
- constant processing ratio of $\lambda=44.4$ - with $\phi 6$ mm product diameter;
- constant extrusion force of approx. 1 MN;
- constant torsional angle of $\gamma=\pm 8^\circ$;
- constant start charge and recipient temperature of 400°C ;
- free product cooling in air;
- constant die rotation frequency of $f=5$ Hz;
- variable die rotation frequency v to maintain constant force.

Fig. 31 shows a view of extruding dies with the KOBO method together with discs in the initial state.

Impact of extrusion conditions and surface treatment on the quality of dies and on the strength properties of products

It was found as a result of extruding an EN AW-7075 alloy with constant torsional speed and frequency at a variable force (1st stage) that the highest initial speed of extrusion of 0.06 mm/s is achieved by using dies with an AlTiCrN+DLC coating (Table 5). It is very similar, however, to the values obtained on other coatings (variance by 0.01 mm/s). An exception is a die with a CrAlSiN+DLC coating where the initial extrusion speed is three times lower. It also translates to the final extrusion force that is higher in this case (0.9 MN). It is very difficult to initiate an extrusion process with the KOBO method using such a variant. A die with a CrN+DLC coating applied and a die after quenching and tempering exhibit similar parameters. A disc was cracked for dies after nitriding. Fig. 32 shows a view of the dies' front surface after the first stage of extrusion.

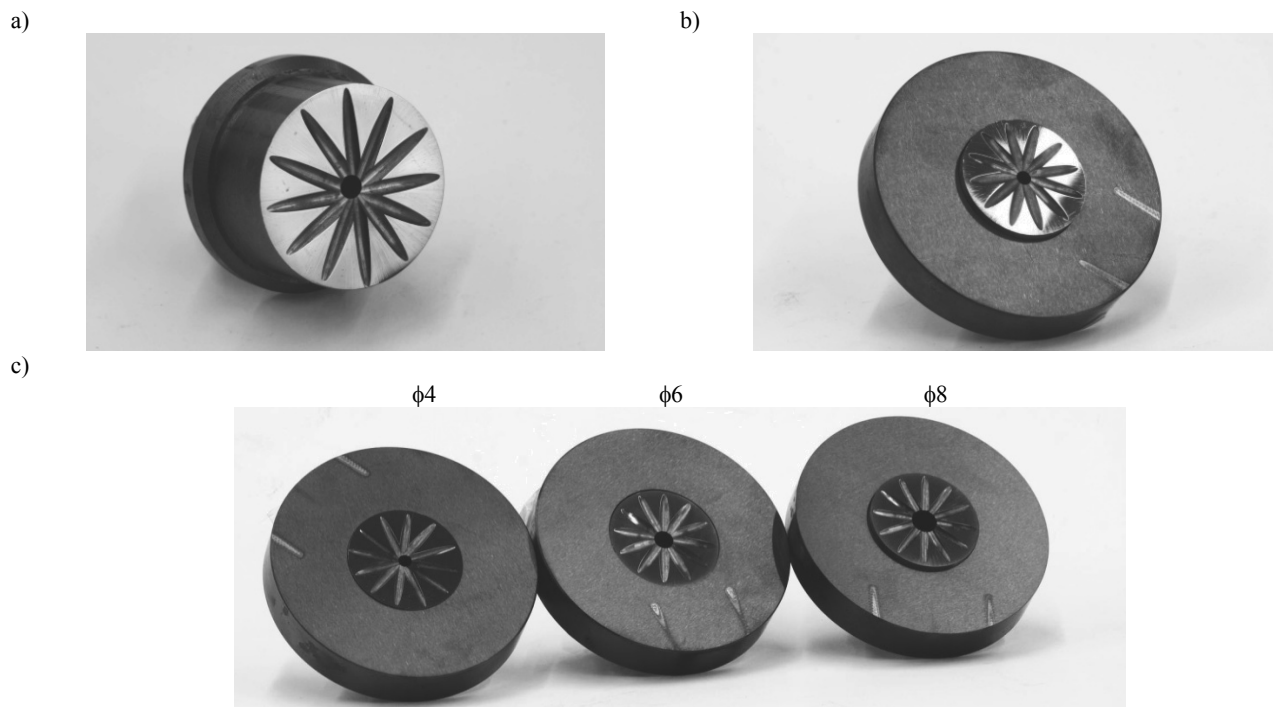


Fig. 31. View of dies with a CrN+DLC coating deposited: a) die $\phi=4$ mm; b) die $\phi=4$ mm placed on a disc; c) set of dies $\phi=4, 6$ and 8 mm for operational tests

Products with a smooth surface without any scratches and cracks are produced when extrusion is carried out with the KOBO with a constant force by gradually decreasing a die rotation frequency from the initial value of 5 Hz (2nd stage) (Table 6). CrN+DLC, CrAlSiN+DLC and AlTiCrN+DLC coatings do not exhibit any signs of wear. An extrusion butt from the extruded material sticks to the die for a CrN+DLC coating, however.

A static tensile test of the wires obtained as a result of extrusion was made in order to characterise the strength properties of the extruded material according to the process conditions, as well as the method and type of the protection layer applied onto the die surface. Figs. 33-38 show the results of tensile strength tests for wires made of EN AW-7075 alloy after extrusion with the KOBO method at constant speed and rotation frequency with a variable force (1st stage), while Figs. 39-44 provide the results of tensile strength tests of wires made of EN AW-7075 alloy after extrusion at constant speed and force with a variable frequency of die rotation (2nd stage). The wire samples were cut in sequence from the beginning to the end of the product produced. Tables 7 and 8 enlist the strength properties of wires. Standard deviations are given to present a differentiation of properties along the length of the wires tested.

In case of extrusion with a constant die rotation frequency, the highest strength properties are exhibited by those wires extruded using dies with an AlTiCrN+DLC coating after quenching and tempering, with tensile strength R_m , respectively, 413 and 418 MPa (Table 7). Elongation of approx. 14% is obtained for wires extruded on dies with AlSiCrN+DLC and AlCrSiN+MoS₂ coatings and on nitrided ones. The lowest and most differentiated values of strength properties are exhibited by an EN AW-7075

alloy after extrusion using a CrN+DLC coating (Fig. 33). The progress of strain-stress curves for dies with an AlCrSiN+DLC coating and nitrided ones (Figs. 35 and 37) are nearest to each other along the entire length, signifying a possibility to achieve constant strength properties in materials.

Extrusion at constant speed reduces differences in strength properties along the tested wires in all cases (Figs. 39-44). The highest strength properties are obtained for wires extruded on dies with CrN+DLC coatings and nitrided and tempered and quenched dies. The lowest strength properties, and at the same time the highest plasticity, is exhibited by a material after extruding on a die with an AlTiCrN+DLC coating (Table 8).

A question arises in view of the untypical progress of an extrusion process and the application of dies whose surface has been modified in thermal and thermochemical treatment processes or by producing protection layers with the PVD and CVD technique about their impact on the progress of strain and stress curves for EN AW-7075 alloy. Four different behaviours can be differentiated by analysing stress and strain curves (Fig. 33-44):

- low elongation and high strength - in particular quenched and tempered (1st stage), AlTiCrN+DLC (1st stage), CrN+DLC (2nd stage), CrAlSiN+DLC (2nd stage);
- Lüders plastic instability - in particular of nitriding (1st stage), quenching and tempering (1st stage), CrN+DLC (2nd stage);
- low strength properties and high plasticity - in particular CrAlSiN+MoS₂ (2nd stage), AlTiCrN+DLC (2nd stage);
- Portevin-Le Chatelier plastic instability - in particular of AlTiCrN+DLC (1st stage), nitriding (1st stage), AlTiCrN+DLC (2nd stage).

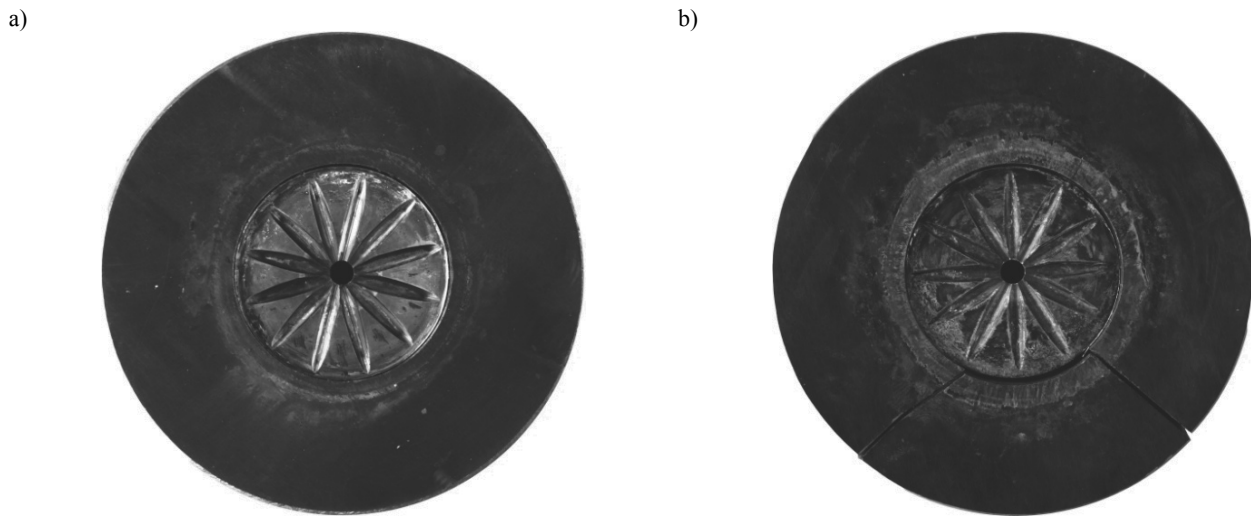


Fig. 32. View of surface of dies and discs after extrusion with constant speed and torsional frequency at constant force (1st stage) with the following coating: a) CrAlSiN+DLC coating, b) nitrided coating

Table 5.

Conditions of extrusion and coating quality during an extrusion process with the KOBO method at constant speed and rotation frequency with constant force (1st stage)

Coating/treatment type	Extrusion force, T		Punch speed, mm/s		Die coating/surface quality	Comments
	start	end	start	end		
CrN+DLC	107	74	0.05	0.5	Visible small signs of coating wear on front surface of die	Extruded material adheres to die surface
AlTiCrN+DLC	108	80	0.06	0.5	Visible small signs of coating wear on front surface of die	Highest start speed
CrAlSiN+DLC	107	90	0.02	0.5	Visible small signs of coating wear on front surface of die	Lowest start speed and highest final extrusion force
CrAlSiN+MoS ₂	107	83	0.04	0.5	Visible coating wear on front surface and in grooves	Extruded material adheres to die surface
Nitriding	107	80	0.04	0.5	Visible wear of front surface of die and disc	Broken disc
Quenching and tempering	107	70	0.05	0.5	Visible wear of front surface of die and disc	Lowest final extrusion force

Table 6.

Conditions of extrusion and coating quality during an extrusion process with the KOBO method at constant speed and force at variable die rotation frequency (2nd stage)

Coating/treatment type	Extrusion force, T		Punch speed, mm/s		Frequency, Hz		Die coating/surface quality	Comments
	start	end	start	end	start	end		
CrN+DLC	107	95	0.01	0.5	5	3.8	No signs of coating wear	Butt sticks to die
AlTiCrN+DLC	107	100	0.01	0.5	5	3.8	No signs of coating wear	Smooth product surface
CrAlSiN+DLC	107	95	0.01	0.5	5	3.5	No signs of coating wear	Smooth product surface
CrAlSiN+MoS ₂	107	95	0.02	0.5	5	2.5	Coating wear on front surface of die	Broken disc
Nitriding	107	95	0.03	0.5	5	4.0	Wear of front surface of die and disc	Broken disc
Quenching and tempering	107	95	0.05	0.5	5	2.2	Wear of front surface of die and disc	Visible small scratches on extruded product

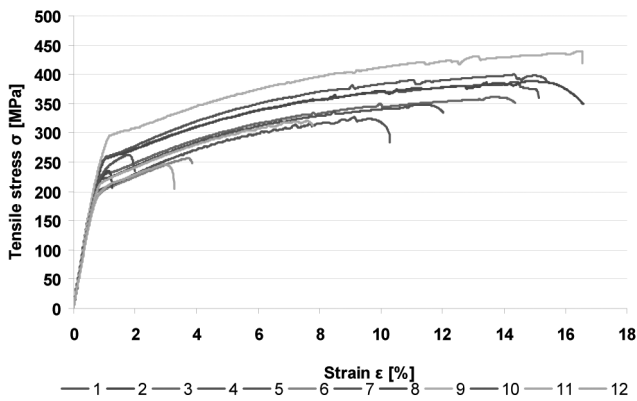


Fig. 33. Tensile curves of wire made of EN AW-7075 alloy after extrusion with the KOBO method with the constant rotation frequency of 5 Hz using a die with a CrN+DLC coating

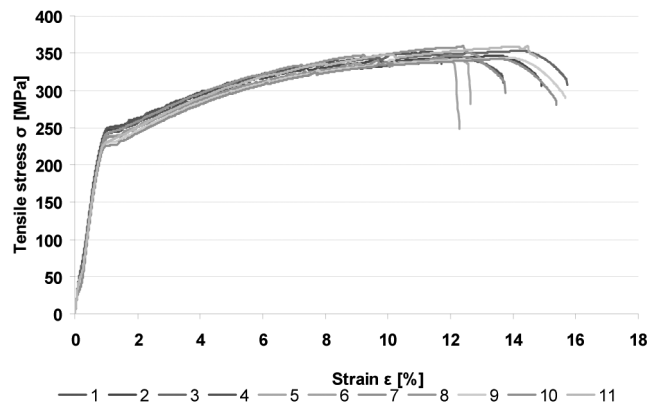


Fig. 35. Tensile curves of wire made of EN AW-7075 alloy after extrusion with the KOBO method with the constant rotation frequency of 5 Hz using a die with a CrAlSiN+DLC coating

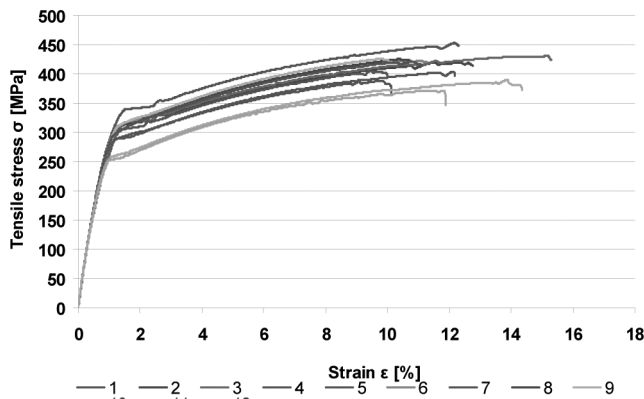


Fig. 34. Tensile curves of wire made of EN AW-7075 alloy after extrusion with the KOBO method with the constant rotation frequency of 5 Hz using a die with an AlTiCrN+DLC coating

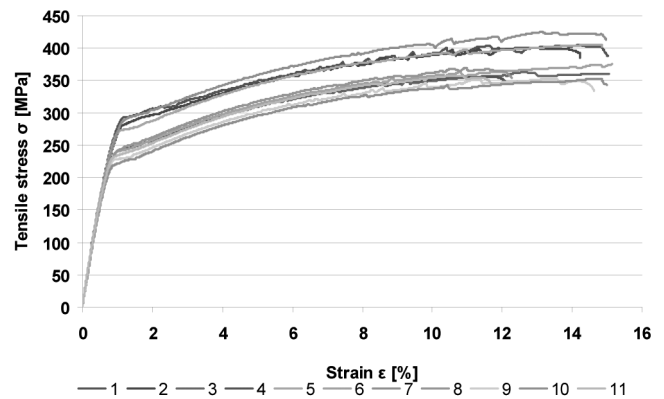


Fig. 36. Tensile curves of wire made of EN AW-7075 alloy after extrusion with the KOBO method with the constant rotation frequency of 5 Hz using a die with a CrAlSiN+MoS₂ coating

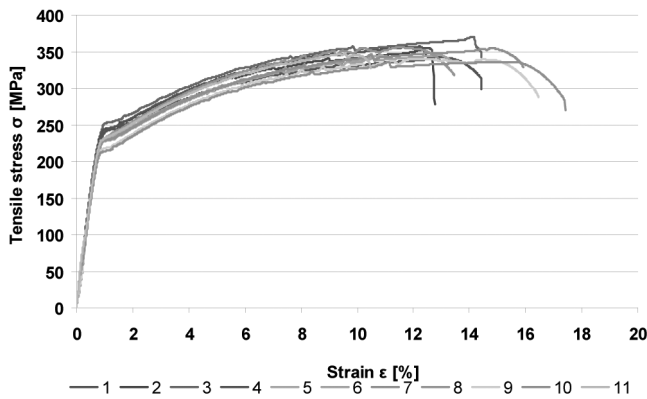


Fig. 37. Tensile curves of wire made of EN AW-7075 alloy after extrusion with the KOBO method with the constant rotation frequency of 5 Hz using a nitrided die

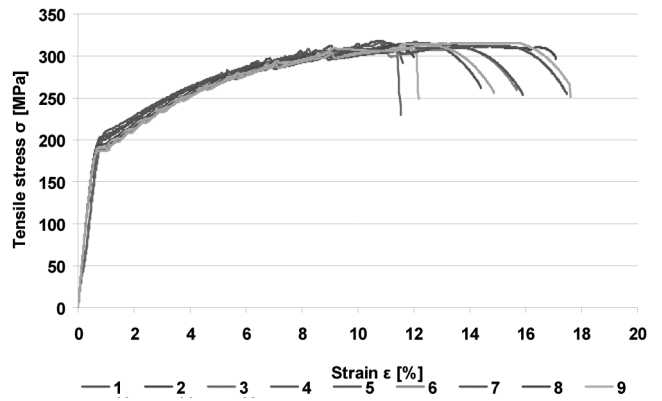


Fig. 40. Tensile curves of wire made of EN AW-7075 alloy after extrusion with the KOBO method with the constant force of 95 T using a die with a AlTiCrN+DLC coating

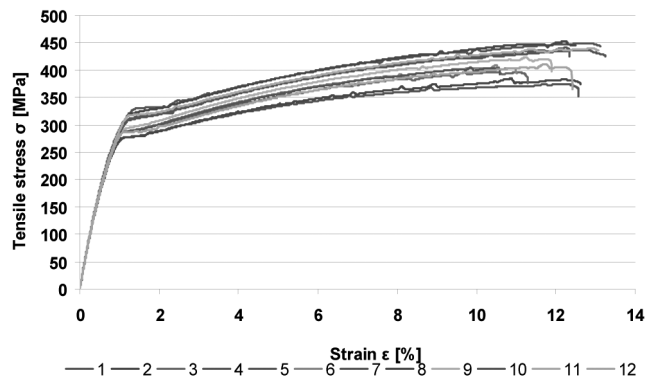


Fig. 38. Tensile curves of wire made of EN AW-7075 alloy after extrusion with the KOBO method with the constant rotation frequency of 5 Hz using a tempered and quenched die

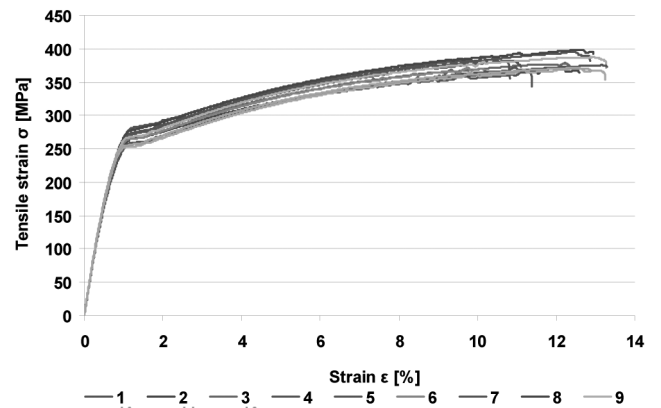


Fig. 41. Tensile curves of wire made of EN AW-7075 alloy after extrusion with the KOBO method with the constant force of 95 T using a die with a CrAlSiN+DLC coating

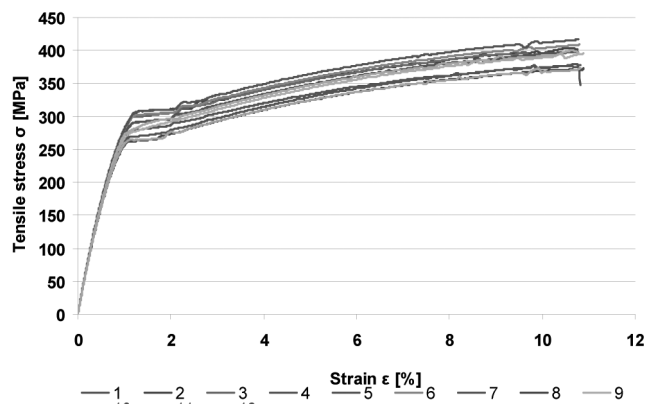


Fig. 39. Tensile curves of wire made of EN AW-7075 alloy after extrusion with the KOBO method with the constant force of 95 T using a die with a CrN+DLC coating

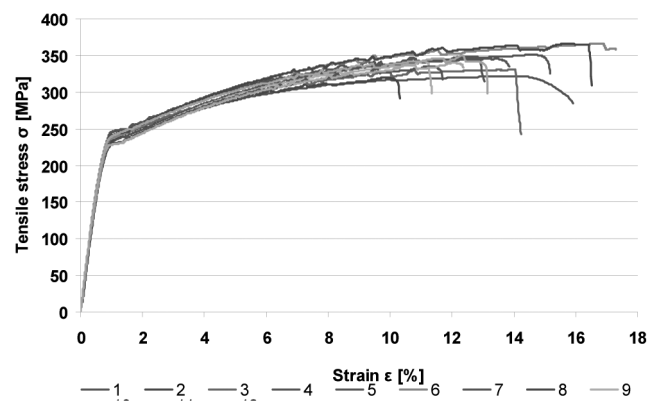


Fig. 42. Tensile curves of wire made of EN AW-7075 alloy after extrusion with the KOBO method with the constant force of 95 T using a die with a CrAlSiN+MoS₂ coating

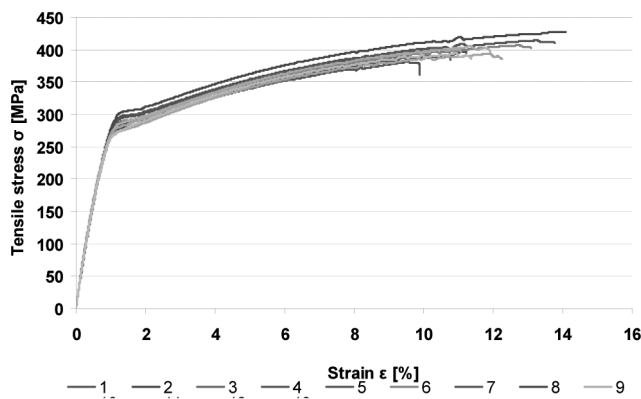


Fig. 43. Tensile curves of wire made of EN AW-7075 alloy after extrusion with the KOBO method with the constant force of 95 T using a nitrided die

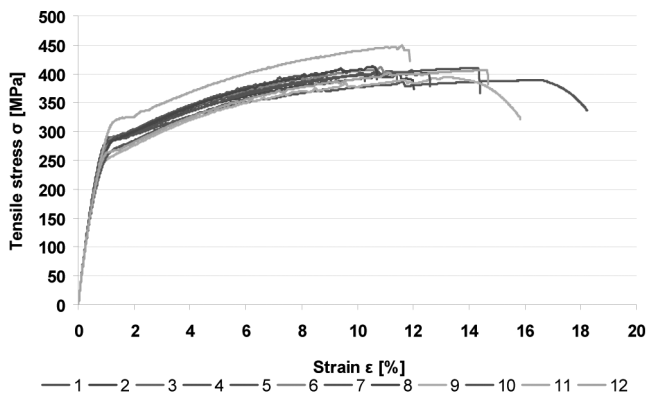


Fig. 44. Tensile curves of wire made of EN AW-7075 alloy after extrusion with the KOBO method with the constant force of 95 T using a tempered and quenched die

Table 7. Mechanical properties of EN AW-7075 alloy wires extruded with the KOBO method with constant die rotation frequency - 1st stage

Coating/treatment type	$R_{0,2}$, MPa	R_m , MPa	A, %
Nitriding	223±15	350±9	13.9±2.0
Quenching and tempering	251±8	418±24	12.2±0.8
AlCrSiN+DLC	225±19	348±6	14.0±1.3
AlCrSiN+MoS ₂	241±16	378±24	14.5±1.7
AlTiCrN+DLC	247±11	413±21	11.9±1.6
CrN+DLC	227±26	331±65	9.9±5.7

Table 8. Mechanical properties of EN AW-7075 alloy wires extruded with the KOBO method with constant extrusion force - 2nd stage

Coating/treatment type	$R_{0,2}$, MPa	R_m , MPa	A, %
Nitriding	238±12	407±14	12.7±2.4
Quenching and tempering	243±6	400±11	11.6±1.4
AlCrSiN+DLC	236±6	378±10	12.2±1.0
AlCrSiN+MoS ₂	228±10	343±14	13.7±2.0
AlTiCrN+DLC	195±8	313±3	14.3±2.3
CrN+DLC	246±9	400±13	12.6±1.7

The Portevin-Le Chatelier (PLC) effect is classified according to the three basic types: A, B and C depending on the time and spatial character of deformation bands' arrangement [146-148]. Type A is equivalent to deformations propagating continuously along the strain axis, being separate plastic waves. Type B means deformation propagation oscillating in time, while type C - a deformation band occurring randomly and not propagating along the specimen subjected to straining. For the specimens tested, the B and C type instability effect is present in the majority of cases.

The tests performed have confirmed it is appropriate to perform extrusion with the KOBO method with constant force. Homogenous properties can thus be obtained along the entire length of extruded products. The best properties are exhibited by wires extruded using dies with AlTiCrN+DLC and CrAlSiN+DLC coatings.

Impact of extrusion conditions and surface treatment on the quality of dies at elevated temperature

Test with a temperature of 400°C with a constant horizontal force of 1 MN (4th stage) were carried out to appraise the effect of temperature, speed and force of extrusion on the wear of coatings. Dies with the eye diameter of 6 mm (processing ratio of $\lambda=44.4$) were used to increase speed controllability.

No external interference with the control system of valves enabling work with the set punch transfer speed was possible during extruding. A constant extrusion force value could not have been successfully reached in any case due to very high speeds. Table 9 shows the conditions recorded each time while conducting the experiments.

The tests performed at this stage point out that a CrN+DLC coating does not exhibit any signs of wear. This can be caused by the lowest heat conductivity of the CrN layer for all the analysed nanocrystalline nitride layers produced in a PVD process. The signs of wear were noticed on the front surface for other coatings. A die with a CrAlSiN+DLC coating is characterised by hindered process initiation and a very high final extrusion force. A coating behaves in a similar way during extrusion with a constant die rotation frequency (1st stage). An extrusion process with the KOBO method at a higher temperature is characterised, for an

AlTiCrN+DLC coating, by the smallest final extrusion force and very high punch transfer speed (Table 9). Wires for extrusion in all the examined cases were characterised by a good surface quality only in the initial stage of extruding (Fig. 45). When the process is held at a temperature of 400°C with final speeds over 3 mm/s, the end pieces of wire break as a result (Fig. 45d).

The purpose of selecting extrusion condition for the 4th stage was, however, to test the dies in extremely hard conditions. The worst wire surface quality was observed after extrusion with a quenched and tempered and nitrided die, which is related to their working surfaces being completely destroyed. Fig. 46 shows a view of front surfaces of dies after extruding EN AW-7075 alloy at a temperature of 400°C.

Impact of surface treatment on dies' service life

An extrusion process with the KOBO method at constant speed and dies rotation frequency (3rd stage) was carried out to

Table 9.

Conditions of extrusion and coating quality during an extrusion process with the KOBO at temperature of 400°C with constant extrusion speed and die rotation frequency at variable extrusion speed

Coating/treatment type	Extrusion force, T		End speed, mm/s	Die coating/surface quality	Wire quality	Comments
	start	end				
CrN+DLC	100	80	3.65	No signs of wear of coating produced on die surface	Good beginning, cracked end	Lowest coating wear
AlTiCrN+DLC	100	75	3.99	Visible coating wear	Good beginning, cracked end	Lowest final extrusion force
AlCrSiN+DLC	100	90	3.65	Small wear of coating	Very good beginning, cracked end	Lowest final extrusion force
Quenching and tempering	100	77	4.05	Destroyed surface of die	Good beginning, cracked centre and end	Worst wire quality, highest final extrusion speed
Nitriding	100	-	-	Destroyed surface of die	Good beginning, cracked centre and end	Substantial die wear

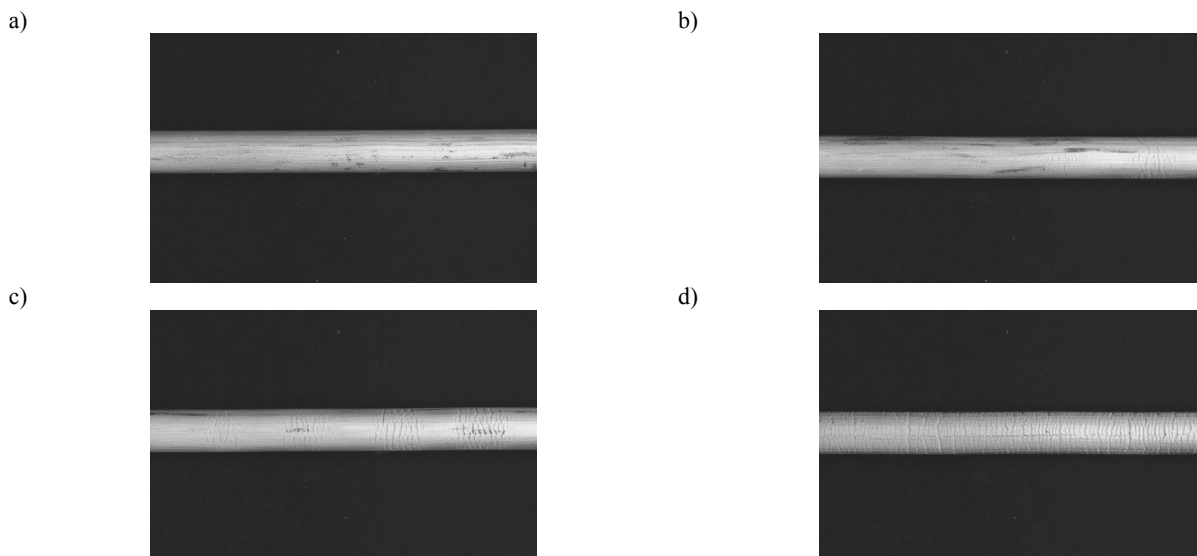


Fig. 45. View of the surface of wire extruded with the KOBO method at temperature of 400°C with processing ratio of $\lambda=44.4$: a) smooth surface; b) surface with first cracks; c) cracks alternately with good wire surface, d) cracks

assess quantitatively a service life of dies. Operational tests held in laboratory conditions enabled to compare the life of dies coated with the layers produced and classic dies subjected to a nitriding or quenching and tempering process only.

The extrusion process can be interrupted by even a small recess or damage of the deposited protection coating or nitride layer and produce a product of an unacceptable quality. Hence a surface condition of the extruded product and wear of the front surface and a device calibrating strip were used as evaluation criteria for a die's service life. Table 10 presents a die in the initial condition after 5 extrusion tests and after 10 tests completed (optionally after fewer tests due to die wear according to the service life evaluation criteria applied).

Table 11 shows the outcomes of operational tests expressed with the number of subsequent passes performed using dies differing in the type of a protection layer, during which the quality of the extruded product and tool was acceptable according to the criteria assumed.

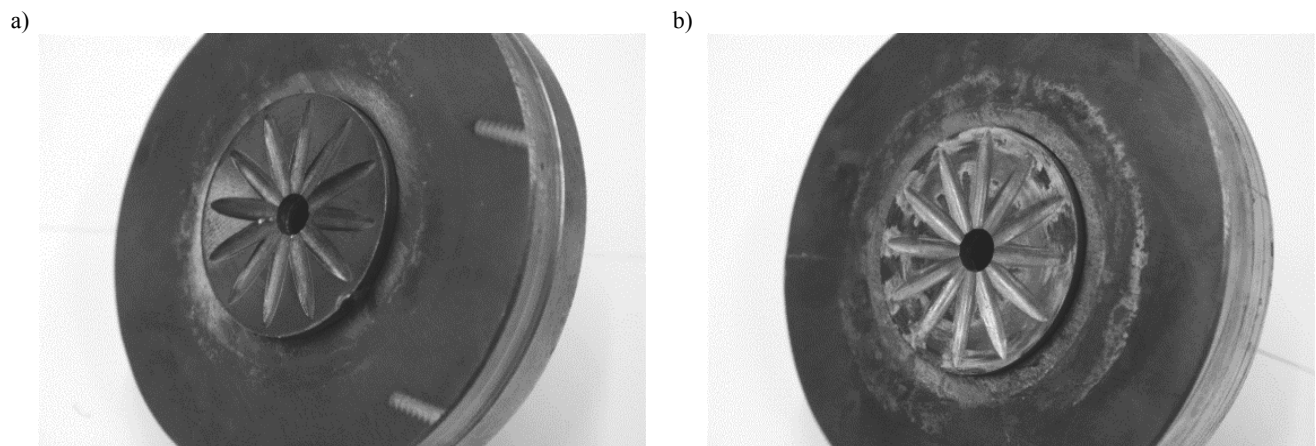


Fig. 46. View of surface of dies and discs after extrusion at temperature of 400°C with constant extrusion speed and die rotation frequency at variable extrusion speed (4th stage) with the following coating: a) CrN+DLC coating, b) nitrided coating

Table 10.

Wear analysis of surface of extrusion dies coated with coatings consisting of a nanocrystalline nitride layer PVD with an additional low-friction layer and subjected to a nitriding or quenching and tempering process (3rd stage)

Die surface appearance	Coating/treatment type					
	CrN+DLC	AlTiCrN+DLC	CrAlSiN+DLC	CrAlSiN+MoS ₂	Nitriding	Quenching and tempering
in initial condition						
after 5 tests						
po ostatniej próbie*						

*5 tests were made for a quenched and tempered die, 8 tests for a nitrided die, 9 tests for a die with CrAlSiN+MoS₂ coating

Table 11.

Lives of extrusion dies coated with coatings consisting of a nanocrystalline nitride layer / low-friction layer and subjected to a nitriding or quenching and tempering process (3rd stage)

Test No.	Coating/treatment type												
	CrN+DLC		AlTiCrN+DLC		CrAlSiN+DLC		CrAlSiN+MoS ₂		nitriding		quenching and tempering		
	die	product	die	product	die	product	die	product	die	product	die	product	
1	⊕	⊕	⊕	⊕	⊕	⊕	⊕	⊕	⊕	⊕	⊕	⊕	⊕
2	⊕	⊕	⊕	⊕	⊕	⊕	⊕	⊕	⊕	⊕	⊕	⊕	⊕
3	⊕	⊕	⊕	⊕	⊕	⊕	⊕	⊕	⊕	⊕	⊕	⊕	⊕
4	⊕	⊕	⊕	⊕	⊕	⊕	⊕	⊕	⊕	⊗	⊕	⊗	⊗
5	⊕	⊕	⊕	⊕	⊕	⊕	⊕	⊕	⊕	⊗	⊗	⊗	⊗
6	⊕	⊕	⊕	⊕	⊕	⊕	⊗	⊕	⊗	⊗	⊗	∅	∅
7	⊕	⊕	⊕	⊕	⊕	⊕	⊗	⊗	⊗	⊗	⊗	∅	∅
8	⊗	⊗	⊕	⊕	⊕	⊕	⊗	⊗	⊗	⊗	⊗	∅	∅
9	⊗	⊗	⊗	⊕	⊗	⊕	⊗	⊗	∅	∅	∅	∅	∅
10	⊗	⊗	⊗	⊗	⊗	⊕	∅	∅	∅	∅	∅	∅	∅

⊕ - acceptable quality according to the criteria adopted
 ⊗ - unacceptable quality according to the criteria adopted
 ∅ - no tests

The surface of dies, in grooves and at peripheries, is gradually wearing in subsequent tests for classical quenched and tempered and nitrided dies during an extrusion process. Over the subsequent passes, the final force of extrusion is dropping, wire quality deteriorating, cracks are visible at the side product surface, especially in the final section of the wire (Fig. 47a). Quenched and tempered and nitrided dies are wearing very quickly (4th pass). This substantially influences a final product's quality.

The dies with CrN+DLC and CrAlSiN+MoS₂ coatings deposited onto their surface exhibit a twice higher service life. Extrusion force decreases over the subsequent passes, and the gradual wear of coatings becomes visible, especially at the peripheries, front surface and dies' grooves. Numerous grooves and scratches (Fig. 47b,c) are visible on the surface of the extruded material manifesting that the calibrating band is not smooth (7th pass).

A 3-fold increase in service life as compared to dies used normally in extrusion processes, i.e. quenched and tempered and nitrided, was found for dies with CrAlSiN+DLC and AlTiCrN+DLC coatings produced on their surface. A surface quality of the extruded alloy is very good (Fig. 47d). Fine scratches (Fig. 47c) on a product surface appear only during the 10th pass as the surface of dies is wearing and as an alloy sticks to a calibrating band.

A distinctive moiré effect originating from reverse die rotation, representing the essence of the KOBO extrusion method,

is visible on a smooth surface of wire with very good quality (Fig. 47d). The lower wire with more rotation traces illustrates a process stage carried out at small extrusion speed, thus a large number of rotations per volume unit (beginning of rotation), where the expected punch transfer speed has not yet been reached. The upper wire illustrates a stage performed with the expected extrusion force.

The observations made have indicated that abrasive wear and abrasive-adhesion wear are the main destruction forms of the analysed dies. The results of microscopic observations are shown in Fig. 48. A die wear degree and intensity analysis provides that the application of the proposed two-layer coatings on an extrusion tool's surface will considerably improve friction effects and extend a service life of dies as compared to quenched and tempered and nitrided dies.

An analysis performed confirms the importance of synergic interaction of individual elements of the coatings produced comprised of a hard nanocrystalline layer produced with a PVD method and a low-friction DLC layer (MoS₂ layer to a smaller extent) in forming the service life of extrusion dies. At the same time, considering the fact that comparable properties were maintained for dies with coatings produced on their surface containing an external low-friction DLC layer, then the factor having a biggest effect on ensuring coatings durability are the properties of PVD nanocrystalline layers.

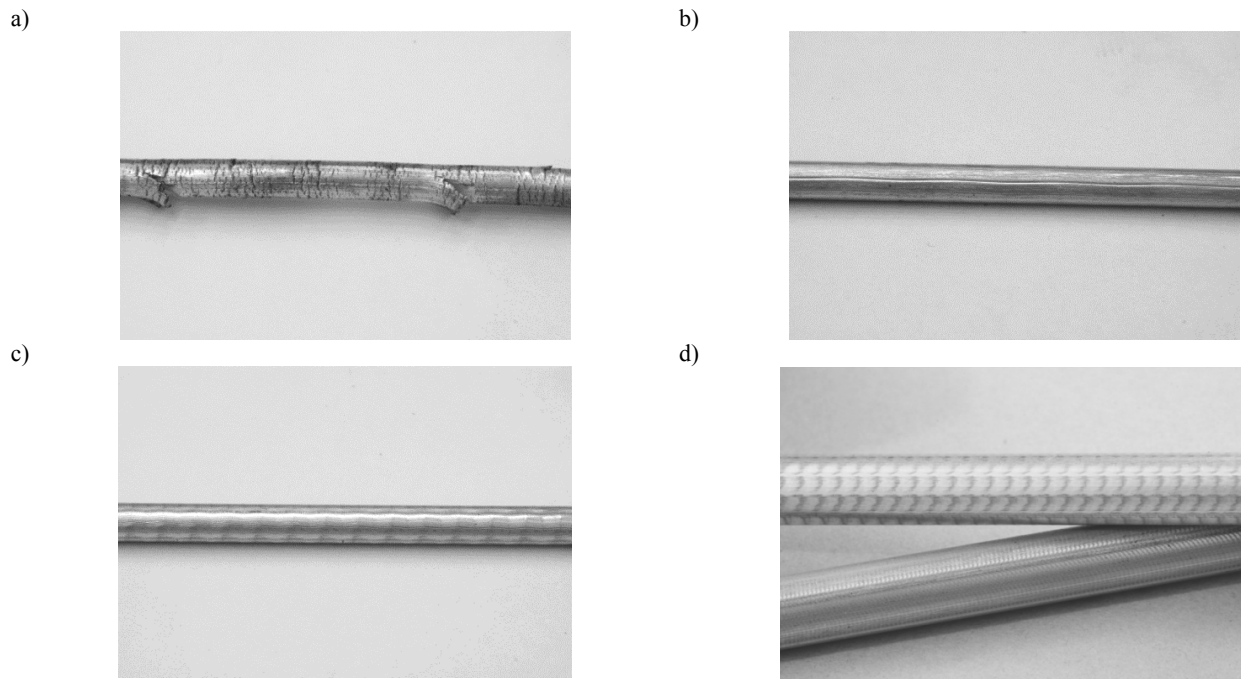


Fig. 47. View of the surface of wire cold-extruded with the KOBO method with processing ratio of $\lambda=100$: a) numerous fine and coarse cracks, b) thick scratch, c) surface with plates scratched along the extrusion direction, d) smooth surface with no scratches with a distinctive moiré effect originating from die rotation

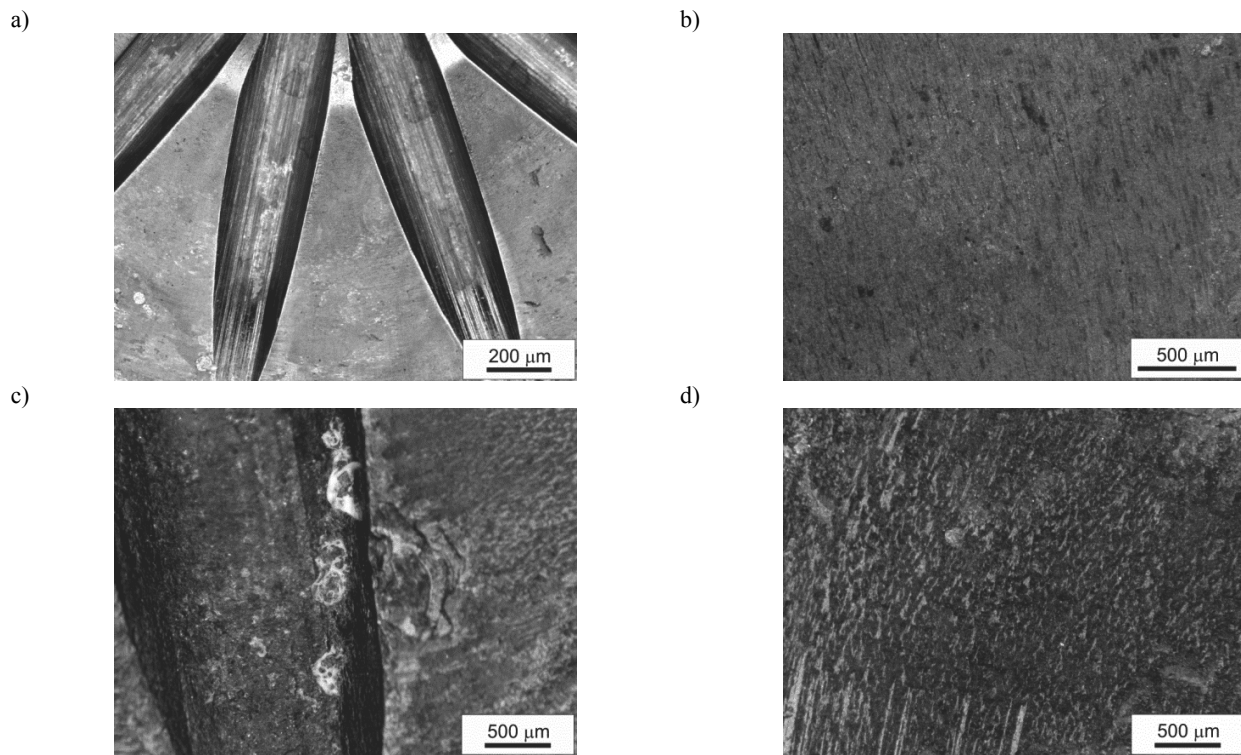


Fig. 48. Results of observations of microscope traces of extrusion dies' wear: a, b) with a CrAlSiN+DLC coating deposited onto their surface, c, d) nitrided dies

5.3. Results of modelling the relationships between the extrusion process conditions and product properties using artificial intelligence tools

Artificial neural networks for more than ten years have been a popular modelling method utilised in multiple, differing areas such as medicine, finance or engineering applications. Numerous examples of this method's applications can be found in material engineering [149-161]. One of the basic advantages of artificial neural networks is a possibility of creating relations between variables without having to describe the analysed problem mathematically. In order to prepare neural networks to perform a particular task, an algorithm does not have to be established and recorded as a programme. This process is replaced by training using a string of typical excitations and the corresponding, desired reactions. An important characteristic of a network is a generalisation ability, i.e. an ability to generalise the knowledge acquired in training for the data that has not been presented in training. A set of examples representative for the examined phenomenon has to be prepared for an artificial neural network trained by means of examples. It is difficult to meet this condition in material engineering as it very often entails time- and cost-intensive experimental investigation.

Artificial neural networks for modelling the relationships between the conditions of 99.5% commercially pure aluminium extrusion process with the KOBO method and the finished product's properties: yield point $R_{0.2}$, tensile strength R_m and strain A . Artificial neural networks were prepared with Statistica Neural Networks 4.0F software.

A neural model design process can be divided into the four repeating stages: preparing a data set for training and network performance evaluation, identification of parameters characterising the network, network training and an assessment of network performance. The essential parameters defined when designing artificial neural networks:

- neural network type and structure;
- error function;
- activation function;
- Post Synaptic Potential function (PSP);
- training method and parameters;
- variables scaling method.

The data set was randomly grouped into two subsets: a training and validation subset. Examples from the training set were used for calculating the values of networks weights, while the data from the validation set was used for assessing network quality in training.

The quality of the developed neural networks was assessed according to the following statistics:

- an average absolute error of a network forecast calculated according to the dependence:

$$E_j = \frac{1}{n} \sum_{i=1}^n (|X_{zi} - X_{oi}|)$$

where:

E_j - error for j -this property,

n - data number in set,

X_{zi} - i -this value of the measured property,

X_{oi} - i -this calculated value.

- a standard deviation quotient for prediction errors and a dependent variable standard deviation,
- Pearson's correlation coefficient.

The correctness of a neural model can only be considered in the case where network forecasts involve a smaller error than a simple estimation of an output value, expressed, for example, by an average value of this variable. An average network response error in such case equals a standard deviation of the variable output value, while a quotient of standard deviations takes on the value 1. A quotient of standard deviations for an error-free prediction takes on the value 0.

A unidirectional MLP (Multi-layer Perceptron) network was selected as an optimum one based on preliminary simulation investigations.

Independent variables in form of the basic process conditions were used for developing a neural network: frequency of reverse die rotation, punch speed and extruded material temperature. The effect of dependent conditions was additionally considered, in particular those dependent on the process initial conditions measured during extrusion: extrusion force and torque moment.

The artificial neural network developed in the work can be assigned to three groups according to independent variables and dependent variables used in the model and according to their intended function:

- *independent variables*: extruded material temperature, frequency of reverse die rotation, punch speed → *dependent variables*: extrusion force, torque moment; *purpose*: simulation of effect of extrusion conditions on the extrusion force and torque moment value, calculation of force and moment as input data for networks calculating product properties;
- *independent variables*: extruded material temperature, frequency of reverse die rotation, punch speed, extrusion force, torque moment → *dependent variables*: yield point $R_{0.2}$, tensile strength R_m and strain A ; *purpose*: calculation of product properties, simulation of process conditions' influence on product properties;
- *independent variables*: extruded material temperature, frequency of reverse die rotation, punch speed → *dependent variables*: yield point $R_{0.2}$, tensile strength R_m and strain A ; *purpose*: simulation of temperature effect, frequency of reverse die rotation and punch speed on product properties.

The response was in each case coded as a single neuron. A neuron activation level in the initial layer was determining a value of one of the dependent variables: yield point, tensile strength, strain, torque moment or extrusion force. The analysis was made at the beginning, in the middle and at the end of the product extruded. The artificial networks were trained with the backward error propagation and the conjugate gradient methods. A training error chart for a training and validation set was observed during training. Training was completed at the time when a validation set error started to grow with an error value for the training set falling. 24 models utilising artificial neural networks with three or five neurons in the input layer and one neuron in the output layer were totally established. A neural network overview is presented in Fig. 49.

Table 12.

Overview of artificial neural networks designed for calculation of yield point $R_{0,2}$, tensile strength R_m and strain A at the end of the aluminium product extruded with the KOBO method

Neural network characteristics		Network designation		
		$R_{0,2}$	R_m	A
Network type/neurons in: input - hidden - output layer		MLP/5-4-1	MLP/5-3-1	MLP/5-4-1
Training method/ training epochs		BP/50 CG/59	BP/50 CG/154	BP/50 CG21
Mean absolute error	training set	5.4 MPa	3.0 MPa	3.0 %
	validation set	5.4 MPa	2.3 MPa	3.0 %
Standard deviations	training set	0.31	0.30	0.36
	validation set	0.35	0.32	0.34
Correlation coefficient	training set	0.95	0.95	0.93
	validation set	0.94	0.95	0.94

error function: sum of squares
activation function in input/ hidden / output layer: linear/ logistic / linear with saturation
Linear Post Synaptic Potential Function(PSP)
BP - Backward Error Propagation method; CG - Conjugate Gradient Method

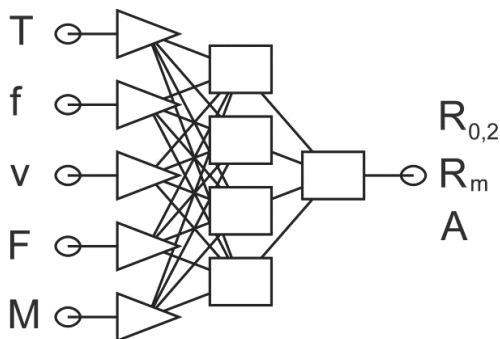


Fig. 49. Artificial neural network scheme (T - extruded material temperature, f - frequency of reverse die rotation, v - punch speed, F - extrusion force, M - torque moment, $R_{0,2}$ - yield point, R_m - tensile strength, A - strain)

Table 12 lists basic information characterising artificial neural networks with the values of the indicators used for network quality evaluation. An example was presented in form of three networks designed for calculating yield point $R_{0,2}$, tensile strength R_m and strain A based on the extruded material temperature, change frequency of reverse dies rotation, punch speed, extrusion force and torque moment.

It should also be noted that generalisation ability, i.e. an ability to generalise knowledge acquired in a training process, is confirmed by similar values of quality evaluation indicators, respectively for: a training and validation set.

Fig. 50-60 present a simulated effect of extrusion conditions with the KOBO method on a product's selected mechanical properties and torque moment and extrusion force for the set values of the other process conditions. The model established can be used for calculating the properties of aluminium and its alloy produced when extruding with the KOBO method for the frequencies of reverse die rotation of 3-8 Hz, punch speed of 0.09-0.5 mm/s and the extruded material temperature of 24-400°C.

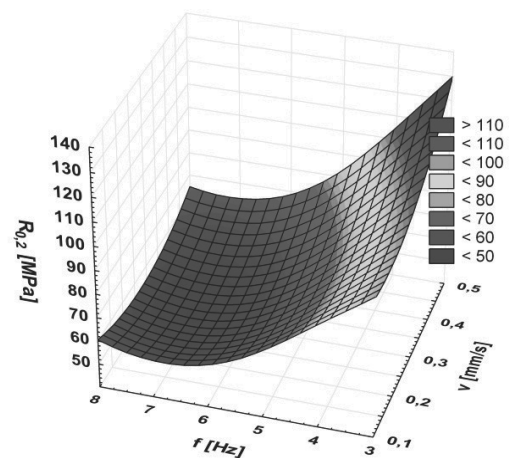


Fig. 50. Simulation of effect of reverse die rotation frequency and punch speed on yield point $R_{0,2}$ at the product end during extrusion with the KOBO method at 24°C

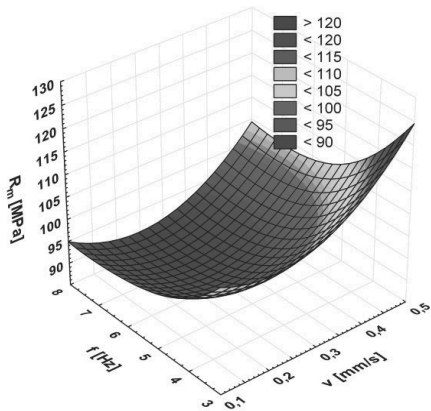


Fig. 51. Simulation of effect of reverse die rotation frequency and punch speed on tensile strength R_m at the product end during extrusion with the KOBO method at 24°C

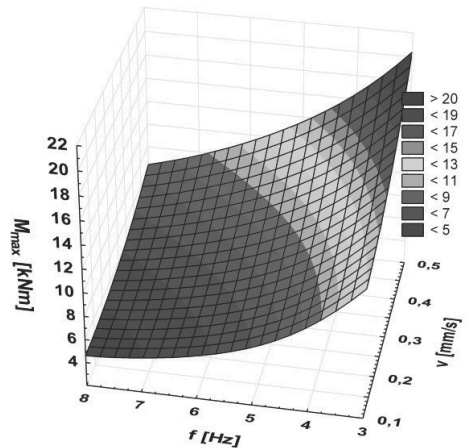


Fig. 54. Simulation of effect of reverse die rotation frequency and punch speed on torque moment M_{max} at the product end during extrusion with the KOBO method at 24°C

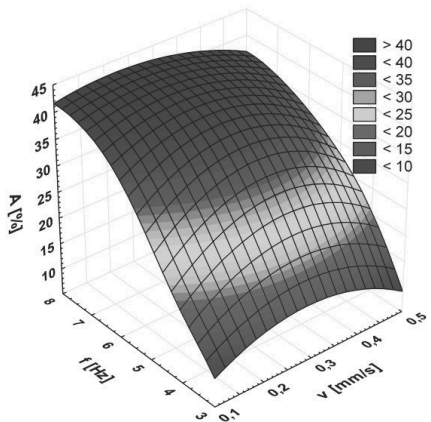


Fig. 52. Simulation of effect of reverse die rotation frequency and punch speed on strain A at the product end during extrusion with the KOBO method at 24°C

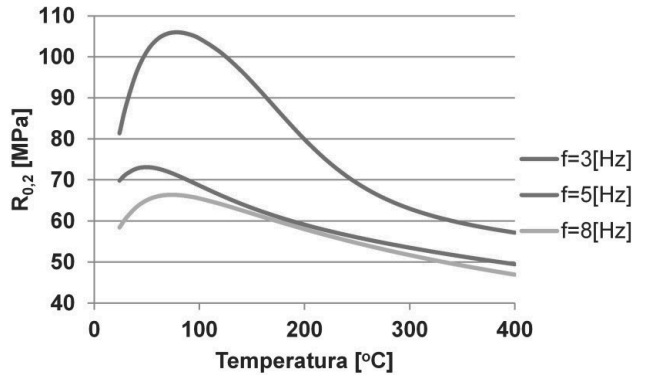


Fig. 55. Simulation of effect of reverse die rotation temperature and frequency for punch speed of $v=0.09$ mm/s on yield point $R_{0.2}$ (the product end, KOBO method extrusion)

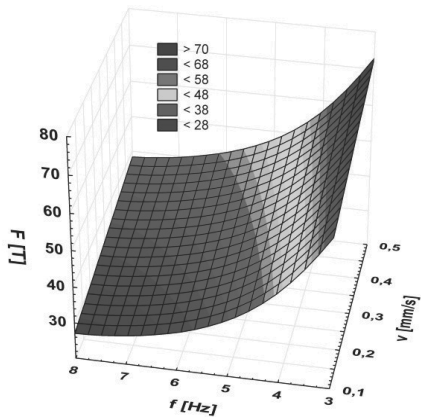


Fig. 53. Simulation of effect of reverse die rotation frequency and punch speed on extrusion force F at the product end during extrusion with the KOBO method at 24°C

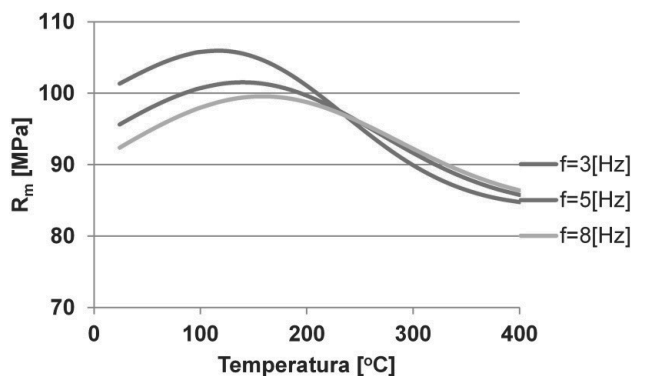


Fig. 56. Simulation of effect of reverse die rotation temperature and frequency for punch speed of $v=0.09$ mm/s on tensile strength R_m (the product end, KOBO method extrusion)

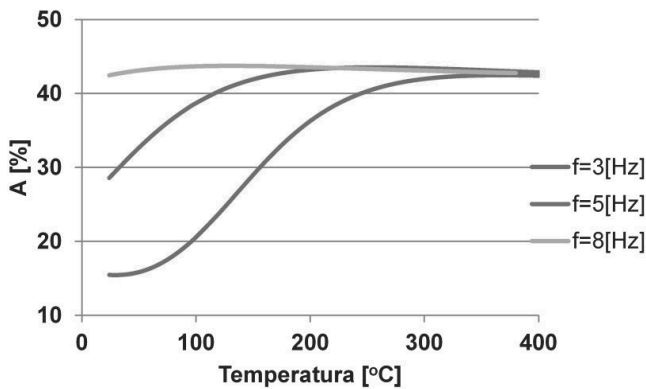


Fig. 57. Simulation of effect of reverse die rotation temperature and frequency for punch speed of $v=0.09$ mm/s on strain A (the product end, KOBO method extrusion)

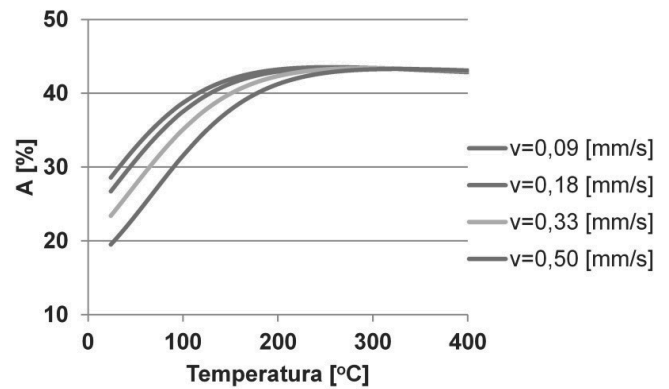


Fig. 60. Simulation of effect of temperature and punch speed for reverse die rotation frequency of $f=5$ Hz on strain A (the product end, KOBO method extrusion)

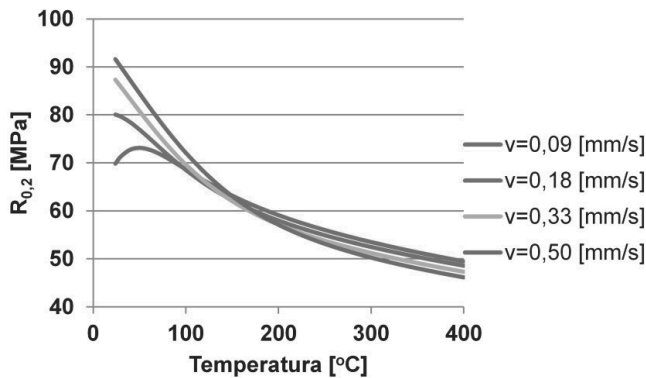


Fig. 58. Simulation of effect of temperature and punch speed on reverse die rotation frequency of $f=5$ Hz on yield point $R_{0.2}$ (the product end, KOBO method extrusion)

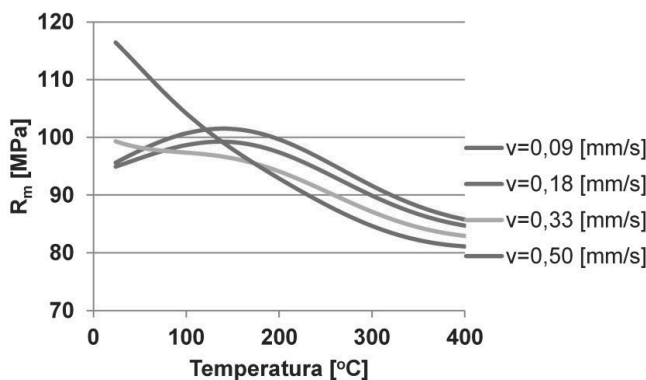


Fig. 59. Simulation of effect of temperature and punch speed for reverse die rotation frequency of $f=5$ Hz on tensile strength R_m (the product end, KOBO method extrusion)

5.4. Structure, chemical and phase composition of coatings

The fractographic tests made with the electron scanning microscope (Figs. 61, 63, 65, 67) allow to assert that the tested coatings, depending on the applied system of layers, indicate a monolayer structure consisting of a hard nitride layer and a double-layer structure consisting of a hard nitride layer and a low-friction layer. It was also found that a chromium-based transient layer exists well bound with a substrate that was fabricated to improve the coatings' adhesion to a hot-work tool steel substrate.

The individual layers are deposited uniformly and tightly adhere to each other and to the substrate material. A morphology of the surface of fractures in the tested coatings is characterised by a compact structure. A column structure exists only for an AlTiCrN layer (Fig. 63). Fractographic tests of the fractures of the tested steel specimens with coatings deposited onto their surface indicate a sharp transition zone between the substrate and the layer, as well as between the layers forming a coating.

The tests of the layers' chemical composition performed using the EDS system (Figs. 62, 64, 66) confirm the existence of the relevant elements in the analysed layers. In the case of an MoS_2 layer, due to its small thickness and the nature of the incident beam, the method applied rendered it impossible to make an accurate quality analysis of chemical composition (Fig. 68).

The observations of the analysed coatings' surface topography using the scanning electron microscopy (SEM) and atomic force microscopy (AFM) methods revealed a varied surface topography of nitride and low-friction layers produced on the surface of hot-work tool steel. Two types of morphology can be differentiated according to the type of layers. The first one occurs in the case of nitride layers produced with Physical Vapour Deposition with the arc method and is characterised by the existence of single droplet-shaped microparticles (Fig. 69). The other one, though, exists for a low-friction DLC layer produced with Plasma-Assisted Chemical Vapour Deposition and is characterised by a high inhomogeneity relating to multiple droplet-shaped or nearly ball-shaped particles existing on the surface (Fig. 70).

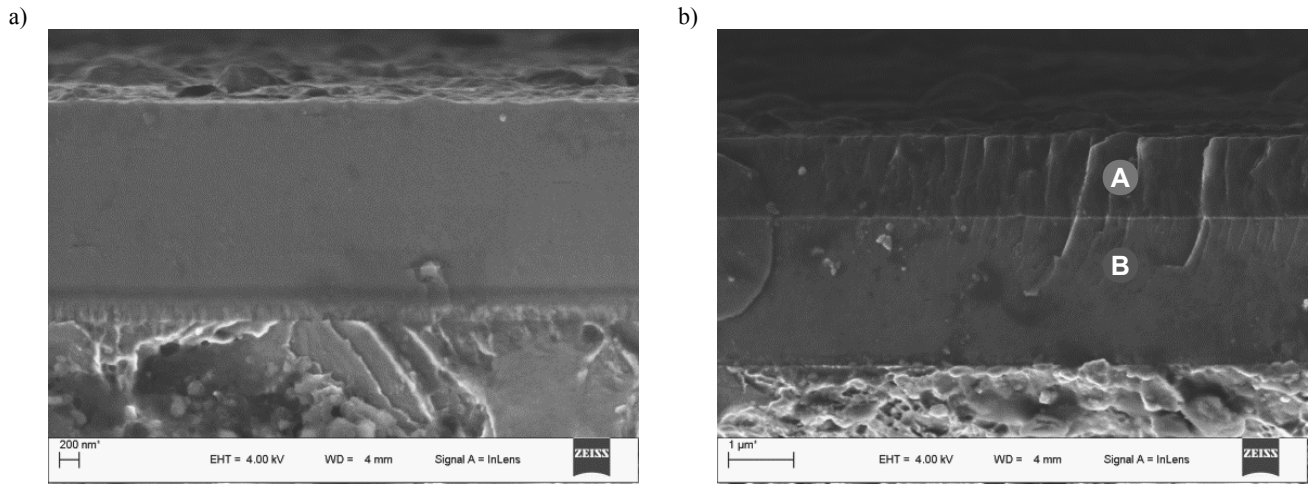


Fig. 61. Coating fracture surface: a) CrAlSiN, b) CrAlSiN+DLC produced on hot-work tool steel X40CrMoV5-1 surface

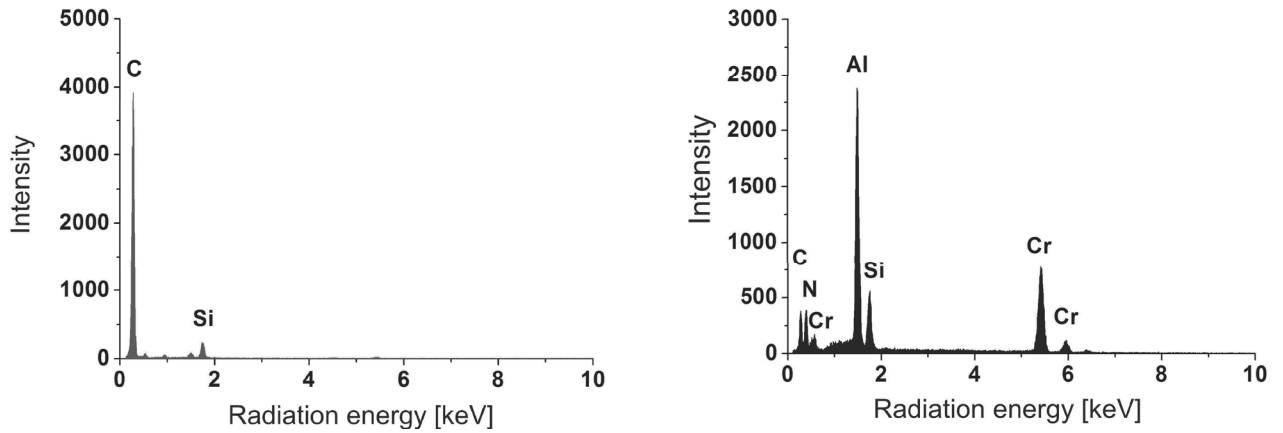


Fig. 62. Diagram of energy of backscatter X-ray radiation from, respectively, the A and B microarea, according to Fig. 61b

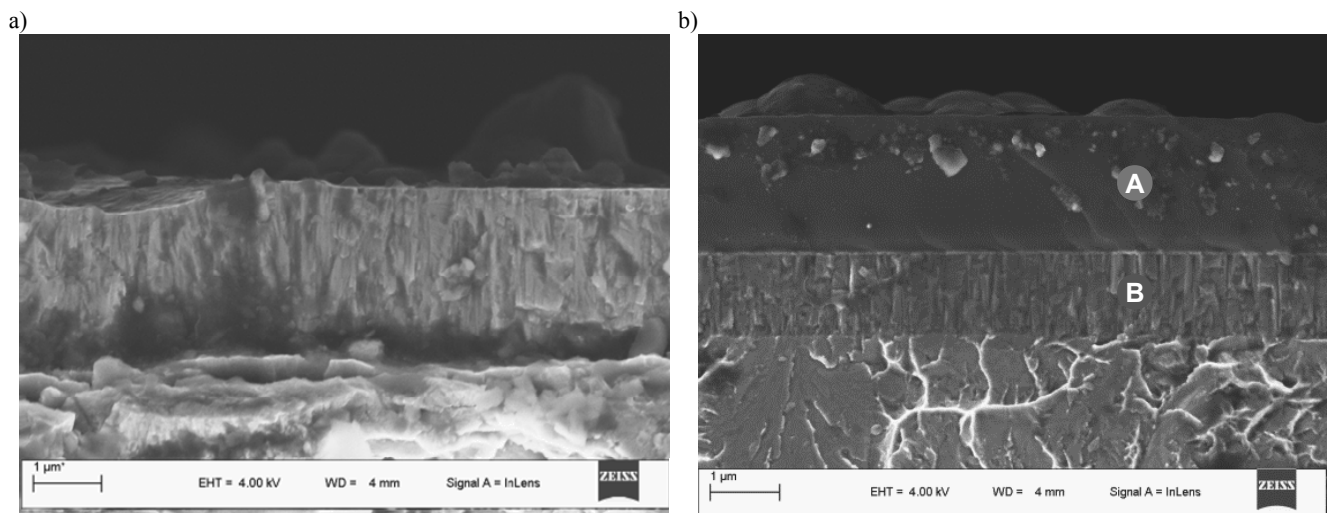


Fig. 63. Coating fracture surface: a) AlTiCrN, b) AlTiCrN+DLC produced on hot-work X40CrMoV5-1 tool steel surface

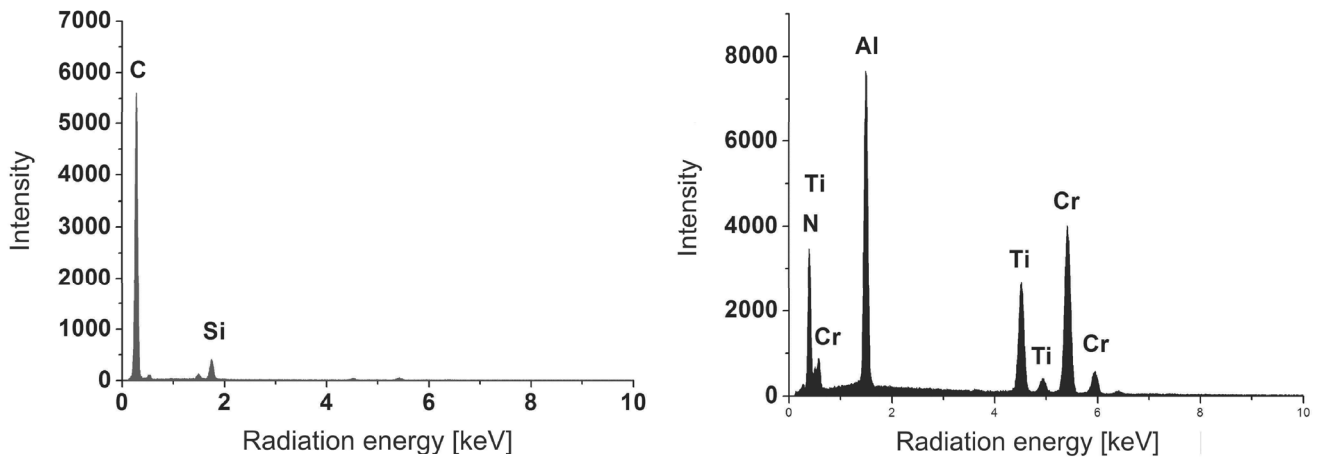


Fig. 64. Diagram of energy of backscatter X-ray radiation from, respectively, the A and B microarea, according to Fig. 63b

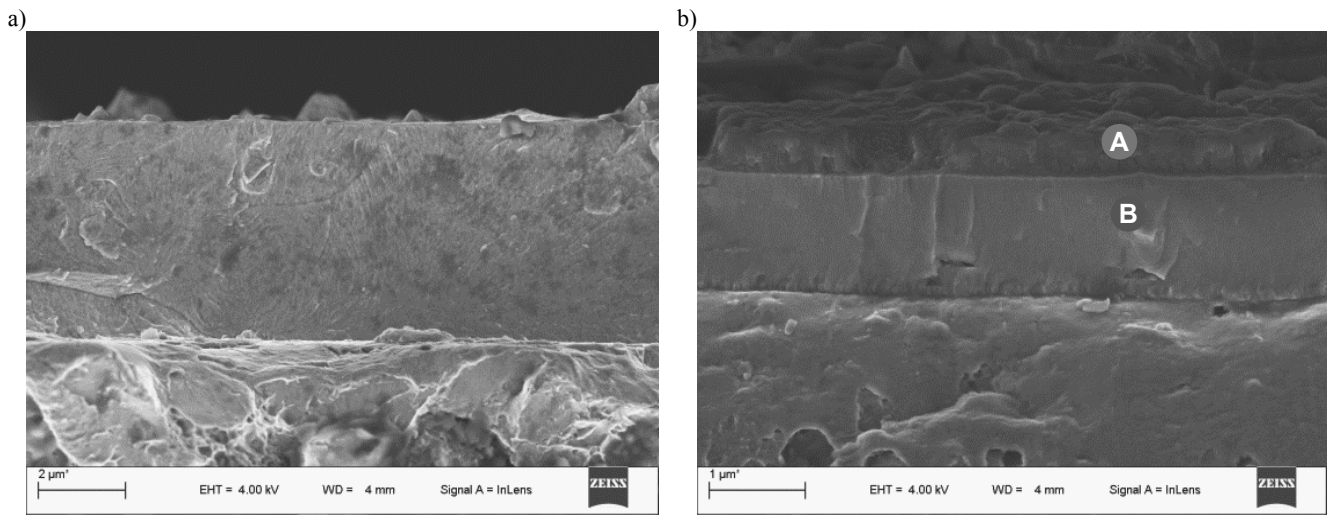


Fig. 65. Coating fracture surface: a) CrN, b) CrN+DLC produced on hot-work X40CrMoV5-1 tool steel surface

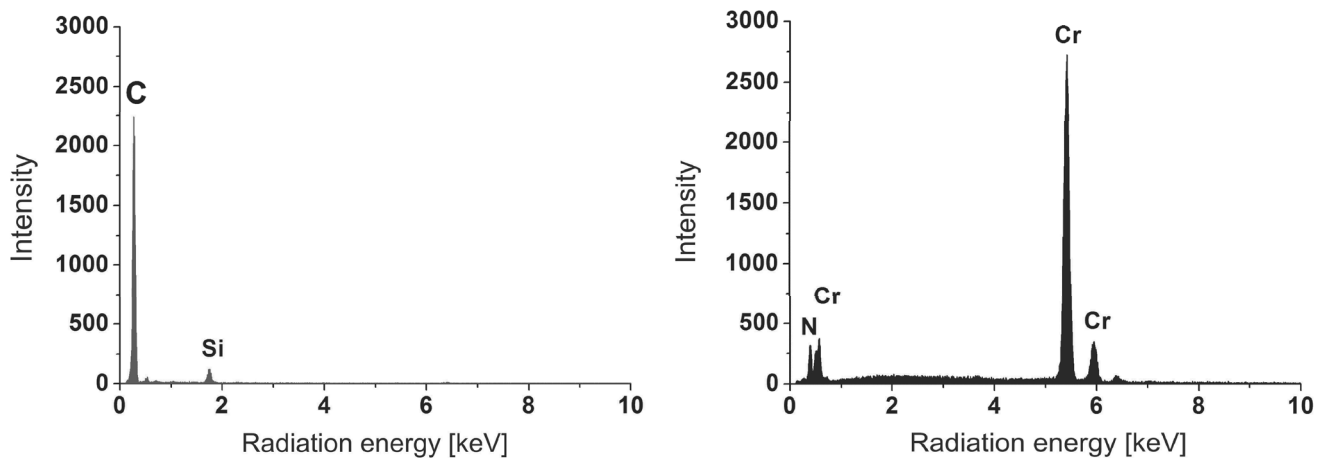


Fig. 66. Diagram of energy of backscatter X-ray radiation from, respectively, the A and B microarea, according to Fig. 65b

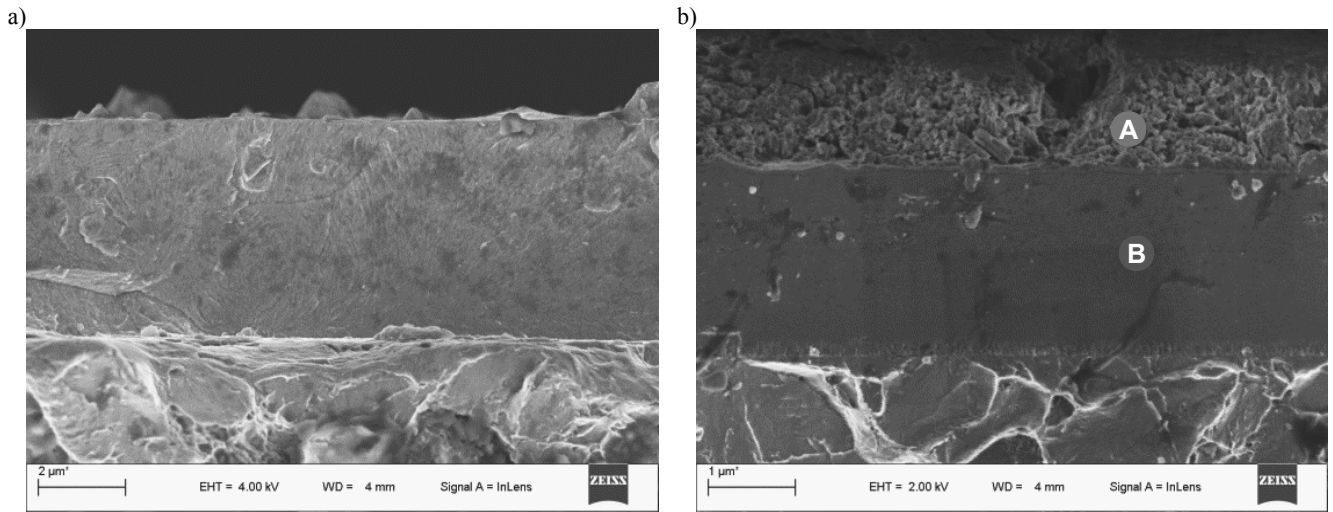


Fig. 67. Coating fracture surface: a) CrAlSiN, b) CrAlSiNN+MoS₂ produced on hot-work X40CrMoV5-1 tool steel surface

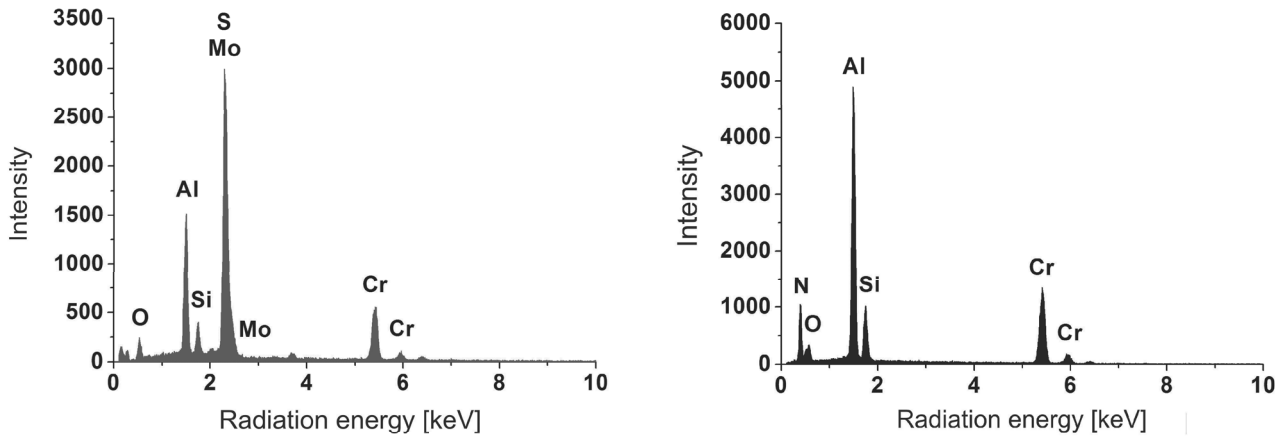


Fig. 68. Diagram of energy of backscatter X-ray radiation from, respectively, the A and B microarea, according to Fig. 67b

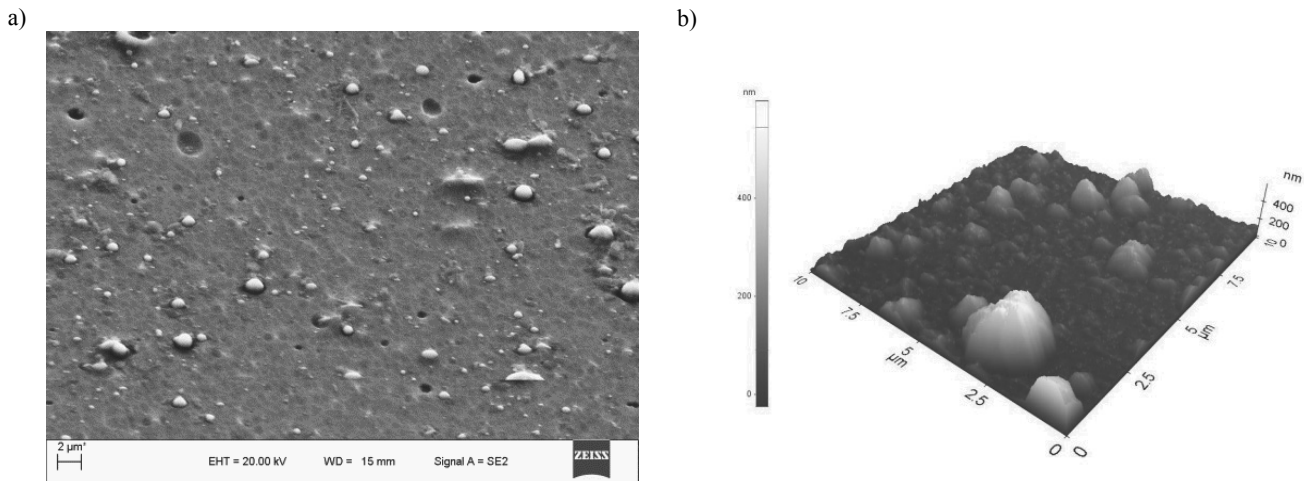


Fig. 69. CrAlSiN coating fracture surface: a) SEM, b) AFM

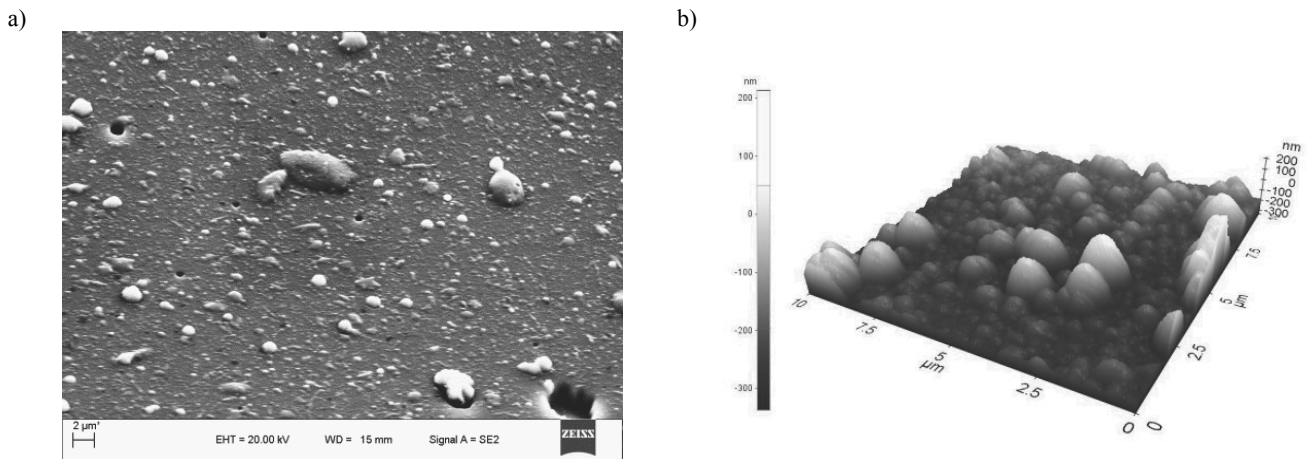


Fig. 70. CrAlSiN+DLC coating fracture surface: a) SEM, b) AFM

An additional surface development analysis performed determining a ratio of the actual area measured for a given specimen according to its orthogonal projection on the XY plane revealed large development for hard nitride layers. Surface development increases by about 5-10 % according to the coating type as a consequence of depositing a low-friction layer onto the surface of nitride layers. The measurements taken also allowed to determine the layers' surface roughness (by R_a).

Tests were carried out, using the high-resolution transmission electron microscope, in order to determine the structure and size of crystallites in the layers produced and to examine the character of transition zones between the substrate and the coating, as well as between the individual layers in the coatings. The size and shape of grains in the deposited layers was determined using the dark field technique and based on electron diffractions obtained signifying an amorphous or nanocrystalline structure of the analysed layers.

The results of the tests obtained using the transmission electron microscopy confirmed the amorphous character of a low-friction DLC layer. The electron diffraction patterns obtained have shown the considerable broadening of diffraction rings (Fig. 71). Fig. 72 presents a TEM image of DLC layers made on different intermediate layers for very high magnifications made without a lens diaphragm. The images do not show the presence of long-range order (typical for an amorphous structure).

It was found by examining thin lamellas from the cross section of nitride layers (CrAlSiN, AlTiCrN and CrN) produced with the PVD technique that the layers feature a compact structure with high homogeneity and a grain size between 5 to 10 nm (Fig. 73) depending on the layer type. It can be concluded already based on TEM images in the light field that the layers have a nanocrystalline structure. Dark areas appearing on the light field image (Fig. 73) are crystallites that are oriented close to the axis of bands relative to an electron beam. Observations in the dark field and the diffraction images made for increasingly smaller areas confirm a nanocrystalline structure of the examined nitride layers.

In addition, small crystalline CrN (CrAlSiN) grains sized several nanometres deposited in an amorphous Si_3N_4 matrix were observed in the tests of the CrAlSiN nitride later structure by

means of high-resolution transmission electron microscopy, which may signify a layer's nanocomposite structure (Fig. 74).

The essence of high adhesion of the layers formed to the substrate material and between individual layers in coatings and the possibility of their synergic interaction is the existence of transition zones for each of the coatings. Shown with the example of a CrAlSiN+DLC layer (Fig. 75) is the character of a joint between an external low-friction DLC layer and a hard nanocrystalline nitride CrAlSiN layer as well as between the core of the coated tool and a CrAlSiN layer.

7 separate subzones providing different contrast on TEM images in the light field can be differentiated for a transition zone between a low-friction DLC layer and a hard CrAlSiN layer:

- proper low-friction DLC layer (designated as DLC1);
- DLC layer with growing Si intensity and decreasing C intensity (designated as DLC2);
- DLC layer with constant Si and C intensity (designated as DLC3);
- CrN layer;
- Cr layer;
- Ti layer;
- proper CrAlSiN layer.

A linear analysis (Fig. 76) was performed with a scattered X-ray radiation energy (EDS) spectrometer and a surface analysis of elements distribution (Fig. 77) using Energy-filtering transmission electron microscopy (EFTEM) was carried out to confirm the existence of a change in chemical composition of individual sublayers between a low-friction DLC layer and a CrAlSiN layer. The character of changes in the intensity of the elements shows that the sublayers mentioned exist.

The DLC layer, starting with about 300 nm, shows an increased concentration of Si (Figs. 76 and 77), and two sublayers are visible - DLC2 and DLC3 (Fig. 78). Growth in an Si concentration and fall in a C concentration occurs in the first layer, while it maintains on a constant level in the other one. They are both amorphous and undifferentiable on a diffraction image. Information about the mass and atomic concentration of individual elements in the microareas of the sublayers DLC1 and DLC3 (Fig. 78, Table 13) was acquired as a result of an X-ray quantitative EDS microanalysis. The individual CrN and Cr and

Ti sublayers (Fig. 79) were produced to improve the adhesion of a low-friction DLC layer to the hard surface of the nitride layer.

4 subzones can be differentiated for a transition zone between a hard CrAlSiN layer and a substrate material:

- proper CrAlSiN layer;
- CrAlSiN layer with much lower Cr concentration;
- CrN layer;
- substrate material.

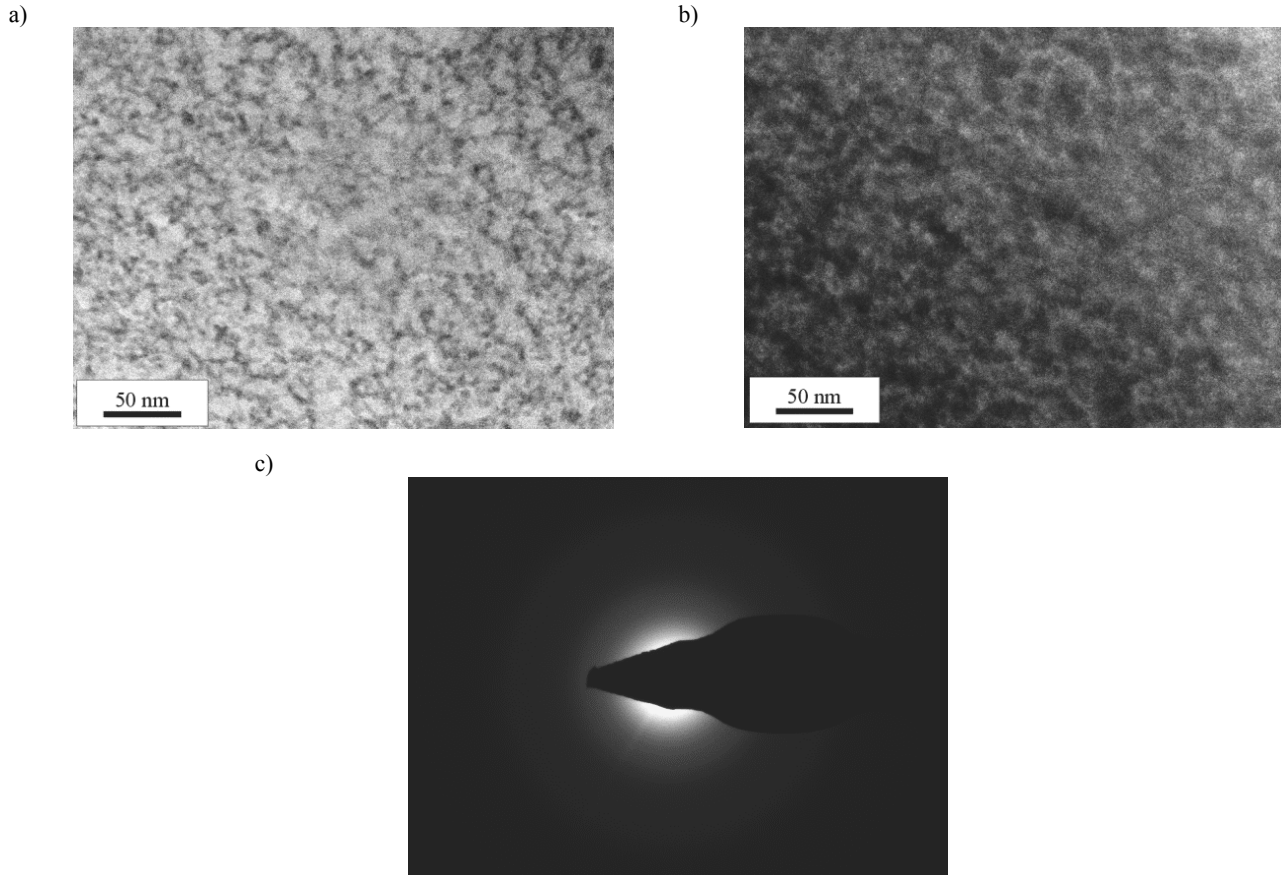


Fig. 71. Structure of DLC layer forming part of AlTiCrN+DLC coating produced on hot-work X40CrMoV5-1 tool steel substrate: a) image in the light field, b) image in the dark field, c) diffraction pattern with the area as in Fig. a) and b)

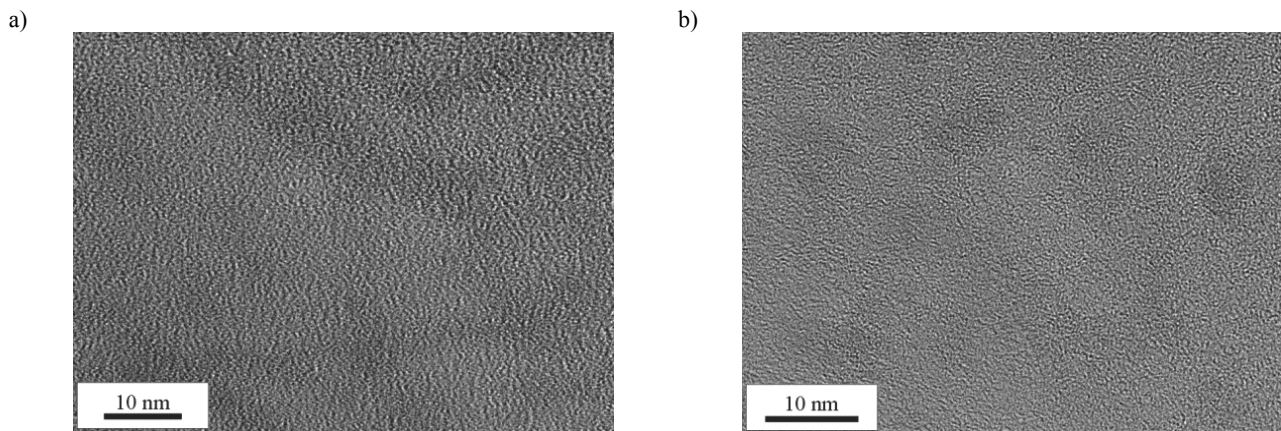


Fig. 72. TEM image for very high magnifications made without diaphragm of DLC low-friction layer produced on hard surface of the layer: a) CrAlSiN, b) CrN

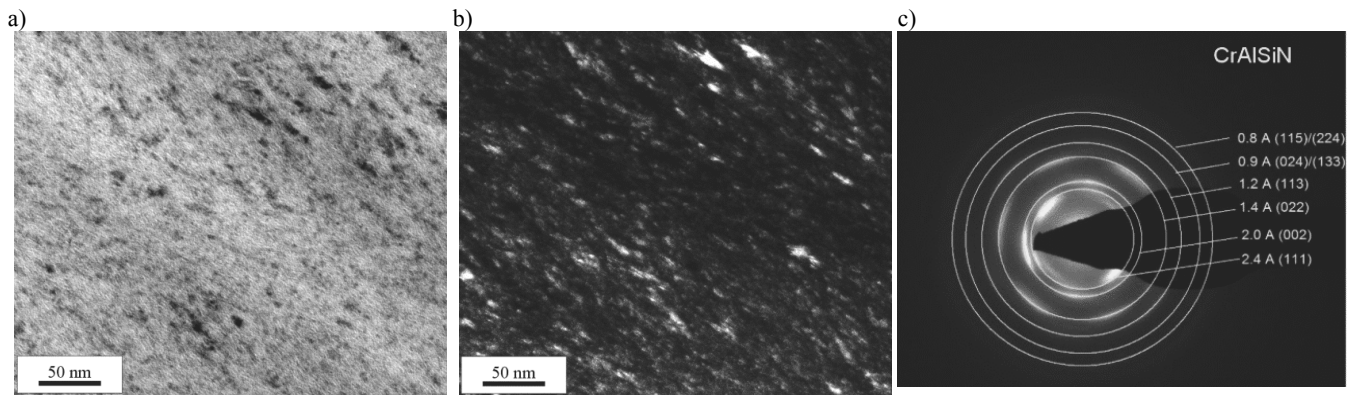


Fig. 73. Structure of CrAlSiN layer produced on hot-work X40CrMoV5-1 tool steel substrate: a) image in the light field, b) image in the dark field, c) diffraction pattern with the area as in Fig. a) and b) with a solution

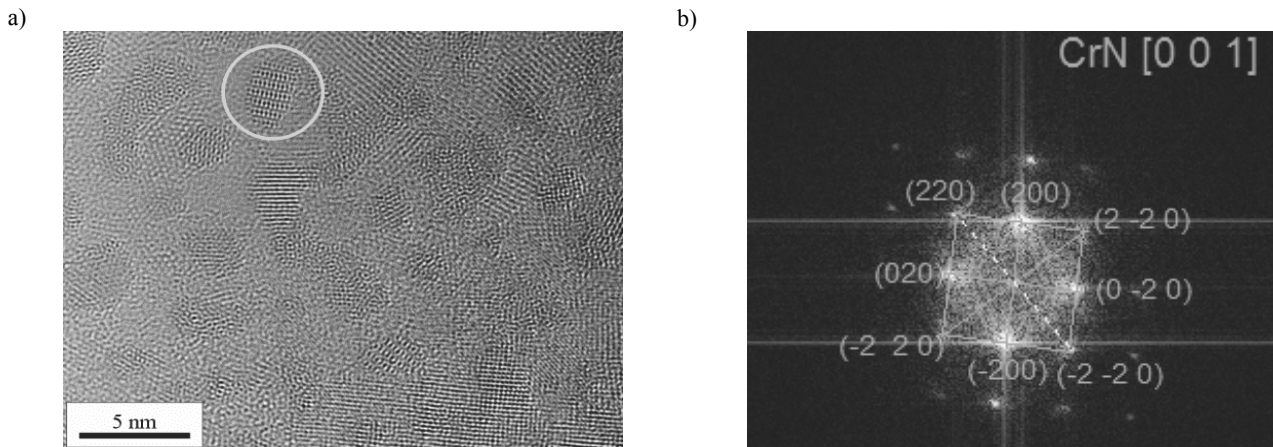


Fig. 74. High-resolution (HRTEM) image of the CrAlSiN layer formed on a hot-work X40CrMoV5-1 tool steel substrate (a) together with the indexed Fourier transform of the marked area (b)

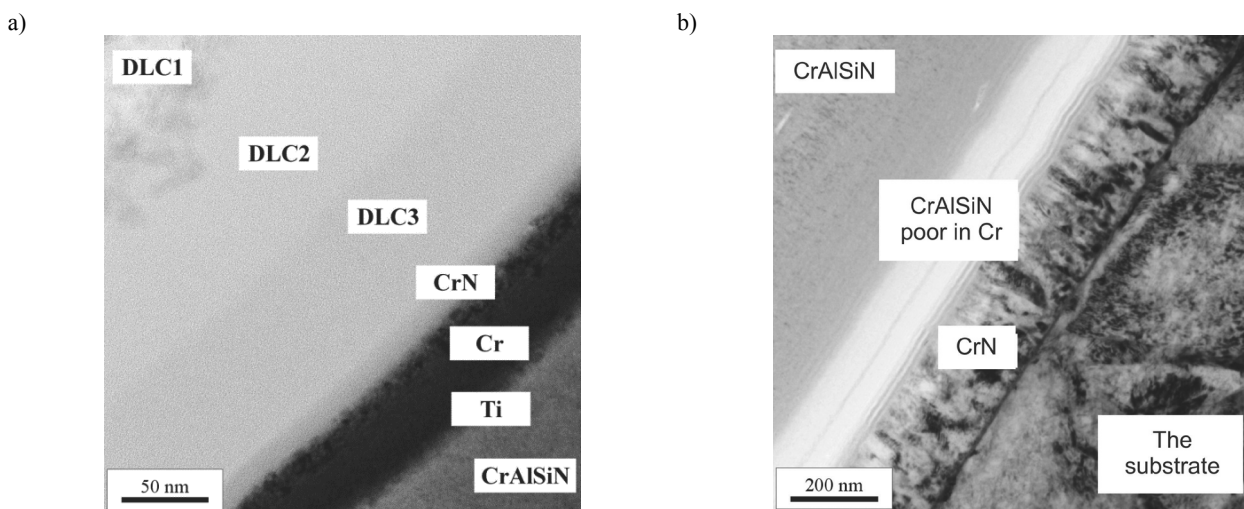


Fig. 75. Structure of transition zones between: a) DLC and CrAlSiN layer, b) CrAlSiN layer and substrate material existing in CrAlSiN+DLC layer formed on a hot-work X40CrMoV5-1 tool steel substrate

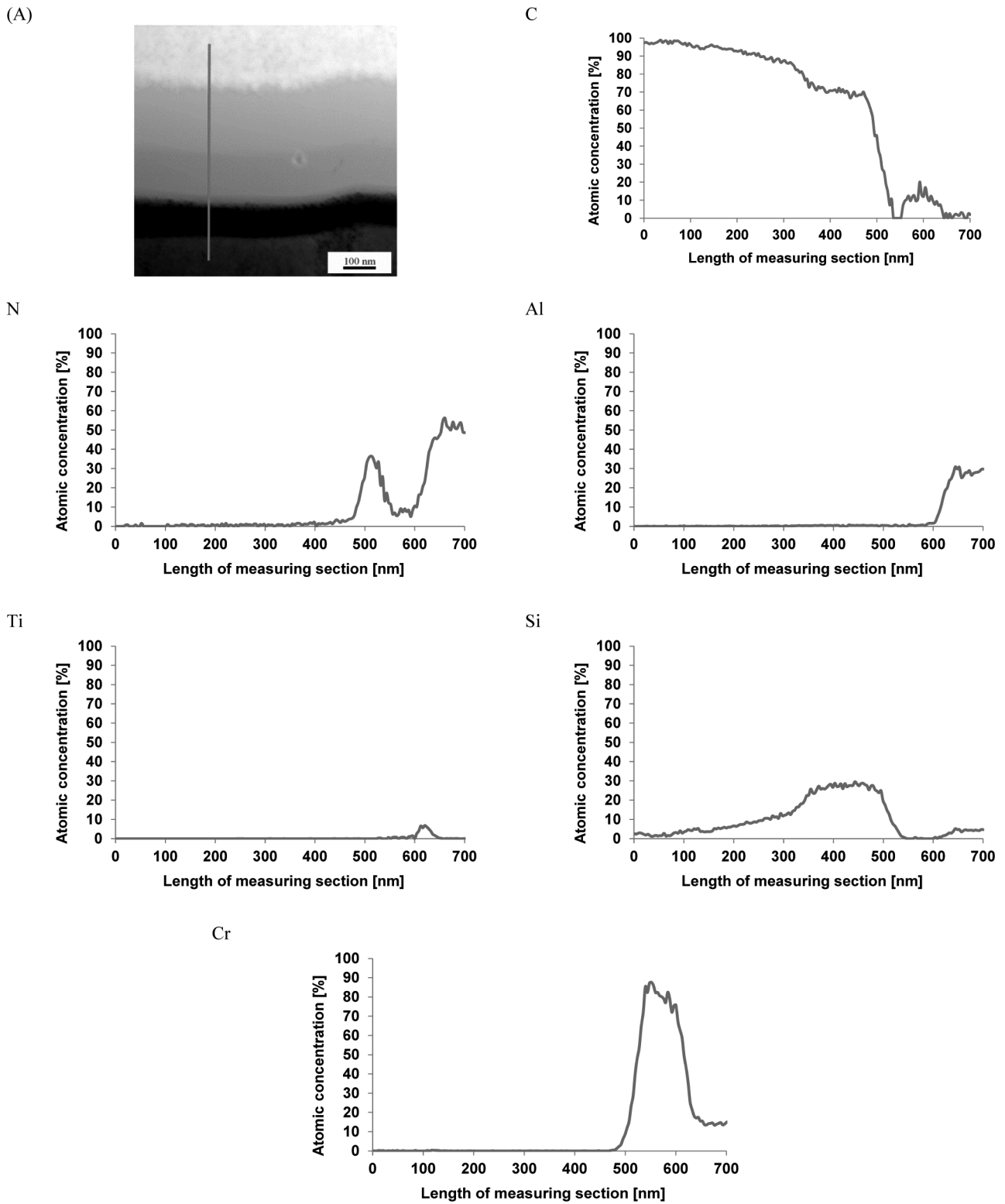


Fig. 76. Structure of a transition zone between a low-friction DLC layer and a hard CrAlSiN layer: image obtained in the STEM (A) mode and linear distribution of elements obtained in STEM mode using EDS

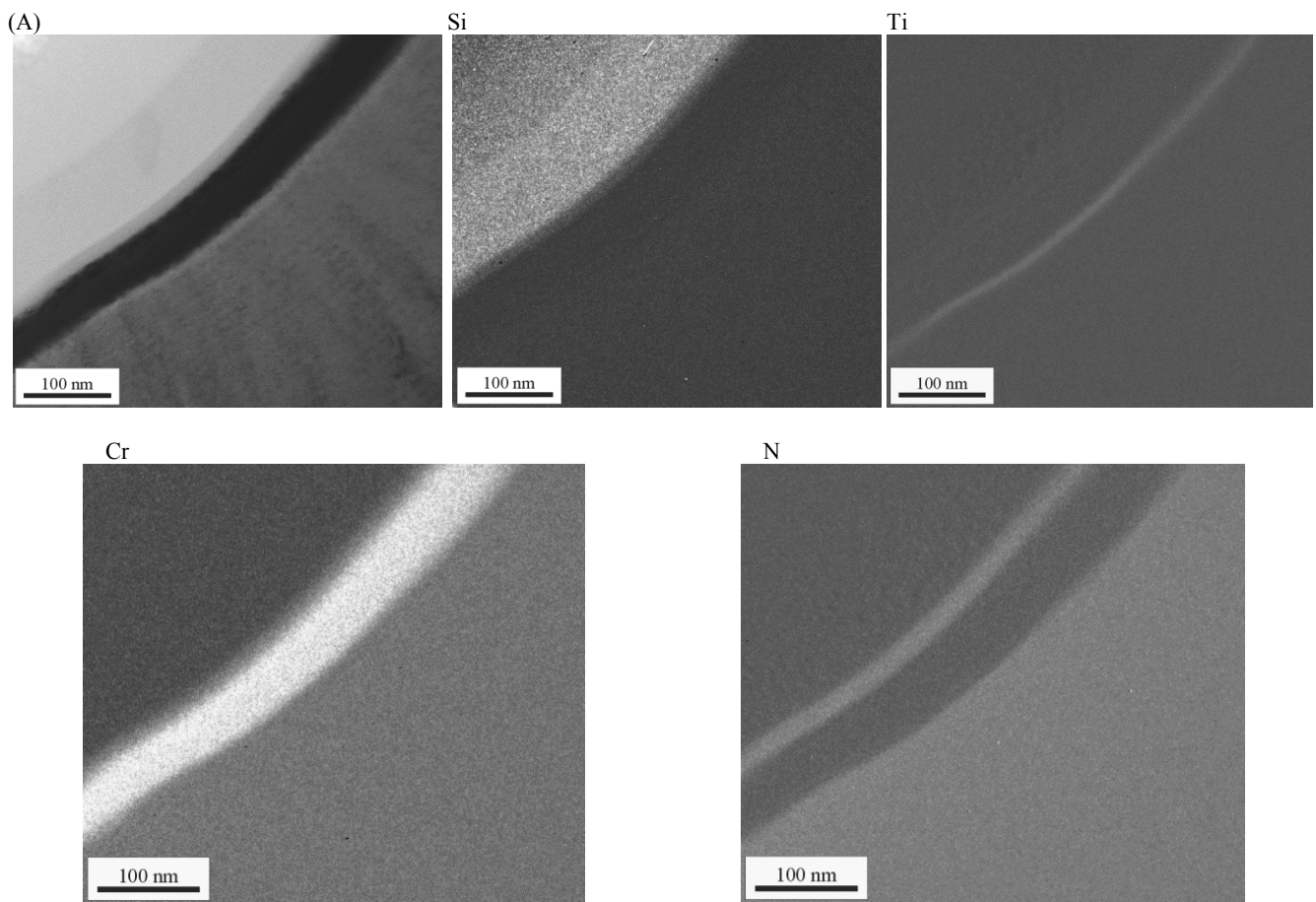


Fig. 77. Structure of a transition zone between a low-friction DLC layer and a hard CrAlSiN layer: image obtained with EFTEM (A) and EFTEM map of elements distribution

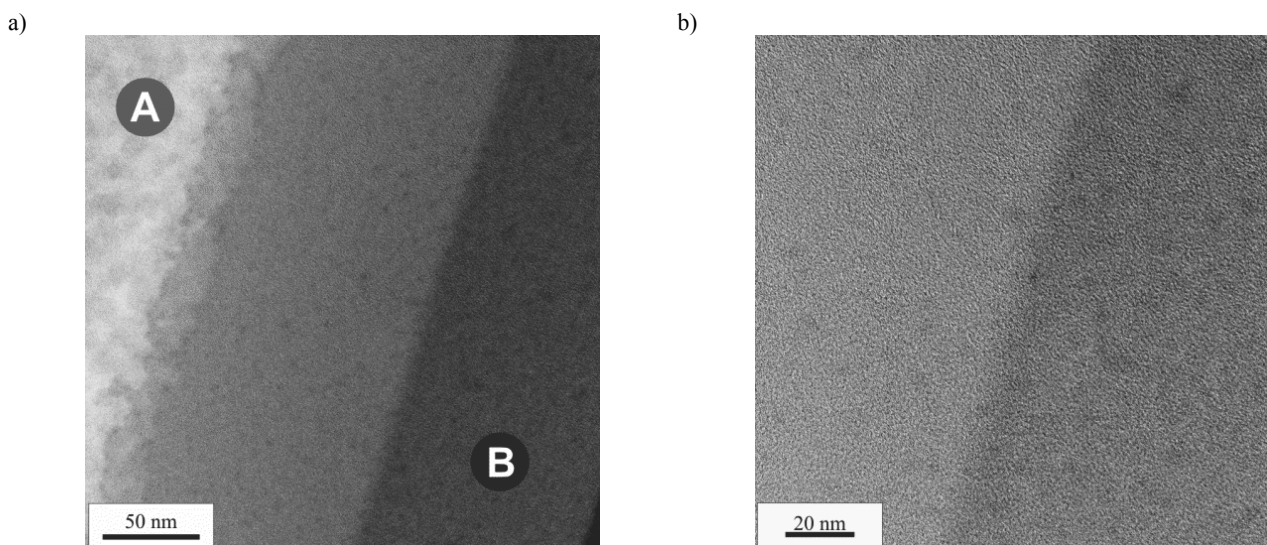


Fig. 78. Structure of DLC layer forming part of CrN+DLC coating formed on a hot-work X40CrMoV5-1 tool steel substrate: a) image of DLC1, DLC2 and DLC3 sublayers, b) image of DLC2 and DLC3 sublayers

Table 13.
Results of quantitative analysis of chemical composition of DLC1 and DLC3 layers on Fig. 78

Element analysed	Concentration, %	
	mass concentration	atomic concentration
	point A	
C	63.9	79.7
O	2.6	2.5
Si	33.5	17.8
	point B	
C	97.9	98.6
O	1.3	1.0
Si	0.8	0.4

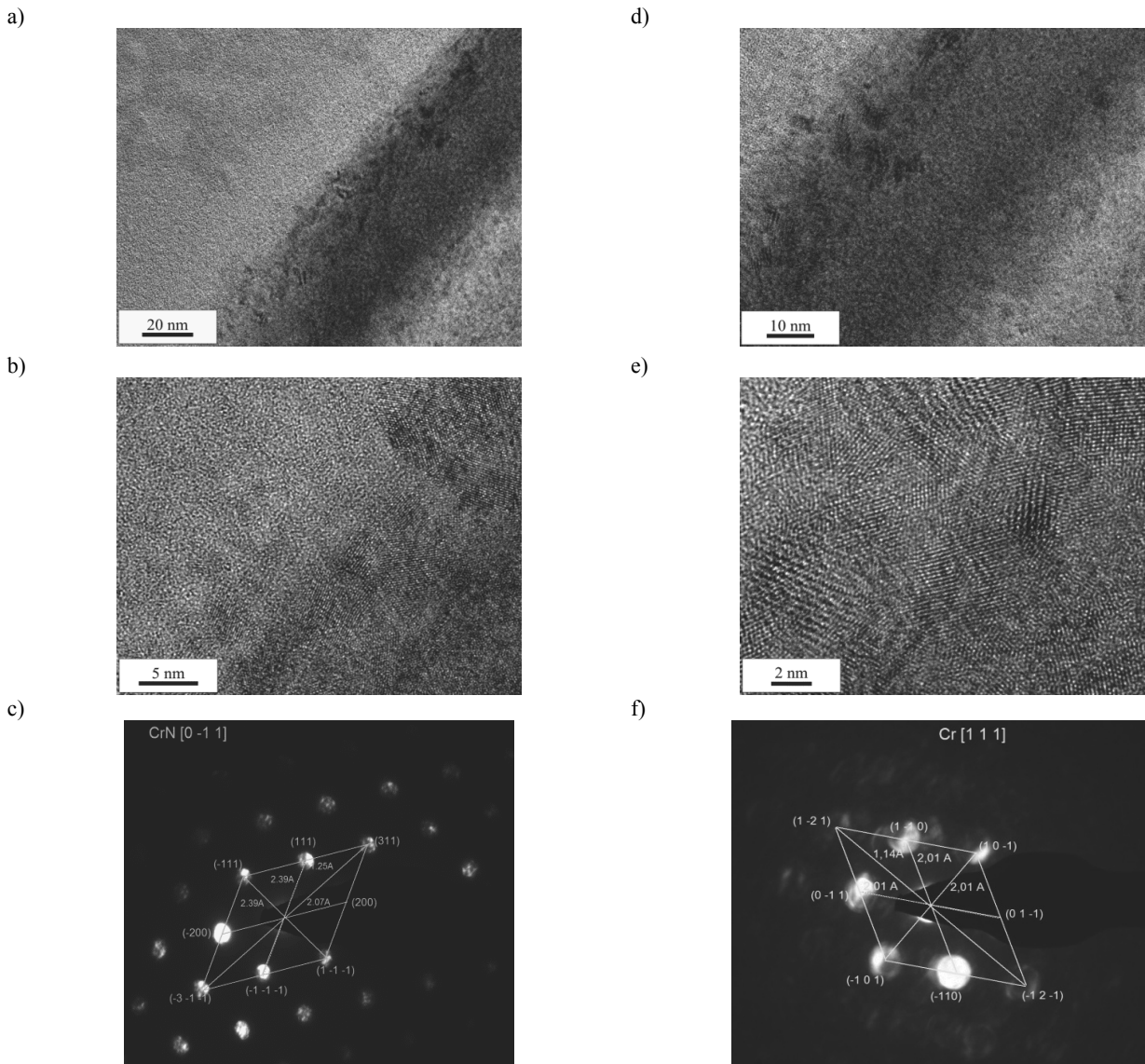


Fig. 79. High-resolution (HRTEM) image of structure of transition zone existing between low-friction DLC layer and hard CrAlSiN layer: a, b) CrN sublayer, c) microdiffraction from the area as in figure c) with a solution, d, e) Cr sublayer, f) microdiffraction from the area as in figure e) with a solution

A linear analysis was performed with a scattered X-ray radiation energy (EDS) spectrometer (Fig. 80) and a surface analysis of elements distribution using Energy-filtering transmission electron microscopy (EFTEM) (Fig. 81) was carried out to confirm the existence of individual sublayers between the hard CrAlSiN layer and the substrate material. The character of changes in the intensity of the elements points out that the sublayers mentioned exist.

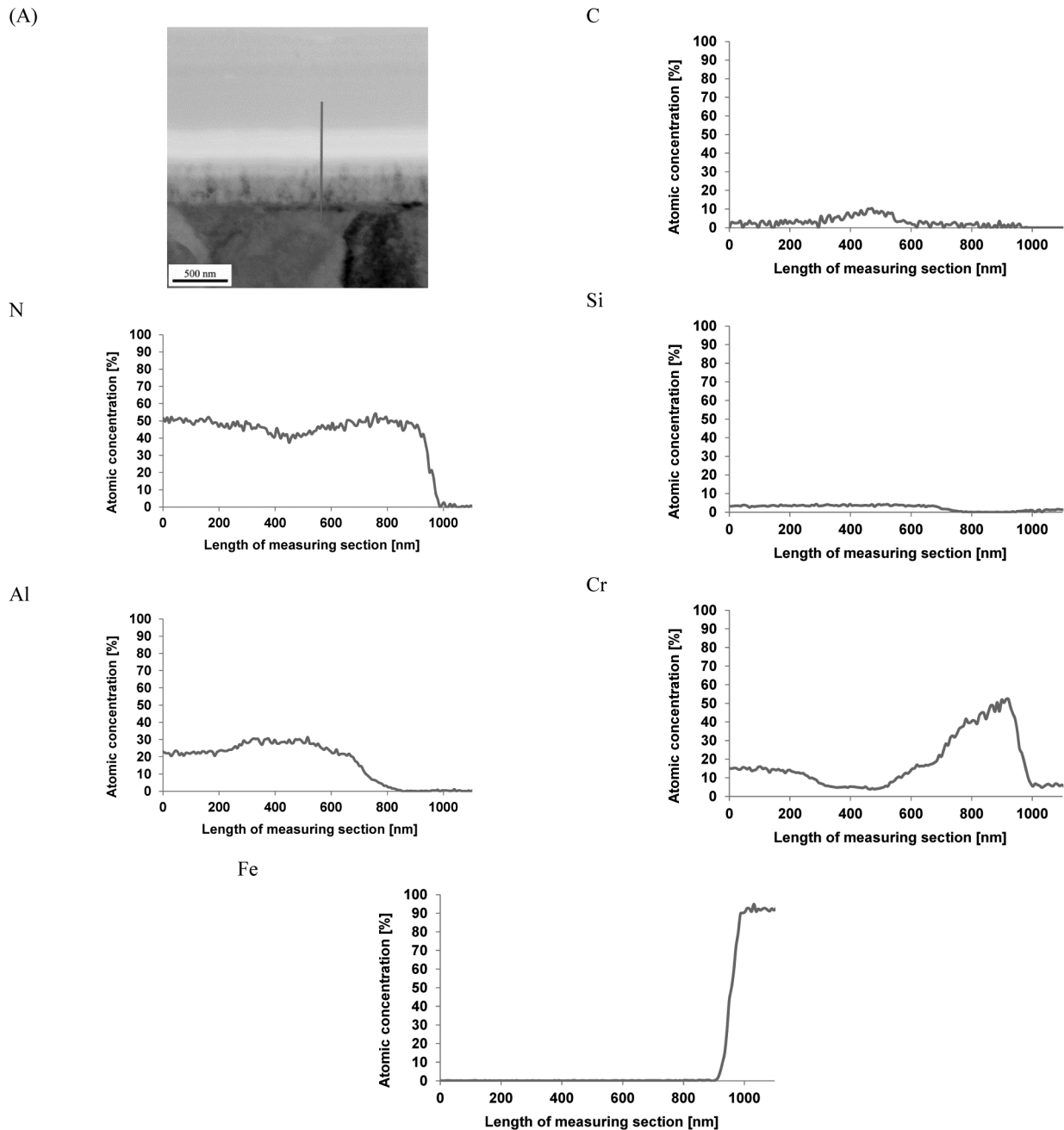


Fig. 82 presents a CrAlSiN sublayer structure with a smaller concentration of Cr, while Fig. 83 shows a structure of a CrN sublayer which form a transition zone between the CrAlSiN layer and the substrate material. It was found in diffraction examinations that the CrAlSiN layer deprived of Cr is amorphous (Fig. 82c) while the CrN layer has a crystalline structure (Fig. 83c).

Fig. 80. Structure of a transition zone between a hard CrAlSiN layer and substrate material: image obtained with the STEM (A) mode and linear distribution of elements obtained with STEM mode using EDS

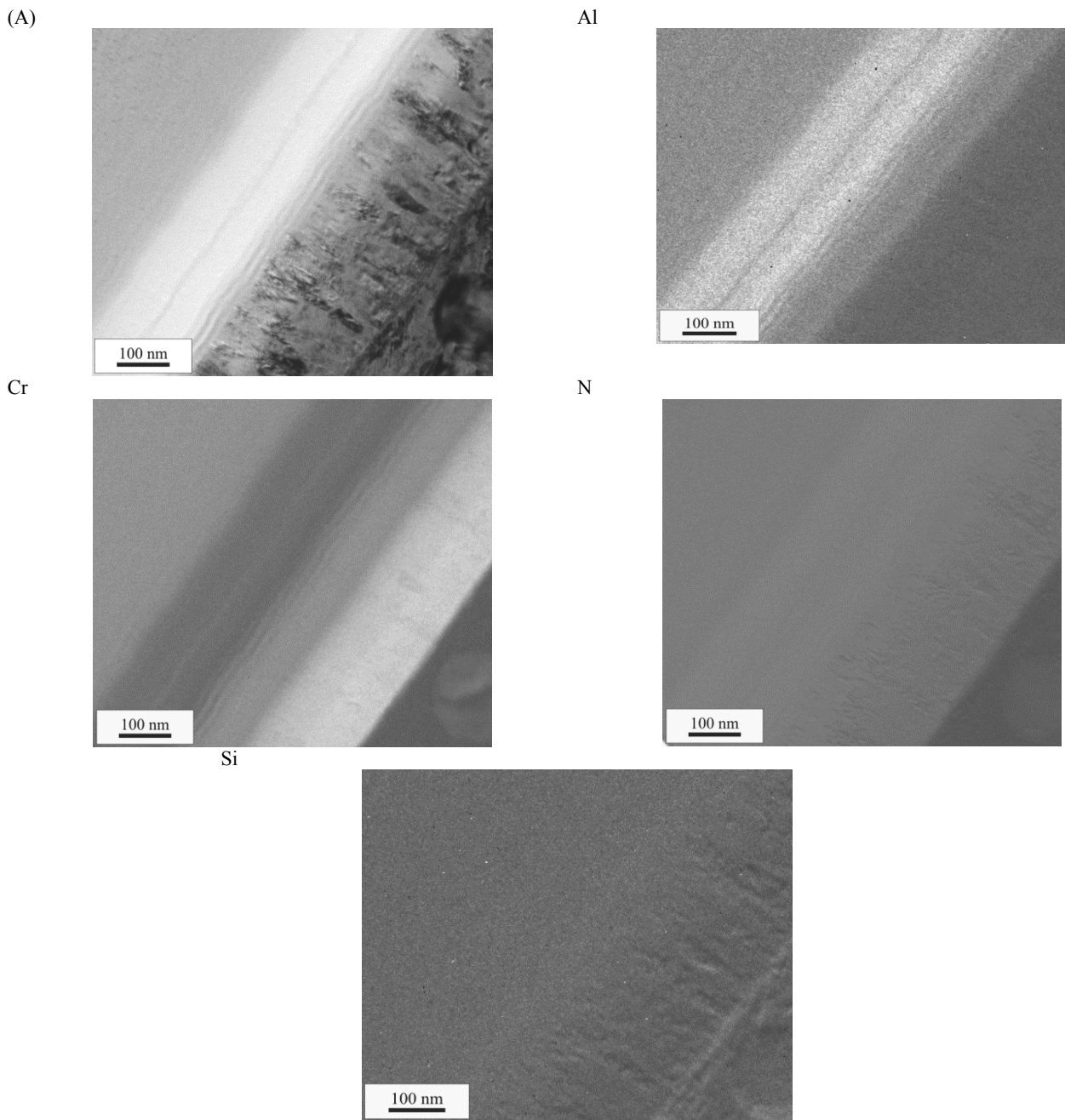


Fig. 81. Structure of a transition zone between a hard CrAlSiN layer and substrate material: image obtained with EFTEM (A) mode and map of elements distribution

The investigations performed indicate the existence of transition areas with a varied concentration of elements occurring in the joint area between the individual layers forming the transition zones. The character of changes in the joint zone, i.e. a higher concentration of elements forming part of the substrate with a lower concentration of elements forming the layer or between the individual layers may prove that diffusion transition areas exist between the individual layers and the substrate

material, influencing the higher substrate adhesion of the coatings deposited.

The tests of X40CrMoV5-1 steel specimens with coatings deposited onto their surface with high-resolution electron transmission microscopy indicate a sharp transition zone between the substrate and the layer (Fig. 84). In general, there are no reasons implying the epitaxial growth of the examined layers.

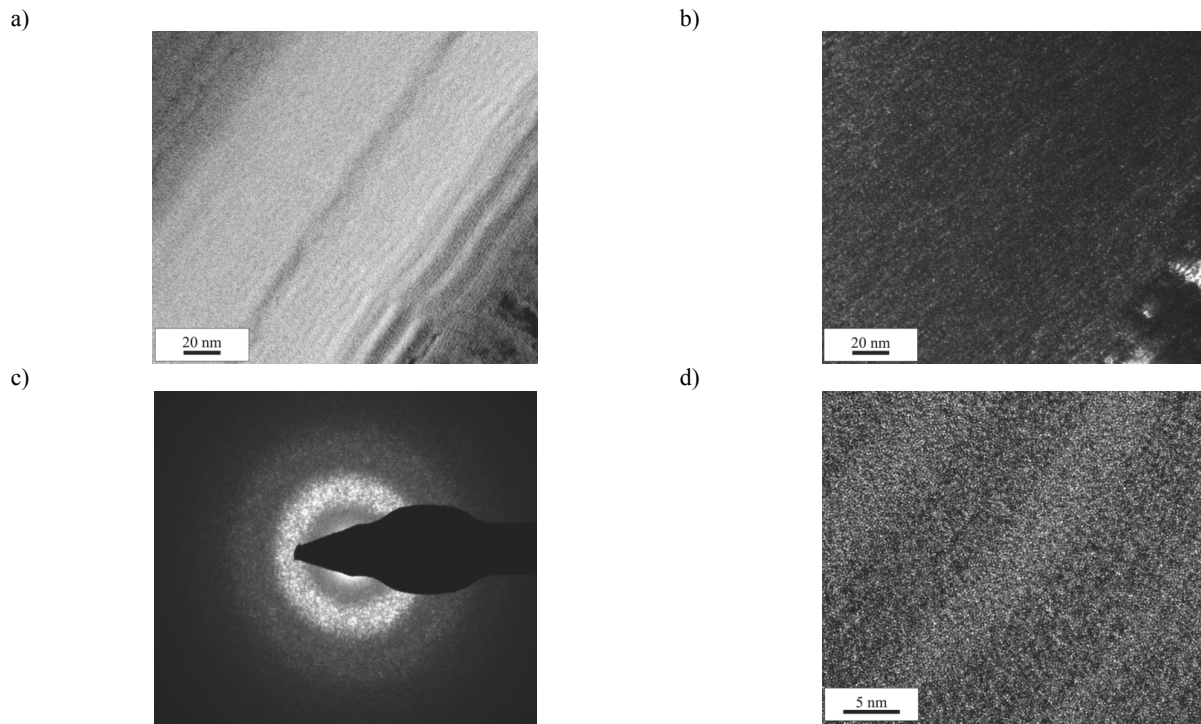


Fig. 82. Structure of CrAlSiN sublayer deprived of Cr of a transition zone between a hard CrAlSiN layer and substrate material: a) image in the light field, b) image in the dark field, c) diffraction pattern with the area as in Fig. a) and b), d) high-resolution image (HRTEM)

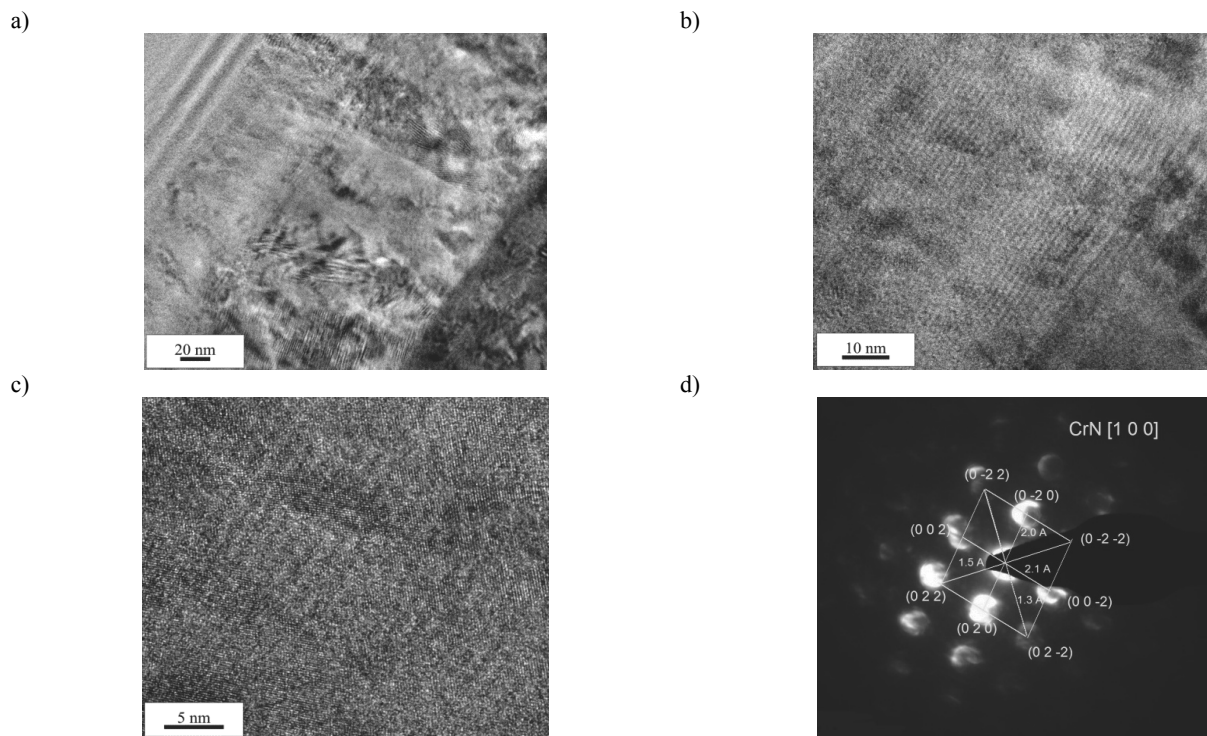


Fig. 83. High-resolution image (HTEM) of the structure of: a, b, c) CrN sublayer of the transition zone existing between the hard CrAlSiN layer and the substrate material, d) microdiffraction from the area as in figure c) with a solution

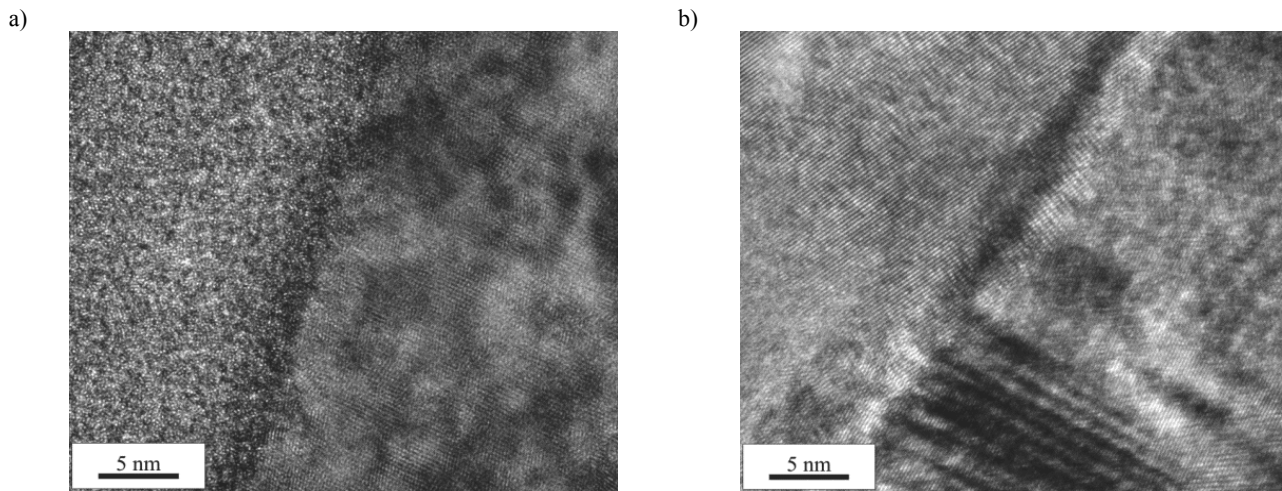


Fig. 84. High-resolution image (HRTEM) of the structure of CrN sublayer formed on the surface of hot-work X40CrMoV5-1 tool steel

5.5. Other results of physicochemical, structural and crystallographic tests of surface layers

Variations in the chemical concentration of layer components and an analysis of the chemical condition of elements were made based on examinations with Auger Electron Spectroscopy (AES) and X-ray Photoelectron Spectroscopy (XPS). A diameter of the crater formed as a result of bombing with Xe⁺ ions is 3.5 mm and depends on the collimation of the incident beam of ions and the set etching area in the ion gun used (Fig. 85a). The three areas visible with a different shade of grey correspond to a low-friction layer (external), hard nitride layer (transient) and X40CrMoV5-1 steel substrate (central) with a diameter of about 1.5 mm. According to the examinations of chemical composition with the AES method within the area of the layers, it was confirmed that the chemical composition of the individual layers forming the coatings is as assumed, while the presence of the elements forming part of the substrate was found on the bottom of a crater created by etching with Xe⁺ ions.

An Auger-electron review spectrum established from the substrate material (hot-work X40CrMoV5-1 tool steel) is shown in Fig. 85b. A group of three reflexes corresponding to the transition of electrons between LMM coatings for iron is visible for the kinetic energy of Auger electrons within the range of 500-800 eV. Small reflexes existing at the kinetic energy value of 500 eV and 300 eV correspond to Cr LMM and C KLL electron transitions. A complex structure of spectral line corresponding to Fe LMM and Cr LMM electron transitions is visible on the spectrum registered within the range of the Auger-electron kinetic energy below 100 eV. The other elements such as molybdenum, vanadium, oxygen, representing alloy additions or admixtures in steel, were recorded with X-ray Photoelectron Spectroscopy (XPS).

An Auger-electron review spectrum obtained from the area where a CrAlSiN nitride layer exists is shown in Fig. 85c.

The characteristic maximums corresponding to electron transitions for N KLL, Cr LMM, Al KLL correspond to the basic components of a CrAlSiN layer. The presence of silicone was confirmed with XPS tests.

The external part of the tested crater corresponds to the existence of a DLC later area etched with xenon ions and, at larger distance, to the areas not etched with a beam of ions. An Auger-electron spectrum obtained from the etched area shows a wide reflex within kinetic energy of 200-300 eV corresponding to KLL transition for carbon atoms (Fig. 85d). Dark surface contrast from the area visible outside the crater corresponds to an unetched DLC layer containing superficial contaminants of oxygen compounds only. A relative relationship of oxygen to carbon concentration determined with tests for the DLC layer with the XPS method is 0.02. Such a low value signifies a high chemical quality of the layer produced.

A distribution of the individual elements present in the tested layers (Fig. 86) was also analysed. The existence of oxygen and carbon should be associated with an effect of contamination. An especially high concentration of carbon and chromium was observed in the transition zone between a DLC layer and nitride layer, which corresponds to the results of earlier investigations performed with the transmission electron microscope.

Survey spectra showing the presence of photoelectric lines distinctive for elements used for creating the examined coatings (Fig. 87) were obtained as a result of examining the analysed coatings deposited onto a hot-work X40CrMoV5-1 tool steel substrate formed with the XPS technique. The chemical composition of layers, determined with measurements of the core lines O1s, Cr2p, N1s, Si2p, Al2p, C1s, Mo3d, S2p with the XPS method, is presented in Tables. 14-19. The photoelectric lines situated by the energy of 670.8 eV and 683.5 eV derive from the 3d band of xenon atoms' electrons used for creating the crater.

An analysis of the chemical condition of the elements forming part of the coatings was made with the XPS method. As shown in Fig. 88 for a CrAlSiN+DLC coating, an analysis was undertaken of carbon 1s, nitride 1s, chromium 2p, aluminium 2p and silicone 2s.

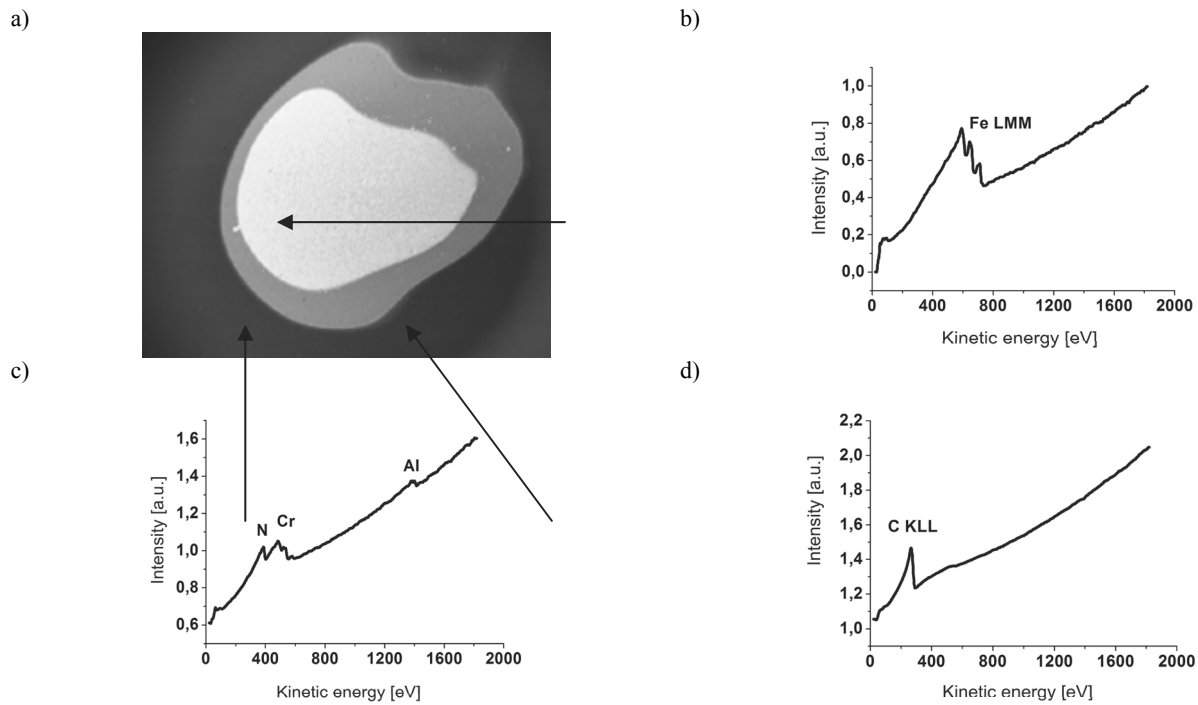


Fig. 85. AES spectrum for individual layers of CrAlSiN coating produced on hot-work X40CrMoV5-1 tool steel surface: a) topography of surface of crater etched with Xe⁺ ions, b) substrate material, c) CrAlSiN layer, d) DLC layer

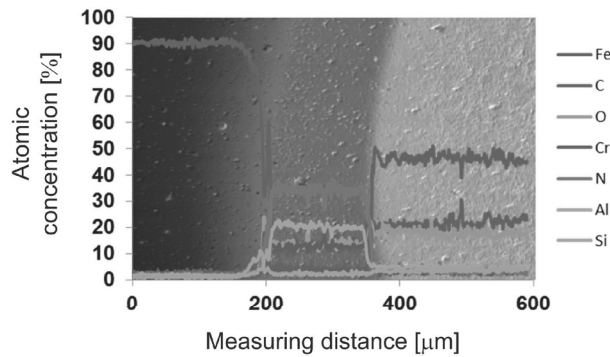


Fig. 86. Linear profile of chemical composition (AES) of CrAlSiN+DLC coating produced on the surface of hot-work X40CrMoV5-1 tool steel

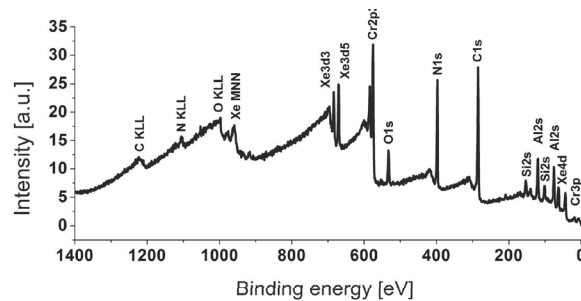


Fig. 87. XPS spectrum obtained for CrAlSiN+DLC coating formed on hot-work X40CrMoV5-1 tool steel surface

Table 14.

Results of quantitative analysis of chemical composition of CrAlSiN (XPS) layer

Element	Cr	Al	Si	N	C	O
Atomic concentration	17.19	14.93	3.54	30.35	17.06	16.93
Mass concentration	38.91	17.53	4.32	18.52	8.92	11.80

Table 15.

Results of quantitative analysis of chemical composition of AlTiCrN (XPS) layer

Element	Cr	Al	Ti	N	C	O
Atomic concentration	20.79	23.56	7.25	31.12	7.11	10.17
Mass concentration	39.34	23.13	12.63	15.87	3.11	5.92

Table 16.

Results of quantitative analysis of chemical composition of TiAlSiN (XPS) layer

Element	Ti	Al	Si	N	C	O
Atomic concentration	21.28	17.49	4.02	34.11	10.47	12.63
Mass concentration	42.28	19.59	4.68	19.84	5.22	8.39

Table 17.

Results of quantitative analysis of chemical composition of CrN (XPS) layer

Element	Cr	N
Atomic concentration	55.5	44.5
Mass concentration	82.6	17.4

Table 18.

Results of quantitative analysis of chemical composition of DLC (XPS from surface) layer

Element	C	O
Atomic concentration	97.9	2.1
Mass concentration	97.2	2.8

Table 19.

 Results of quantitative analysis of chemical composition of MoS₂ (XPS) layer

Element	Mo	S
Atomic concentration	67.8	32.2
Mass concentration	86.3	13.7

A Cr2p line spectrum indicates a single doublet for the binding energy of 574.1 eV for the Cr2p_{3/2} condition characteristic for binding energy of chromium atoms in the coatings. Binding energy for the line N1s of 397 eV correspond to the CrN compound. The shape of the line C1s comprises four constituents of which two are clearly visible for the energy of 284.8 eV and 282.1 eV (Fig. 88e). The constituent with the highest intensity with the energy of 284.8 eV may be assigned to surface carbon (aliphatic compounds of carbon) not originating from the coating deposition process. The position of the lines with a smaller binding energy of 282.1 is typical for carbides. The complex shape of the line observed for the binding energy of about 288 eV corresponds to the carbon oxides adsorbed on the

coating surface. The constituent occurring for the energy of 286 eV, though, may be assigned to the C-N binding (existing in the layer) or to the C-O binding (as a result of oxidation or contamination).

For the AlTiCrN layer, a Ti2p line spectrum shows a single doublet with the binding energy of 454.7 eV for the Ti2p_{3/2} condition distinctive for only one chemical surrounding of titanium atoms.

Moreover, to fully identify the structure of a DLC layer produced with the PACVD method, tests were carried out using a Raman spectrometer (Fig. 89). Raman spectroscopy is a very useful method in diagnosing different carbon phases and also allows to determine clearly the fraction of carbon phases according to the line D and G. A monocrystalline phase of

graphite is characterised by an intensive reflex occurring for the dislocation of 1580 cm^{-1} . Diamond features almost a 100% fraction of sp^3 bonds and a narrow band occurring for 1332 cm^{-1} .

Intermediate phases, such as DLC or amorphous carbon, are forming sp^2 bonds and are represented by broad D bands ($1345\text{--}1360\text{ cm}^{-1}$) and G bands ($1500\text{--}1580\text{ cm}^{-1}$).

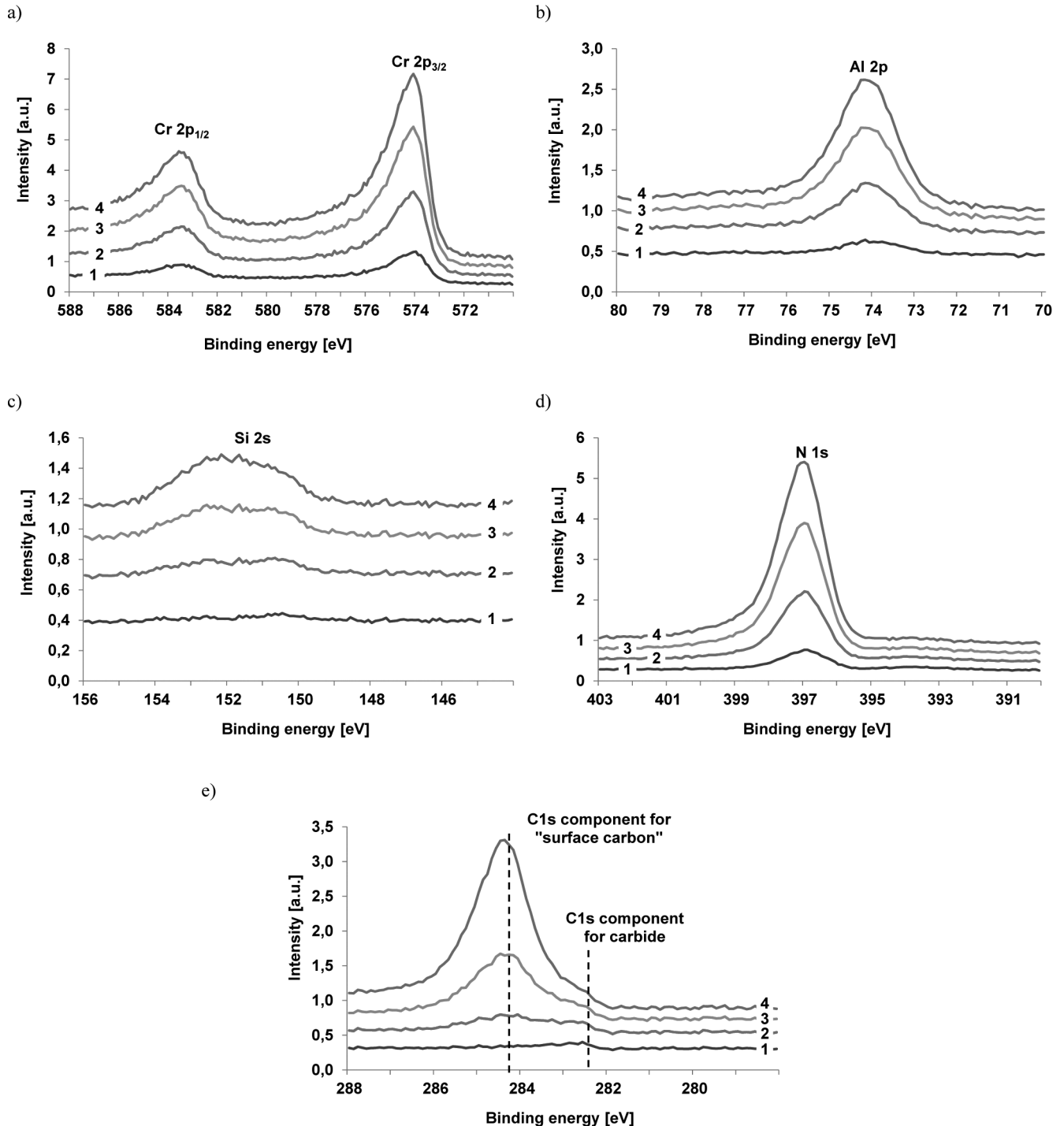


Fig. 88. XPS spectra obtained for CrAlSiN+DLC coating from the area of: (1) substrate material, (2, 3) CrAlSiN layers, (4) DLC layers; a) Cr2p, b) Al2p, c) Si2s, d) N1s, e) C1s

A Raman spectrum obtained is presented as a sum of two Gauss curves occurring for the Raman offset value of approx. 1359 cm^{-1} (D band), characteristic for sp^3 -type bonds, i.e. for diamond and 1581 cm^{-1} (G band) corresponding to sp^2 -type bonds, i.e. graphite. The visible double band is typical for an amorphous carbon DLC layer (with sp^2 -type bonds prevalent) which also confirms the amorphous character of the DLC layer. The quotient of intensity of reflexes corresponding to the phases of diamond and graphite was $I_D/I_G = 1.1$.

The tests of chemical composition made with Glow Discharge Optical Emission Spectrometry (GDOES) confirm that chemical elements are present in the coatings produced forming part of the analysed layers (Figs. 90, 91).

The character of changes in the joint zone, and in particular in the transition zone substrate/coating material, i.e. a higher concentration of elements forming part of the substrate, with an accompanying dropping concentration of elements forming the coatings may signify that a diffusion transient layer exists between the substrate material and a coating influencing the adhesion of the deposited coatings to the substrate.

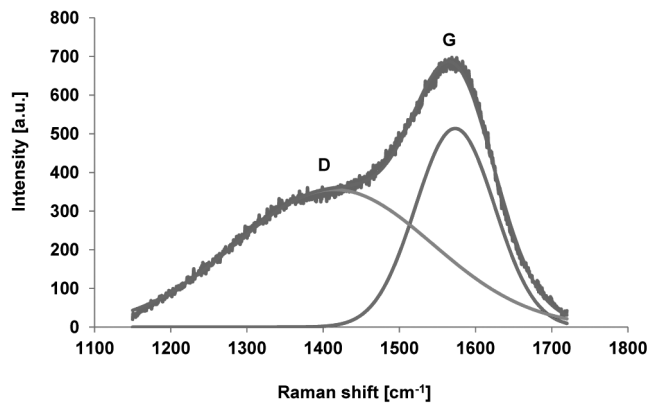


Fig. 89. Raman spectrum of low-friction DLC coating formed with PACVD method

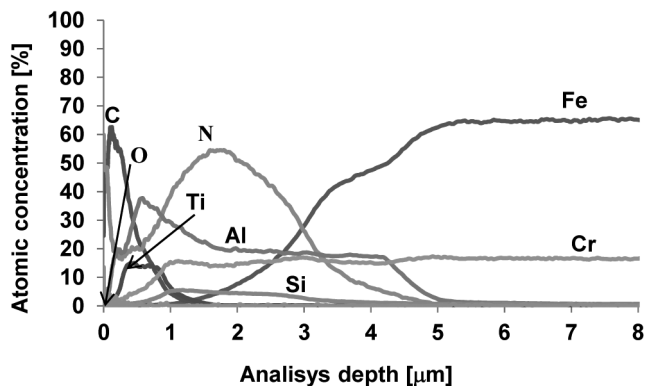


Fig. 90. Changes in the concentration of CrAlSiN+DLC coating components deposited onto X40CrMoV5-1 hot-work tool steel

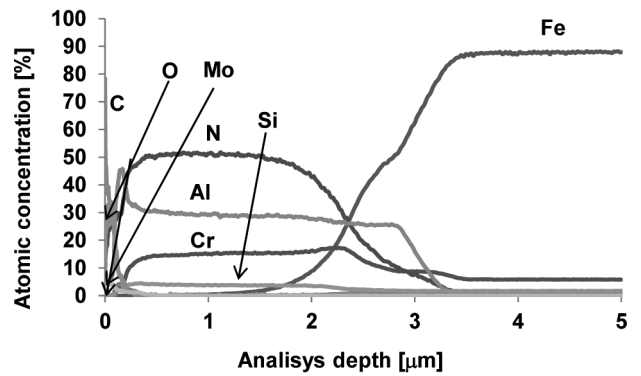


Fig. 91. Changes in the concentration of CrAlSiN+MoS₂ coating components deposited onto X40CrMoV5-1 hot-work tool steel

The results of an X-ray qualitative phase analysis performed with Bragg-Brentano geometry confirm that relevant phases exist in the tested coatings, as well as in a hot-work tool steel substrate. Some of the reflexes identified on the diffraction patterns established are shifted towards higher or lower reflection angles and their intensity varies from the values given in JCPDS files, which may mean that a texture exists or compressive or tensile stresses within the layers analysed [162-165]. As reflexes of the substrate material and coatings are overlapping in certain cases and considering their intensity making it difficult to analyse the results obtained, the diffraction technique was additionally applied with the constant incidence angle of the primary X-ray beam. This technique enables to produce diffraction lines from thin layers as a result of increasing the volume of the material taking part in diffraction. Reflexes from the thin surface layers were only registered for different incidence angles of the primary beam selected experimentally, individually for each type of coating (Figs. 92, 93).

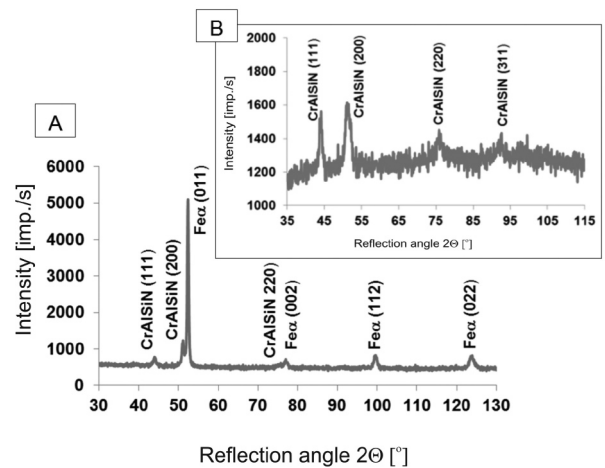


Fig. 92. (A) X-ray diffraction pattern of CrAlSiN+DLC coating deposited onto a hot-work X40CrMoV5-1 tool steel surface created with the Bragg-Brentano method and (B) X-ray diffraction pattern created for the constant incidence angle geometry of $\alpha=4^\circ$

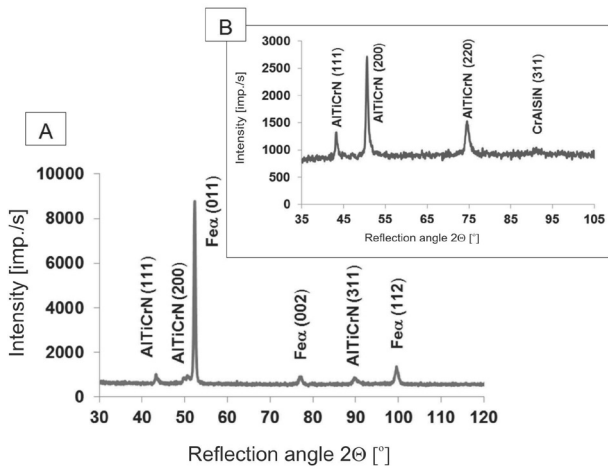


Fig. 93. (A) X-ray diffraction pattern of AITiCrN+DLC coating deposited onto a hot-work X40CrMoV5-1 tool steel surface created with the Bragg-Brentano method and (B) X-ray diffraction pattern created for the constant incidence angle geometry of $\alpha=3^\circ$

A texture analysis of the investigated coatings was performed with the reflection method. A concentric intensity distribution of pole figures varying along the axis of such figures indicates the presence of a constituent axial texture of layers produced with the PVD technique. The intensity growth areas on the registered figures correspond to the presence of fibres $\langle 311 \rangle$, and $\langle 111 \rangle$ for TiAlSiN. A texture image of an example of a layer formed with the PVD technique is presented as experimental pole figures designated as CPF (Fig. 94), ODF (Orientation Distribution Function) (Fig. 95) and complete pole figures calculated with the ODF marked as RPF (Fig. 96).

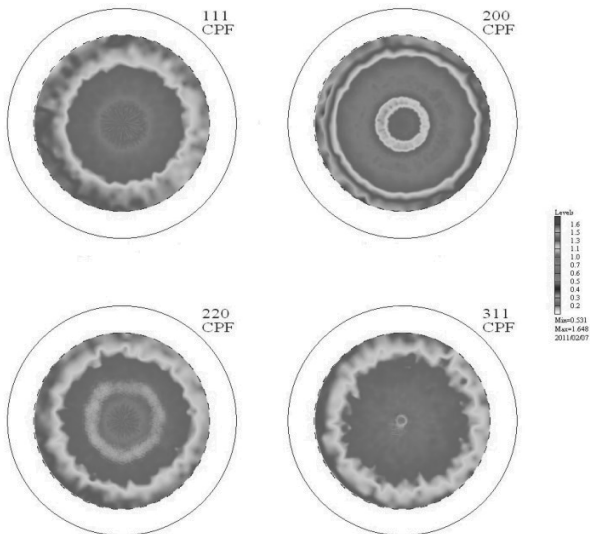


Fig. 94. Experimental pole figures (111), (200), (220) and (311) of the CrAlSiN layer formed with the PVD technique on a hot-work X40CrMoV5-1 tool steel surface

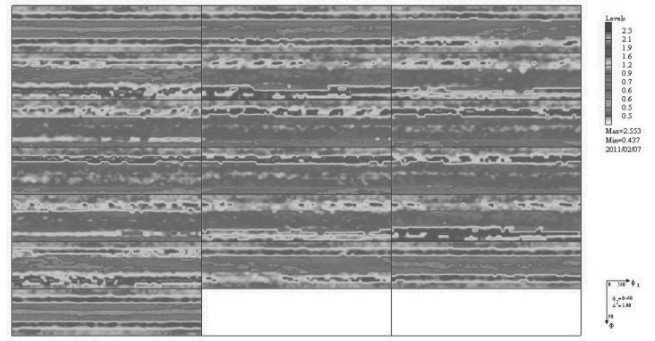


Fig. 95. Orientation distribution function of CrAlSiN layer formed with PVD technique on a hot-work X40CrMoV5-1 tool steel (ϕ_2 cross section - for the subsequent values of $\phi_2: 0, 10 \dots 90^\circ$)

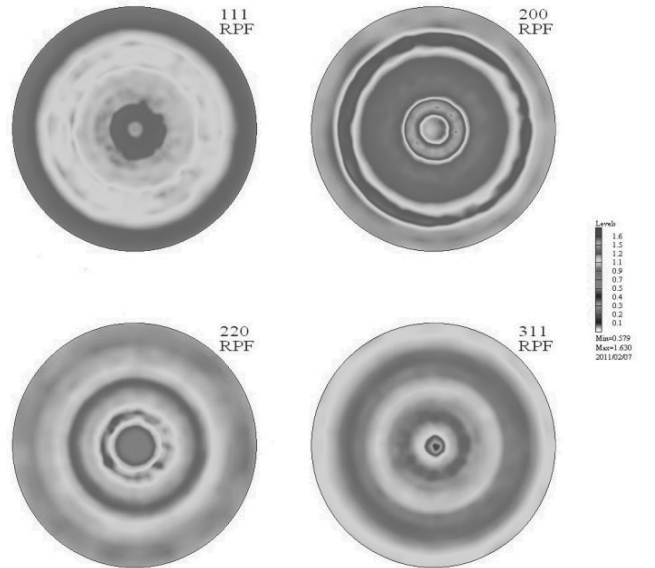


Fig. 96. Pole figures (111), (200), (220) and (311) of the CrAlSiN layer formed with the PVD technique on a hot-work X40CrMoV5-1 tool steel surface calculated with the ODF

Table 20.

Volume fractions of texture and results of measurements of stresses of the analysed layers produced with the PVD technique

Type of coating	Texture	Volume fraction for component in areas covered by diffraction, %	Stresses, MPa	
			method $g\text{-sin}^2\psi$	method $\text{sin}^2\psi$
CrAlSiN	311	25	-3475±65	-3539±126
AITiCrN	311	21	-1343±47	-1579±67
CrN	-	-	-	-
TiAlSiN	111	15	-	-2625±62

The calculations of volume fractions of the marked texture components were made using their integration in the ODF space. Angle broadening ($\Delta\Phi, \Delta\phi_1, \Delta\phi_2$) within the range of 10° to 15° was

taken into consideration in calculating the volume fractions of the identified texture components. The results of fraction calculations of the identified components are given in Table 20.

5.6. Results of tests of coatings' mechanical properties

Coating adhesion of the substrate material is one of the crucial concepts concerning the deposition of hard ceramic material onto tools. Hence adhesion is one of the most important properties of coatings produced with physical and chemical vapour deposition [166-169]. If adhesion is inappropriate, the whole functionality of a coating may be compromised. It is hard to define an unambiguous definition of adhesion of thin layers to the substrate material influenced by a material structure, external loads and the environmental aspects of surroundings.

The critical load L_{C1} and L_{C2} values were determined with a scratch test with a growing load allowing to determine the values of the force causing coating damages. The load at which the first coating damages occur is termed in the literature [170,171] as the first critical load L_{C1} . This damage is represented by a first weak acoustic emission signal (Fig. 97). A value of the first critical load is related to cohesion damages connected with the chipping of a material inside the coating, without exposing (uncovering) the substrate material, though (Fig. 98a). The second critical load L_{C2} is characterised by the total destruction of a coating. This damage is considered to be a bending point of a rising friction force curve on the chart (Fig. 97). This point corresponds to the first contact of a diamond indenter on the substrate when extensive coating chipping takes place (Fig. 98b). Acoustic emission and friction force patterns have their curve disturbed behind this point. An aggregate list of the tests' results is presented in Table 21. The highest values of the critical load L_{C1} and L_{C2} account for, respectively, 36 and 76 N, and, therefore, the best coating adhesion to the substrate was achieved for CrAlSiN+DLC coatings. The other critical load values measured, signifying coating adhesion to the substrate, do not exceed 70 N.

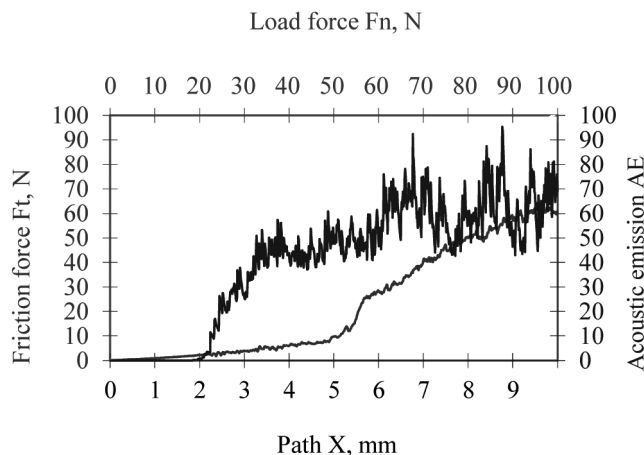


Fig. 97. Diagram of dependence between acoustic emission (AE) and friction force F_t and load for CrN+DLC coatings

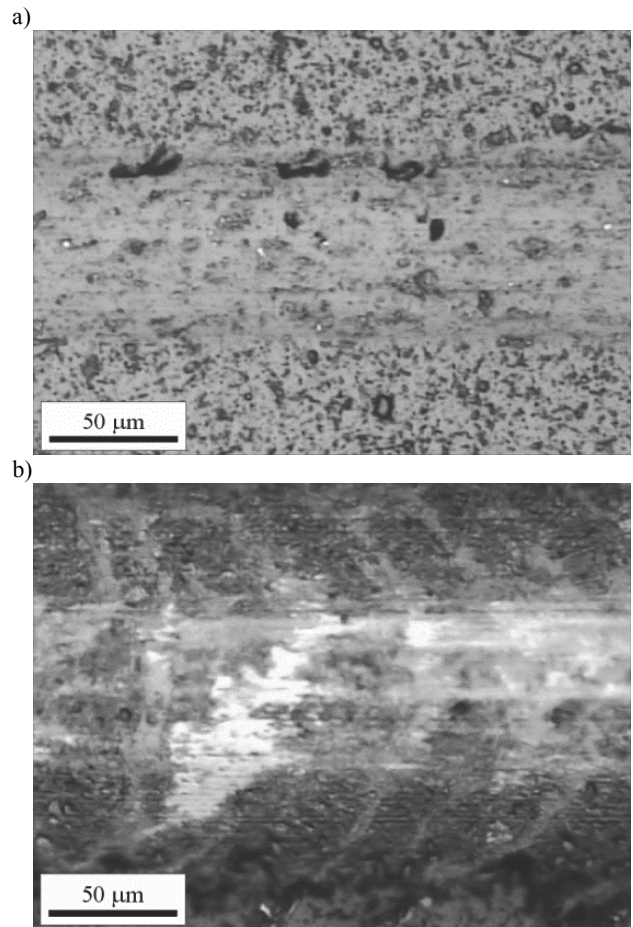


Fig. 98. Scratch mark of CrN+DLC coating surface with diamond indenter in the scratch test method with critical load of: a) L_{C1} , b) L_{C2}

A critical load registered during an adhesion test does not depend only on mechanical strength (adhesion, cohesion) of the coating-substrate system but also on various properties related to the coating and substrate material, such as: substrate hardness and roughness, coating hardness and roughness, coating thickness, friction coefficient between a coating and indenter, internal stresses in the coating as well as the conditions of the test itself.

Table 21. Aggregate list of mechanical properties

Type of coatings	Hardness HV	Critical load L_{C1} , N	Critical load L_{C2} , N
CrAlSiN/DLC	$3846 \pm 471 / 1980 \pm 160$	36 ± 4	76 ± 6
AlTiCrN/DLC	$3384 \pm 359 / 1659 \pm 92$	28 ± 3	67 ± 8
CrN/DLC	$2442 \pm 235 / 1894 \pm 105$	18 ± 3	46 ± 4
CrAlSiN/MoS ₂	$3798 \pm 569 / 1086 \pm 63$	19 ± 2	63 ± 2

Tests with the scanning electron microscope were held to determine the nature of damages created during the adhesion test. In general, the first symptoms of a damaged coating in the majority of the tested coatings are represented by arch-like cracks caused by stretching and chipping occurring at the bottom of the scratch formed during a scratch test. In few cases, minor chipping occurs at the scratch peripheries. As the load increases, semicircles are developed caused by conformal cracking, leading to delamination and cracks, as a result of which local coating delamination occurs.

The tests of internal stresses existing within coatings were carried out with X-ray analysis methods. The measurements of stresses within the analysed layers were performed with the $\sin^2\psi$ and $g\text{-}\sin^2\psi$ methods and the results obtained are provided in Table 20. The values of stresses could only have been determined for hard nitride layers due to an amorphous character of DLC and MoS_2 layers. The reflexes recorded at higher 2θ angle values are preferred for the evaluation of stresses in the $\sin^2\psi$ method due to a smaller error of the results obtained, which is not always possible, however, in experimental tests. Stresses were evaluated with the $\sin^2\psi$ method according to an analysis of shift of reflex deprived of influence on its shape and situation of other constituents of the specimen tested (other layers forming part of the coating or a substrate material). The position of the recorded reflexes was determined with the Gaussian curve adjustment method. On the other hand, the $g\text{-}\sin^2\psi$ method, contrary to the classical $\sin^2\psi$ method, is characterised by the use of multiple diffraction lines from planes $\{hkl\}$ and almost constant X-ray radiation penetration depth into the tested material.

A "negative" inclination of the specimens obtained during the measurements of stresses (Figs. 99, 100) indicates that internal compressive stresses exist in the coatings (Figs. 99, 100).

Depending on their values, internal stresses may positively or negatively influence the coating-substrate material system which directly relates to a service life of tools coated with protective layers. Compressive stresses produced for the analysed layers improve cracking resistance and enhance coating adhesion to the substrate. Tensile stresses, though, accelerate the coating destruction process with an external load applied [172-174].

An abrasive wear resistance test in dry slide friction conditions with the ball-on-disk method at room temperature was performed to determine the tribological properties of the tested coatings deposited on a hot-work X40CrMoV5-1 tool steel substrate. Fig. 101 illustrates the diagrams of changes in a dry friction coefficient μ obtained during tests of wear in relation to an Al_2O_3 counterspecimen at the temperature of 20°C for a wear track of 1000 m. Nearly all the friction curves for coatings with a low-friction DLC layer have a similar characteristic, with the initial transient state with an unbalanced curve, during which a friction coefficient decreases as the wear track increases until the set state is reached, which usually takes place after approx. 100-200 m. The registered friction coefficient for the examined combinations stabilises within 0.03-0.06 according to the coating type (Table 22) in the conditions of dry technical friction, after the a running-in period. The coatings were not worn through entirely in any of the cases as the maximum depths of wear are smaller than their thickness (Fig. 102). The visible build-ups on the wear surfaces of the tested specimens (Fig. 103) may influence

deviations in the friction coefficient on the charts recorded during wear tests.

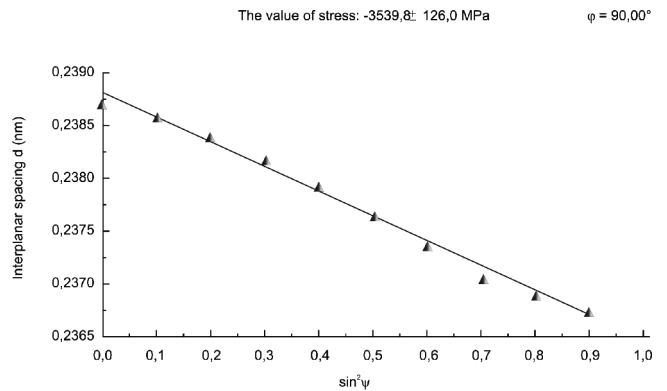


Fig. 99. Changes in interplanar spacing value d of reflex (111) of CrAlSiN layer in the function of $\sin^2\psi$ (measurement of stresses with the $\sin^2\psi$ method for different φ values of specimens' position with regard to a goniometer axis)

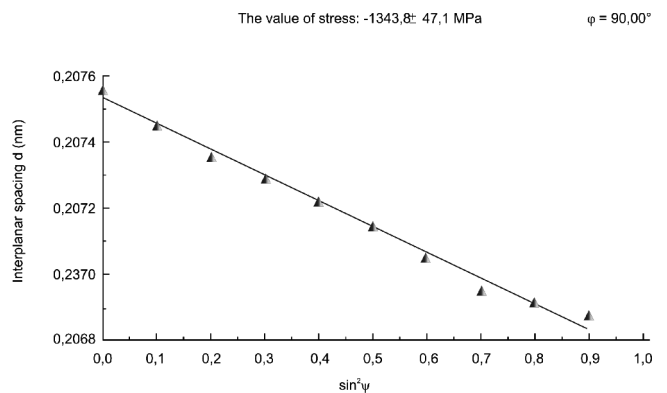


Fig. 100. Changes in interplanar spacing value d of reflex (200) of AlTiCrN layer in the function of $\sin^2\psi$ (measurement of stresses with the $\sin^2\psi$ method for different φ values of specimens' position with regard to a goniometer axis)

It can be assumed based on the observations of traces of coatings' wear made with a confocal microscope that relative displacement of the material of the coating and counterspecimens occurs during friction. The layers formed are characterised by high hardness (Table 21) and resistance to abrasive wear (Table 22) resulting in a narrow and shallow wear track in all the cases. The coatings and counterspecimens examined exhibit high tribological properties. The values of the coating K_c and counterspecimen K_b wear coefficients were recorded at the level of $10^{-7} \text{ mm}^3/\text{Nm}$ and $10^{-9} \text{ mm}^3/\text{Nm}$ (Table 22). For a CrAlSiN+ MoS_2 coating, however, where the majority of build-ups existed, the highest μ friction coefficient was noticed and most intensive counterspecimen wear. A friction coefficient μ for AlTiCrN+DLC, CrAlSiN+DLC and CrN+DLC coatings and a value of K_c and K_b indicators are lower, accordingly, evidencing their high resistance to abrasive wear.

Table 22.

Aggregate list of tests results of abrasive wear at temperature of 20°C

Type of coatings	Thickness, μm	Friction coefficient μ	Wskaźnik zużycia powłok k_{vc} , mm^3/Nm	Wskaźnik zużycia przeciwpróbkę k_{vb} , mm^3/Nm
CrAlSiN/DLC	2.0/1.3	0.06	4.54×10^{-7}	9.71×10^{-9}
AlTiCrN/DLC	1.2/1.9	0.03	3.30×10^{-7}	4.53×10^{-9}
CrN/DLC	1.1/0.5	0.04	1.58×10^{-7}	6.56×10^{-9}
CrAlSiN+MoS ₂	2.0/0.3	0.15/0.72	2.22×10^{-6}	4.83×10^{-8}

Table 23.

Aggregate list of tests results of abrasive wear at temperature of 400°C

Type of coatings	Thickness, μm	Friction coefficient μ	Wskaźnik zużycia powłok k_{vc} , mm^3/Nm	Wskaźnik zużycia przeciwpróbkę k_{vb} , mm^3/Nm
CrAlSiN/DLC	2.0/1.3	0.06	4.54×10^{-7}	9.71×10^{-9}
AlTiCrN/DLC	1.2/1.9	0.03	3.30×10^{-7}	4.53×10^{-9}
CrN/DLC	1.1/0.5	0.04	1.58×10^{-7}	6.56×10^{-9}
CrAlSiN+MoS ₂	2.0/0.3	0.15/0.72	2.22×10^{-6}	4.83×10^{-8}

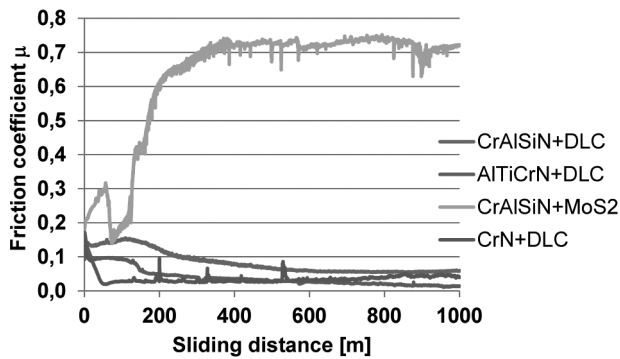


Fig. 101. Relationship between the friction coefficient and wear track obtained based on a wear resistance tests with the ball-on-disk method for the coatings analysed at the temperature of 20°C

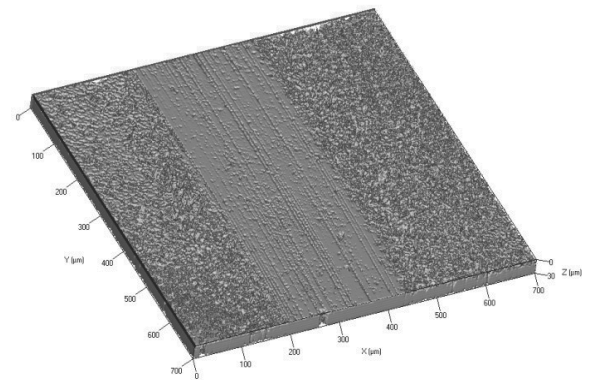


Fig. 103. Three-dimensional topography of wear area of the AlTiCrN+DLC coating, confocal microscope

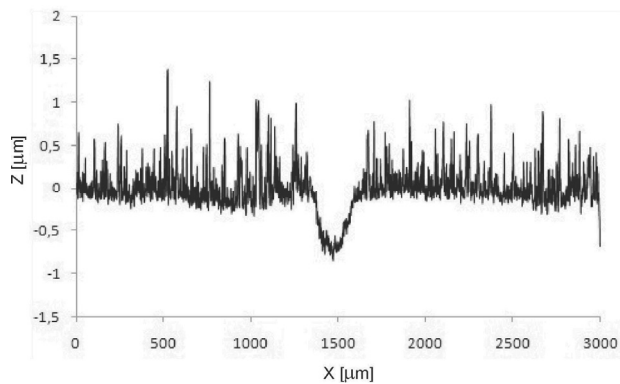


Fig. 102. AlTiCrN+DLC coating wear track profilogram after an abrasive resistance test with the ball-on-disk method

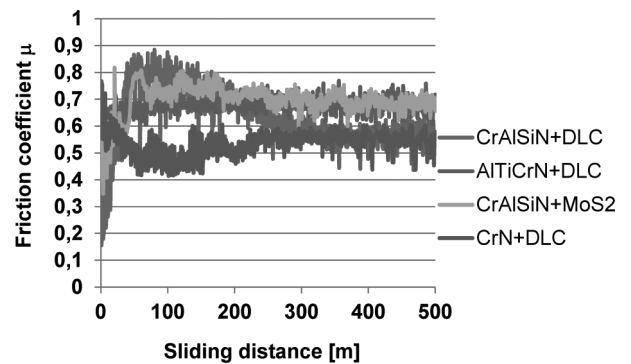


Fig. 104. Relationship between the friction coefficient and the wear track obtained based on a wear resistance test with the ball-on-disk method for the coatings analysed at the temperature of 400°C

Fig. 104 illustrates the diagrams of changes in the dry friction coefficient μ obtained during the tests of wear in relation to a Al_2O_3 counterspecimen at the temperature of 400°C for a wear track of 500 m for a load of 5 N. The lowest value of the K_c coating and K_b specimen wear indicators (Table 23) were noted for a CrN+DLC coating which confirms its high wear resistance at elevated temperature and is consistent with the results of operational tests performed at 400°C .

5.7. Fractal and multifractal analysis

The coatings produced with the physical and chemical vapour deposition methods exhibit numerous physical traits conditioned by their chemical composition and structure [175]. They also exhibit specific geometric characteristics with their description being connected with the concept of morphology, topography and surface shape. An analysis of works [176-178] points out that a surface morphology of coatings is inherently linked to their fabrication technique and properties. It is very important to determine them because surface morphology strongly influences such coating properties as hardness, roughness, friction coefficient and wear resistance [179,180]. The modern research methods allow to determine relationships between functional properties and a fractal dimension of coating structure and topography [181,182].

A modified Projective Covering Method (PCM) developed by W. Kwaśny [183] was employed in this paper to determine the fractal dimension of the investigated coatings' surface. A fractal and multifractal analysis of coatings was carried out based on the results obtained with the atomic forces microscope (Figs. 105a-b). Preliminary measurements were made within the scanning range of 2, 5 and 10 μm . The appropriate scanning range, considering a possibility to compare the results obtained for all the coatings, is, however, 5 μm .

One can concluded according to the analyses undertaken that all the considered coatings exhibit a fractal character of the surface, as signified by linear bilogarithmic charts, within specific ranges, for determination of the fractal dimension D_s (Figs. 105c-d). The highest fractal dimension value $D_s=2.024$ is exhibited by

a CrAlSiN+MoS₂ coating while the smallest value ($D_s=2.006$) is noted for a CrN+DLC coating.

Higher fractal dimension values may prove a more irregular, developed surface connected with the existence of a greater number of more densely packed columns improving the hardness of coatings. The results obtained are closely linked to the shape of the analysed coatings' surfaces and coincide with the earlier references in the literature [183].

A summary list of the results obtained and the R_a roughness parameter values for the tested coatings is shown in Table 24.

It can be concluded by analysing the multifractal spectrum shape that the surfaces examined are homogenous. The dimension values in individual layers for homogenous surfaces vary to a small extent only, which is visible as a narrow spectrum described by a low value of the $\Delta\alpha$ parameter (Fig. 105e). For those surfaces having an inhomogeneous topography, the dimension values in individual fragments are differentiated, which is manifested by a wide range of the spectrum $\Delta\alpha$ (Fig. 105f).

The results of the analyses made point out that hardness is correlated with the fractal dimension value described with the analytical dependence $y=90476x-178706$. Fig. 106 shows a dependence between a microhardness measurement and the fractal dimension value of the tested coatings.

The statistical analyses performed showed a positive linear correlation (correlation factor $r=0.794$) between the value of fractal dimension and hardness. To assess the relevance of the correlation factor, a value of empirical test statistics of $t=3.463$ had been calculated that was then compared to the critical value $t_{kryt}=2.365$ (read from the Student's T distribution table for the relevance level of $\alpha_{stat}=0.05$). As $t > t_{kryt}$, the correlation factor evaluated was considered relevant.

The hardness dependence obtained from the fractal dimension value is more accurately described with the exponential dependence $y=-0.01121\exp(-164.73x+342.27)+4137.66$. An increase in the fractal dimension value influences an increase in the analysed coatings' hardness, however, after exceeding the value $D_s=2.010$, saturation is observed, and hardness maintains on a constant level (Fig. 107). A positive correlation was found in this case between the fractal dimension value and hardness (correlation factor of $r=0.886$, test statistics empirical value of $t=30.962$, critical value of $t_{kryt}=1.969$).

Table 24.

Results of fractal and multifractal analysis and of R_a value of coatings deposited onto a hot-work X40CrMoV5-1 tool steel surface

Type of coatings	R_a	D_s	α_{min}	α_{max}	$\Delta\alpha$
CrN	23	2.008	1.7884	2.0074	0.2190
CrN+DLC	8	2.006	1.8592	2.0035	0.1443
AlTiCrN	17	2.007	1.8211	2.0050	0.1838
AlTiCrN+DLC	46	2.009	1.8890	2.0061	0.1171
CrAlSiN	52	2.017	1.6289	2.0122	0.3833
CrAlSiN+DLC	56	2.014	1.6818	2.0088	0.3269
CrAlSiN+MoS ₂	100	2.024	1.7548	2.0268	0.2720
TiAlSiN	25	2.015	1.6708	2.0145	0.3437
TiAlSiN+DLC	31	2.019	1.7875	2.0164	0.2289

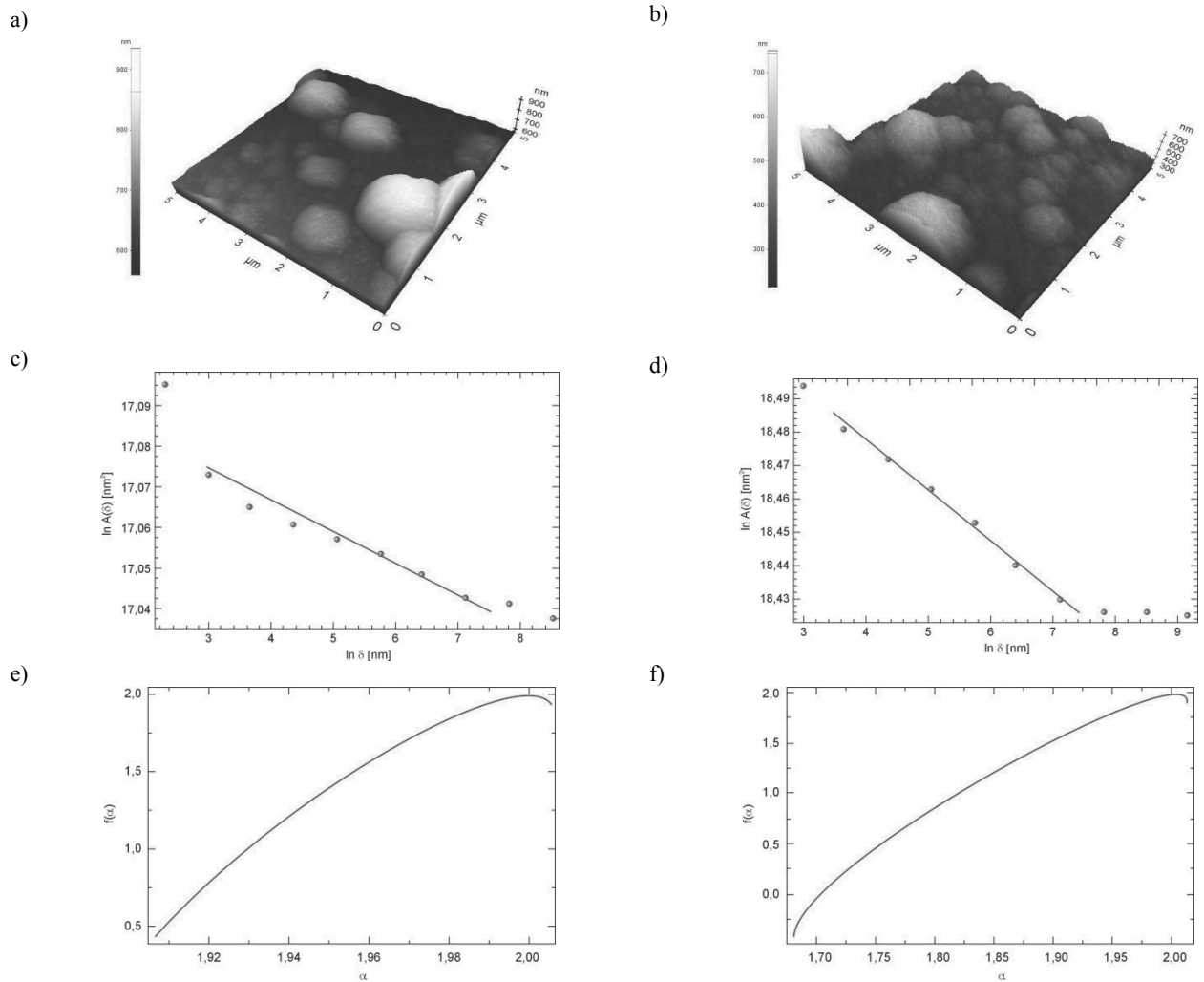


Fig. 105. a, b) Image of topography of coating surface deposited onto a hot-work X40CrMoV5-1 tool steel surface (AFM, 5 μm), c, d) bilogarithmic relationship of the approximated value of the field of the analysed surface in relation to the size of the mesh side used for its determination, e, f) multifractal spectrum of the analysed surface for the coating, respectively, for AITiCrN+DLC and CrAlSiN+MoS₂ coating

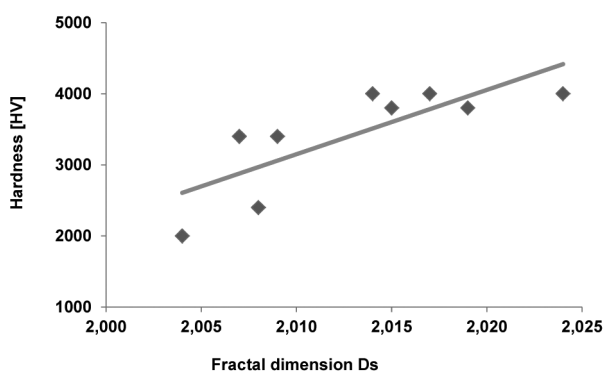


Fig. 106. Linear dependence of the obtained values of the fractal dimension and of the tested coatings' hardness

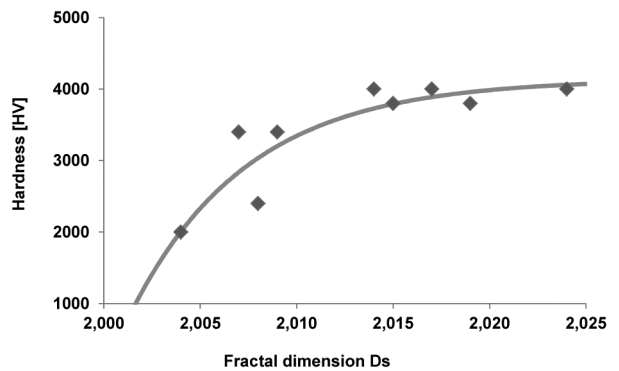


Fig. 107. Exponential dependence of the obtained values of the fractal dimension and of the tested coatings' hardness

5.8. Designing of surface layers

It was revealed by analysing the results of the tests that the effectiveness of hard nanocrystalline layers with a thin low-friction layer for improving the life of dies for plastic working of non-ferrous metals considering the specificity of extrusion with a reversely rotating die (KOBOD) is dependent, due to extremely hard working conditions, upon the properties of its constituent elements. An appropriately shaped structure and properties of hybrid coatings are required consisting of a nanocrystalline nitride layer formed with the PVD technique, of a low-friction layer formed with the CVD technique, as well as of transition zones between a core and a coating and between individual layers produced on a die's working surfaces (Figs. 75-82). The technological factors present during die operation have to be analysed thoroughly to establish criteria for optimising the properties of the investigated layers and to become familiar with the mechanisms of wear during extrusion.

The appropriate formation of the structure and properties of anti-wear coatings, their fabrication conditions and material properties must be optimised [24]. Essential for the actual improvement in the quality of different coating systems is high hardness, adequate state of stresses and a possibly lowest friction coefficient [97,109,183]. The impact of temperature on the tool material is limited by a low heat conductivity factor of coatings fabricated with the physical vapour deposition method [17].

The life of dies as a result of the effective influence of a coating (system of layers) can only be extended until the moment it preserves the required cohesion and appropriate adhesion to the die substrate with the participation of diffusion and adhesion [199]. For this reason, the properties of a transition zone between a core and a coating and between the individual layers are very important. The larger adhesion of a coating to a substrate material improves resistance to tribological wear.

As stated in the work [144], it is very important to employ the right management procedure to design and select adequately a system of layers, which in turn contributes to enhanced durability of a die for plastic working of non-ferrous metals in working conditions and to improved quality and strength properties of the extruded products according to the schematic assumptions in Fig. 14. Fig. 108 shows a diagram of a management procedure to design coatings on extrusion tools with a reversely rotating die.

6. Summary and conclusions

It is a continued endeavour of all tool material designers to develop and produce a perfect tool as resistant to wear in working conditions as possible. Considering a widespread use of such products as extrusion dies, it becomes necessary to intensify efforts to select not only appropriate tool materials, but also the technologies of depositing modern coatings onto them improving their life, and to develop and verify them in industrial conditions.

Innovative advancements in the methods of intensive plastic working of metals (SPD), notably in the area of extrusion, have led to the development of new forms of dies working in extremely disadvantageous operating conditions. Their specificity imposes completely new limitations as to product formability in a single operation than for other plastic working processes. During extrusion, the majority of non-ferrous metals and their alloys have

an unlimited ability to plastic deformations resulting from a possibility of three-axial compression with high stress values. Any limitations stem primarily from dies' strength and durability [68,184-186].

The destruction mechanisms existing mainly on the tool surface can be more broadly analysed and identified accurately through interpreting adequately mutual dependencies between the surface layer and substrate properties and structure and the external factors. It also appears to be of utmost importance to ensure the simultaneous development of both, the tool materials production and working technology, especially a technology of forming and protecting their surface, which in turn will allow to maintain balance between the substrate material and the protective coating.

The outcomes of the own research and of literature studies point out that a solution for problems concerning the life of dies for plastic working of non-ferrous metals in extremely hard operating conditions is mainly sought in the formation of physicochemical properties of tools' surface. By employing the surface treatment technologies of tool materials with the physical vapour deposition (PVD) methods, and also chemical vapour deposition methods (CVD) in selected cases to fabricate a layer with high wear resistance, also at a high temperature, the properties of such material in extrusion conditions can be improved, in particular by lowering the friction coefficient, improving tribological contact conditions within the contact area of the tool-worked material, and also to secure against adhesion wear.

It has become necessary to develop an own research programme as a result of an analysis into the use of dies in the extrusion process with a reversely rotating die, which - as the only one - allows to form hard-deformable metallic materials with very high degrees of processing at a low temperature and high speeds and as a result of tribological conditions of the die-extruded material system. An effective technology of formation and control of functional properties of tools with protective layers deposited onto their surface can be effectively applied as a consequence (Figs. 14, 108). A management algorithm encompasses the basic phases including the necessary technologies and investigations into dies' structure and properties.

A thesis should be considered substantiated in the light of the research pursued to date that a correctly formed structure, mechanical and tribological properties and a synergy of the individual layers are decisive for the life of dies for the plastic working of metals in the extrusion process, modified by forming protective layers with a complex multi-layer structure.

A technique was developed in the initial phase of working the form of a die used for the research, and an analysis and preliminary experiments verifying its material and functional properties had to be performed. The long-term experience of the Chair of Structure and Mechanics of Solids of the AGH University of Science and Technology, Kraków, was used to determine a shape and functional properties of the dies.

The service and functional life of dies produced of hot-work X40CrMoV5-1 tool steel can be extended by modifying their surface layer with the vapour deposition technique, as proven in the framework of the comprehensive own research. In order to achieve the appropriate properties, the conditions of layers' formation were defined based on microhardness and tribological resistance tests.

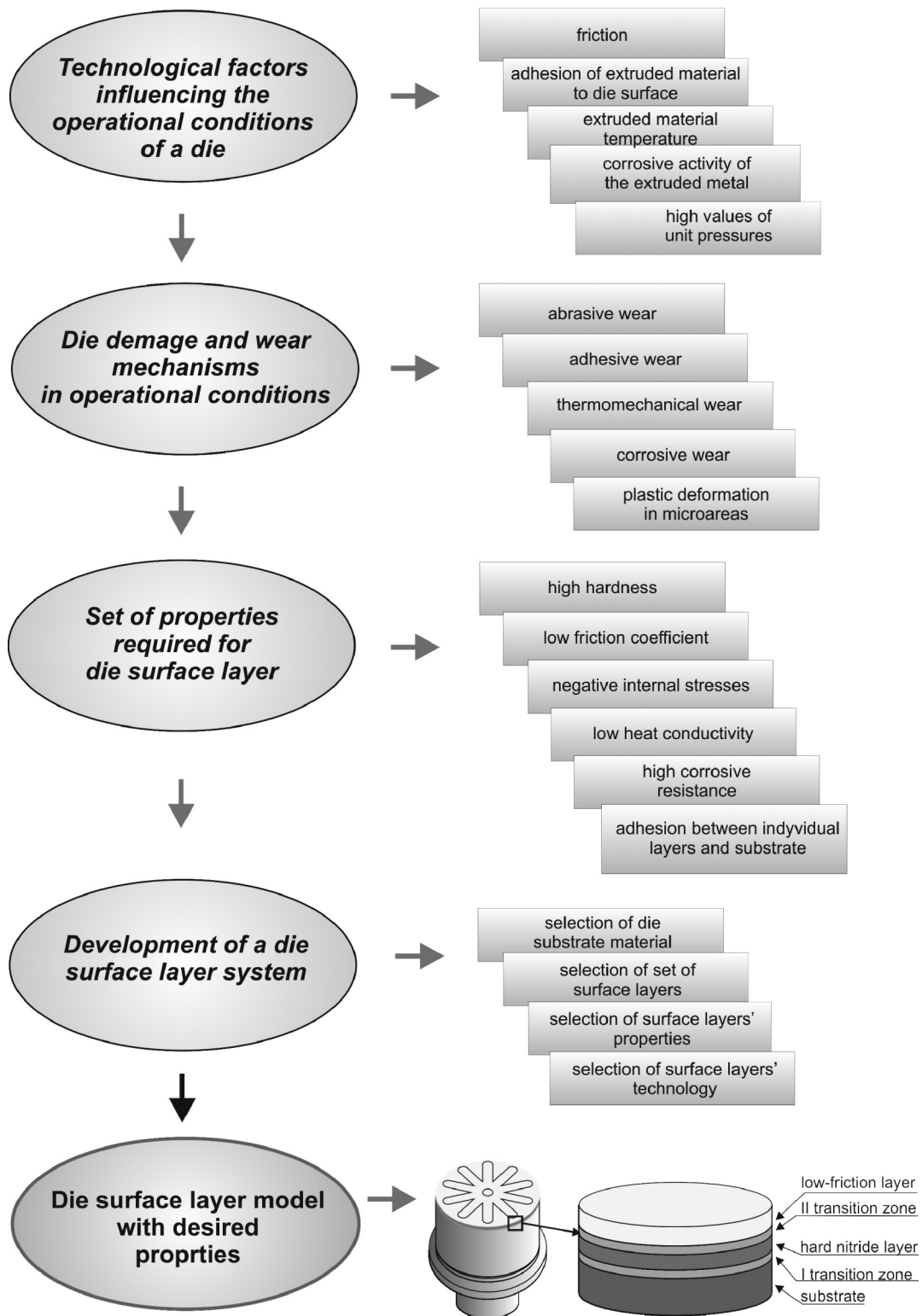


Fig. 108. A diagram of management algorithm in the process of designing hard nanocrystalline coating with a low-friction external layer for extrusion dies (prepared acc. to J. Smolik's procedure [144])

A numerical analysis of the die-extruded material system was made for the form of the die used with protective layers formed. The modelling of the system is a very complex concept as the extrusion force, torque moment, extrusion speed as well as two additional parameters, i.e. die rotation angle and frequency, are interdependent. The calculations allowed to determine the distribution of reduced stresses in the layers and in the die and the distribution of individual elements, as shown in 5.1 (Figs. 26-30).

It was most significant for such a thesis to compare the life of dies coated with the developed coatings in operating conditions. Studies into the kinetics of KOBO extrusion and into the impact of the process conditions on the life of dies and mechanical properties of the products fabricated, have become reasons for selecting the parameters of the experiments carried out for the purpose of this paper. Costly and time-consuming investigations were given up where materials are extruded under the process conditions normally used. Tests were undertaken, though, in extremely difficult conditions unmet (but likely to arise) in industrial practice and in laboratory tests as a result of using high extrusion speeds and large degrees of processing. Appropriate coatings were selected for extrusion based on the results of the preliminary studies and an EN AW-7075 alloy belonging to the group of hard-deformable material was used. A 3-fold increase in service life as compared to dies used normally in extrusion processes, i.e. quenched and tempered and nitrided (Tables. 10, 11) was found during the experiments held for dies with CrAlSiN+DLC and AlTiCrN+DLC coatings produced on their surface. 10, 11). A surface quality of the extruded alloy is very good (Fig. 47). The observations made indicated that abrasive wear and abrasive-adhesion wear were the main forms of the analysed dies' destruction.

The works performed to date [54,56,145] suggest dependencies between the mechanical properties of extruded materials and process conditions. They indicate that mechanical properties are strongly dependent on the extrusion method and conditions. The products extruded conventionally are characterised by the stability of mechanical properties along their length. Two additional parameters exist in the extrusion process with the KOBO method, i.e. angle and frequency of die rotation. The progress of the process can be adjusted directly by changing the frequency of reverse die rotation. The experiments connected with a direct measurement of temperature during conventional extrusion and extrusion with the KOBO method have proven that extrusion force is a factor conditioning the level of strength and plastic properties of the material, and also their stability along the product examined [49,54,145,187-189]. The experiments held have confirmed it is appropriate to perform extrusion with the KOBO method with constant force. The best strength properties are exhibited by wires extruded using dies with AlTiCrN+DLC and CrAlSiN+DLC coatings. Stable and homogenous properties along the entire length of the products tested can be achieved by using the coatings developed. The right conditions of extrusion have to be chosen, though.

Artificial neural networks were employed in this work for modelling dependencies between the conditions of the extrusion process with the KOBO method and the finished product's properties: yield point $R_{0.2}$, tensile strength R_m and strain A (Table 12, Fig. 50-60). The results of own works were used, and also the data included in the work [190]. The similar values of quality evaluation indicators calculated respectively for: a training and

validation set confirm an ability to generalise knowledge collected in the training process. The model established can be used for calculating the properties of aluminium and aluminium alloy products produced when extruding with the KOBO method.

An abrasive wear resistance test with the pin-on-disc method was performed to fully determine the functional and operating characteristic of the coatings analysed (Figs. 101-104, Tables 22-23). It was found after carrying out the tests that coatings with a low-friction DLC layer exhibit the smallest friction coefficient, which is consistent with the data acquired from the extrusion tests where the highest service life was identified for coatings with a DLC layer.

The factors decisive for the suitability of the proposed coatings modifying the working surfaces of dies are, to a large extent, the chemical composition and structure of such coatings. For this reason, the chemical composition and structure of the individual layers were examined in the next stage of the work. Research methods ensuring high measuring accuracy had to be applied considering a small thickness of the formed PVD and low-friction layers.

A chemical composition analysis carried out with the X-ray Photoelectron Spectroscopy method revealed an equilibrium concentration of nitride and metallic elements forming the layers for the layers produced with the PVD technique. A varying concentration of silicone on the cross section of the layer (Figs. 76-78, Table 13) for a DLC layer provides additional opportunities of enhancing mechanical and functional properties. The external zone - a layer of amorphous nitrided carbon a-C:H characterised by the lack of silicone shows a small friction coefficient. If an Si concentration is increased in the internal zone, an a-C:H:Si layer is obtained with a small value of internal stresses, improved resistance to high temperatures and better adhesion, which is especially significant due to direct adhesion to a hard nitride layer. Tests using the transmission electron microscopy confirmed an amorphous character of a low-friction DLC and MoS₂ layers. With regard to the layers formed with the PVD technique, the size and shape of grains was determined based on the structure obtained using the dark field technique and based on electron diffractions obtained signifying a nanocrystalline structure of the analysed layers and a grain size between 5 to 10 nm. Small, crystalline grains sized several nanometres deposited in an amorphous Si₃N₄ matrix were observed for a CrAlSiN layer, which may signify the layer's nanocomposite structure [191-194]. An analysis of the chemical condition of elements held using the AES and XPS spectroscopy technique evidences a high chemical quality of the layers formed.

The roughness of the coatings' surface and the surface development factor was successfully determined with atomic forces microscopy.

A phase composition analysis of the DLC layer with the Raman spectroscopy method showed the presence of bonds distinctive for diamond (sp³ type) and graphite (sp²), which does not differ from data in the literature [195-197].

The last stage of laboratory works was to assess the adhesion of the developed coatings to the substrate material. The essence of high adhesion of the layers formed to the surface of dies and between the individual layers in coatings, and the possibility of their synergic interaction is the existence of transition zones for each of the coatings, as characterised in detail in 5.3. using transmission and scanning electron microscopy (Figs. 75-83), as

well as in 5.4. using X-ray Photoelectron Spectroscopy (XPS) and Auger Electron Spectroscopy (AES) - Figs. 85-86, and in 5.5. using a glow discharge spectroscope (GDOS) - Fig. 90-91. The tests performed indicate that transition areas exist with a varied concentration of elements existing between the individual layers forming the transition zones, influencing improved adhesion of the coatings deposited onto a substrate. It should be considered that the areas are created with the participation of diffusion [198-200]. It can also be concluded that they were formed in connection with the activity of high-energy ions causing the displacement of elements in the joint zone, the higher desorption of the substrate surface and the defects occurring in the substrate or individual layers, as also noted in the works [201,202]. The existence of transition zones should be linked to good adhesion of the coatings deposited to the substrate. This may be evidenced by the high values of the critical load L_{C2} (Figs. 97-98, Table 21) of the coatings analysed. A layer damage mechanism revealed as a result of performing an adhesion test is connected with an arch-like cracks caused by stretching and chipping occurring at the bottom of the forming scratch.

The measurements of internal stresses of the coatings analysed were taken with the X-ray $\sin^2\psi$ method and the multi-reflection $g\text{-}\sin^2\psi$ method. Negative (compressive) internal stresses exist in all the tested coatings (Table 20) substantially influencing the growth of tribological and strength properties, including coatings' adhesion to the substrate, which is consistent with the earlier literature references [172,183,203].

An analysis of the tested coatings' texture was carried out with the pole figures method. A full analysis of orientation distribution was undertaken under the work presented for the layers formed with the PVD technique by performing a quality and quantity texture analysis. X-ray tests confirmed a privileged orientation of their growth $\langle 311 \rangle$ differentiated according to volume fractions of the identified texture components.

The numerous interdisciplinary investigations and analyses carried out in the field of materials science, production technology and computer techniques confirmed that the thesis adopted in the paper is correct. The results obtained set a basis for the formation of the structure and tribological properties of dies with controlled technological process conditions. It can be concluded that the required, final quality and life of tools for plastic working of metals in the extrusion process was achieved and this was verified in operating conditions.

An original achievement was the developed two-layer coating produced in a single process, consisting of an internal hard PVD layer ensuring appropriate hardness, strength, small heat conductivity and limiting the impact of external factors on the destruction process of dies for extruding non-ferrous metals and an internal low-friction layer ensuring good tribological properties, which - coupled with an adequately formed transition zone between the substrate material and the coating, as well as between the individual layers in the coating ensuring the relevant high adhesion - enabled to improve the service life of dies, as demonstrated in the work.

A physical interpretation of the phenomena accompanying the creation and use of surface layers; the tests of the structure, properties and a character of the joint existing between the developed layers and the core of the coated tool; as well as the results obtained from the performed extrusion tests, all bring a major contribution into knowledge about tool materials with

layers formed on their surface highly resistant to wear and about the processes of plastic formation of non-ferrous metals.

The following conclusions have been formulated on the basis of the results of the experimental tests and the analyses performed:

1. The thesis of the paper has been proven as it had been demonstrated that the required functional characteristics of dies for plastic working of metals in the extrusion process are a result of correct structure formation, mechanical and tribological properties of the hard nanocrystalline layer - thin low-friction layer-type as a consequence of their synergic interaction in the operational process.
2. The improved adhesion of coatings to a substrate material and an extended life of dies during operation was ensured by creating layers on the surface of tools for plastic working of non-ferrous metals in the extrusion process meeting the accurately defined functions and at the same time forming correctly a joint zone between the substrate and the coating, as well as between the individual layers in coatings and an advantageous distribution of stresses.
3. The efficiency of computer tools in the field of material engineering was confirmed. A numerical analysis of the coating - material system using the finite elements method in the extrusion process simulation conditions enabled to select the geometric characteristics and properties of the material intended for dies, the correctness of which was verified in operational tests. The charts established illustrating the impact of extrusion conditions on the extrusion force and torque moment value, the impact of process conditions on product properties, as well as the effect of temperature, reverse die rotation frequency and punch speed on product properties using neural networks enabled to successfully develop a model of dependencies between the properties of aluminium and its alloys produced during extrusion with the KOB0 method and the extrusion conditions. The results obtained in the network response enabled to fully integrate the knowledge in the field of materials science and IT tools, proving that the model after a simulation is consistent with the outcomes of the experiments undertaken, which also proves the correctness of the computer analyses presented precluding a necessity to pursue costly and time-consuming experimental tests.
4. The operational tests of dies for plastic working of non-ferrous metals with coatings deposited onto their surface in working conditions point out not only the improved durability of the elements coated with them but also the improvement of durability properties of the non-ferrous metal products extruded depending on the coating type applied.

Acknowledgements

Research was financed partially within the framework of the Polish State Committee for Scientific Research Project No N N507 550738 headed by Dr Krzysztof Lukaszewicz.

References

- [1] L.A. Dobrzański, *Materiały inżynierskie i projektowanie materiałowe, Podstawy nauki o materiałach*

- i metaloznawstwo, Wydział II zmienione i uzupełnione, Wydawnictwa Naukowo-Techniczne, Warszawa, 2006.
- [2] L.A. Dobrzański, Podstawy kształtowania struktury i własności materiałów metalowych, Wydawnictwo Politechniki Śląskiej, Gliwice, 2007.
- [3] H. Dybiec, Submikrostrukturalne stopy aluminium, Uczelniane Wydawnictwa Naukowo-Dydaktyczne AGH, Kraków, 2008.
- [4] S. Veprek, M.J.G. Veprek-Heijman, Industrial applications of superhard nanocomposite coatings, *Surface and Coatings Technology* 202 (2008) 5063-5073.
- [5] M. Betiuk, Rozwój technologii PA PVD-Arc - powłoki nanowarstwowe na narzędziach, *Inżynieria Powierzchni* 3 (2008) 16-22.
- [6] C. Donnet, A. Erdemir, Historical developments and new trends in tribological and solid lubricant coatings, *Surface and Coatings Technology* 180-181 (2004) 76-84.
- [7] W. Bochniak, Teoretyczne i praktyczne aspekty plastycznego kształtowania metali, Wydawnictwa AGH, Kraków, 2009.
- [8] S. Tomovic-Petrovic, O. Jensrud, Extrusion of silicon-rich AlMgSi alloys, *Journal of Materials Processing Technology* 212 (2012) 1437-1442.
- [9] H.I. Demirci, H. Evlen, Effect of extrusion ratio on the wear behaviour of Al-Si and Al-Mg alloys, *Journal of Alloys and Compounds* 510 (2012) 26-32.
- [10] X. Ma, M.B. de Rooij, D.J. Schipper, Friction conditions in the bearing area of an aluminium extrusion process, *Wear* 278-279 (2012) 1-8.
- [11] F. Krumphals, T. Wlanis, R. Sievert, V. Wieser, C. Sommitsch, Damage analysis of extrusion tools made from the austenitic hot work tool steel Bohler W750, *Computational Materials Science* 50 (2011) 1250-1255.
- [12] T. Bjork, R. Westergard, S. Hogmark, Wear of surface dies for aluminum extrusion - a case study, *Wear* 249 (2001) 316-323.
- [13] L.A. Dobrzański, K. Lukaszewicz, Mechanical properties of monolayer coatings deposited by PVD techniques, *Archives of Materials Science and Engineering* 28/9 (2007) 549-556.
- [14] K. Lukaszewicz, L.A. Dobrzański, A. Zarychta, L. Cunha, Mechanical properties of multilayer coatings deposited by PVD techniques onto the brass substrate, *Journal of Achievements in Materials and Manufacturing Engineering* 15 (2006) 47-52.
- [15] K. Lukaszewicz, L.A. Dobrzański, Structure and mechanical properties of gradient coatings deposited by PVD technology onto the X40CrMoV5-1 steel substrate, *Journal of Materials Science* 43 (2008) 3400-3407.
- [16] K. Lukaszewicz, L.A. Dobrzański, W. Kwaśny, K. Labisz, M. Pancielejko, Microstructure and mechanical properties of nanocomposite coatings deposited by cathodic arc evaporation, *Journal of Achievements in Materials and Manufacturing Engineering* 42 (2010) 156-163.
- [17] A.A. Voevodin, J.S. Zabinski, Nanocomposite and nanostructured tribological materials for space applications, *Composites Science and Technology* 65 (2005) 741-748.
- [18] D. Yu, C. Wang, X. Cheng, F. Zhang, Microstructure and properties of TiAlSiN coatings prepared by hybrid PVD technology, *Thin Solid Films* 517 (2009) 4950-4955.
- [19] A.A. Voevodin, J.G. Jones, T.C. Back, J.S. Zabinski, V.E. Strel'nitzki, I.I. Aksenov, Comparative study of wear-resistant DLC and fullerene-like CN_x coatings produced by pulsed laser and filtered cathodic arc depositions, *Surface and Coatings Technology* 197 (2005) 116-125.
- [20] L.A. Dobrzański, K. Lukaszewicz, Comparison of structure and properties of the electroplating, hybrid (electroplating + PVD) and PVD coatings deposited onto the brass substrate, *Materials Science Forum* 591-593 (2008) 860-864.
- [21] M. Sokovic, J. Kopac, L.A. Dobrzański, J. Miłkula, K. Gołombek, D. Pakuła, Cutting characteristics of PVD and CVD-coated ceramic tool inserts, *Tribology in Industry* 28 (2006) 3-8.
- [22] K. Lukaszewicz, A. Kriz, J. Sondor, Structure and adhesion of thin coatings deposited by PVD technology on the X6CrNiMoTi17-12-2 and X40CrMoV5-1 steel substrates, *Archives of Materials Science and Engineering* 51/1 (2011) 40-47.
- [23] A. Dobrzańska-Danikiewicz, K. Lukaszewicz, Strategiczne kierunki rozwojowe technologii nakładania powłok PVD na stop miedzi z cynkiem, *Inżynieria Materiałowa* 4 (2011) 381-384.
- [24] L.A. Dobrzański, W. Kwaśny, R. Shishkov, J. Madejski, Effect of the deposition parameters on the properties of the two-layer surface coatings obtained using magnetron sputtering, *Journal of Materials Processing Technology* 113 (2001) 495-501.
- [25] L.A. Dobrzański, M. Staszuk, K. Gołombek, A. Śliwa, M. Pancielejko, Structure and properties PVD and CVD coatings deposited onto edges of sintered cutting tools, *Archives of Metallurgy and Materials* 55 (2010) 187-193.
- [26] L.A. Dobrzański, M. Polok-Rubinić, M. Adamiak, PVD coatings deposited onto plasma nitrided X37CrMoV5-1 type steel, *International Journal of Materials and Product Technology* 33 (2008) 226-239.
- [27] L.A. Dobrzański, M. Polok, M. Adamiak, M.G. Faga, Improvement wear resistance of hot-work tool steel by plasma nitriding and PVD coatings, *Proceedings of the 1st International Conference "Heat Treatment and Surface Engineering of Tools and Dies" IFHTSE2005, Pula, Croatia, 2005, 185-191.*
- [28] L.A. Dobrzański, M. Polok, M. Adamiak, Struktura i własności powłok PVD na azotowanej stali narzędziowej X37CrMoV5-1 do pracy na gorąco, *Materiały 3 Konferencji Naukowej „Materials, Mechanical and Manufacturing Engineering” M³E`2005, Gliwice-Wisła, 2005, 159-166.*
- [29] M. Bonek, L.A. Dobrzański, E. Hajduczek, A. Klimpel, Structure and properties of laser alloyed surface layers on the hot-work tool steel, *Journal of Materials Processing Technology* 175 (2006) 45-54.
- [30] L.A. Dobrzański, K. Labisz, M. Piec, J. Lełatko, A. Klimpel, Structure and properties of the 32CrMoV12-28 steel alloyed with WC powder using HPDL laser, *Materials Science Forum* 530-531 (2006) 334-339.
- [31] L.A. Dobrzański, A. Polok, E. Jonda, Structure and properties of surface layers obtained by alloying of the hot work tool steels, *Journal of Achievements in Materials and Manufacturing Engineering* 17 (2006) 329-332.

- [32] L.A. Dobrzański, J. Domagała-Dubiel, K. Labisz, E. Hajduczek, A. Klimpel, Effect of laser treatment on microstructure and properties of cast magnesium alloys, *Journal of Achievements in Materials and Manufacturing Engineering* 37/1 (2009) 57-64.
- [33] L.A. Dobrzański, G. Matula, A. Varez, B. Levenfeld, J.M. Torralba, Fabrication methods and heat treatment conditions effect on tribological properties of high speed steel, *Journal of Materials Processing Technology* 157-158 (2004) 44-51.
- [34] A. Kloc, L.A. Dobrzański, G. Matula, J.M. Torralba, Effect of manufacturing methods on structure and properties of gradient tool materials with non-alloy steel matrix reinforced with the HS6-5-2 type high-speed steel, *Materials Science Forum* 539-543 (2007) 2749-2754.
- [35] J. Adamczyk, E. Hajduczek, Wpływ powierzchniowych warstw dyfuzyjnych na zmęczenie cieplne stali narzędziowych do pracy na gorąco WCLV, *Metaloznawstwo i Obróbka Ciepła* 66 (1983) 9-14.
- [36] L.A. Dobrzański, J. Mazurkiewicz, E. Hajduczek, J. Madejski, Comparison on thermal fatigue resistance and structure of the 47CrMoWVTiCeZr16-26-8 hot-work tool steel with X40CrMoV5-1 type one, *Journal of Materials Processing Technology* 113 (2001) 527-538.
- [37] L.A. Dobrzański, Structure and properties of high-speed steels with wear resistant casus or coatings, *Journal of Materials Processing Technology* 109 (2001) 44-51.
- [38] L.A. Dobrzański, W. Kasprzak, A. Zarychta, M. Ligarsli, J. Mazurkiewicz, Structure and properties of W-Mo-V-Co 11-0-2-5 type and W-Mo-V 11-0-2 type high-speed steels, *Journal of Materials Processing Technology* 64 (1997) 93-99.
- [39] W. Libura, Płynięcie metali w procesie wyciskania, *Uczelniane Wydawnictwa Naukowo-Dydaktyczne, Kraków*, 2008.
- [40] P.K. Saha, Aluminium extrusion technology, *ASM International, Materials Park, Ohio*, 2000.
- [41] M. Bauser, G. Sauer, K. Siegert (eds.), *Extrusion*, ASM International, Materials Park, Ohio, 2006.
- [42] J. Richert, *Innowacyjne metody przeróbki plastycznej metali*, Wydawnictwa AGH, Kraków, 2010.
- [43] Z. Rdzawski, *Miedź stopowa*, Wydawnictwo Politechniki Śląskiej, Gliwice, 2009.
- [44] W. Bochniak, A. Korbel, R. Szyndler, R. Hanasz, F. Stalony-Dobrzański, L. Błaż, P. Starski, New forming method of bevel gears from structural steel, *Journal of Materials Processing Technology* 173 (2006) 75-83.
- [45] W. Bochniak, A. Korbel, KOBO type forming: forging of metals under complex conditions of the process, *Journal of Materials Processing Technology* 134 (2003) 120-134.
- [46] A. Korbel, W. Bochniak, Refinement and control of the metal structure elements by plastic deformation, *Scripta Materialia* 51 (2004) 755-759.
- [47] W. Bochniak, K. Pantof, Structure of cooper subjected to changes of the loading scheme during rolling, *Journal of Materials Processing Technology* 208 (2008) 366-371.
- [48] A. Korbel, W. Bochniak, Sposób ciągnięcia materiałów zwłaszcza metalicznych - Patent RP Nr 179347 (pat. udzielono 31.08.2000).
- [49] A. Walocha, A. Korbel, W. Bochniak, P. Ostachowski, Efekt cieplny w procesie wyciskania aluminium metodą KOBO, *Rudy i Metale Nieżelazne* 11 (2009) 773-777.
- [50] W. Bochniak, P. Ostachowski, A. Korbel, K. Piela, Superplastic flow of metals extruded by Kobo method, *Materials Science Forum* 667-669 (2011) 1039-1044.
- [51] L. Błaż, M. Sugamata, J. Kanek, J. Sobota, G. Wloch, W. Bochniak, A. Kula, Structure and properties of 6061 + 26 mass% Si aluminum alloy produced via coupled rapid solidification and KOBO-extrusion of powder, *Journal of Materials Processing Technology* 209 (2009) 4329-4336.
- [52] W. Bochniak, A. Korbel, L. Błaż, A. Brzostowicz, Wytwarzanie droбноziarnistych wyrobów ze stopu aluminium 7075 w procesie wyciskania metodą KOBO, *Przegląd Mechaniczny* 10 (2009) 33-37.
- [53] K. Piela, W. Bochniak, A. Korbel, P. Stachowski, L. Błaż, Wpływ sposobu odkształcenia na strukturę, własności mechaniczne i stabilność cieplną cynku, *Rudy i Metale Nieżelazne* 6 (2009) 356-361.
- [54] P. Ostachowski, A. Korbel, W. Bochniak, M. Łagoda, Własności mechaniczne drutów aluminiowych otrzymanych metodą KOBO, *Rudy i Metale Nieżelazne* 11 (2009) 707-711.
- [55] A. Brzostowicz, A. Korbel, W. Bochniak, L. Błaż, W. Suder, Zjawisko Ludersa w aluminium wyciśniętym metodą KOBO, *Rudy i Metale Nieżelazne* 11 (2009) 663-665.
- [56] A. Korbel, W. Bochniak, P. Stachowski, L. Błaż, Viscoplastic flow of metal in dynamic conditions of complex strain scheme, *Metallurgical and Materials Transactions A* 42 (2011) 2881-2897.
- [57] A. Korbel, R. Szyndler, Innowacyjne rozwiązania w obszarze obróbki plastycznej, *Obróbka Plastyczna Metali* 3 (2010) 203-216.
- [58] L.A. Dobrzański, A.D. Dobrzańska-Danikiewicz, *Obróbka powierzchni materiałów inżynierskich*, Open Access Library, Volume 5 (2011) 1-480.
- [59] M. Pellizzari, High temperature wear and friction behaviour of nitrided, PVD-duplex and CVD coated tool steel against 6082 Al alloy, *Wear* 271 (2011) 2089-2099.
- [60] M. Blicharski, *Inżynieria powierzchni*, Wydawnictwa Naukowo-Techniczne, Warszawa, 2009.
- [61] P. Kula, *Inżynieria warstwy wierzchniej*, Wydawnictwo Politechniki Łódzkiej, Łódź, 2000.
- [62] M. Gierzyńska-Dolna, *Tarcie, zużycie i smarowanie w obróbce plastycznej metali*, Wydawnictwa Naukowo-Techniczne, Warszawa, 1983.
- [63] R. Skoblik, L. Wilczewski, *Odlewnictwo i obróbka plastyczna: laboratorium*, Wydawnictwo Politechniki Gdańskiej, Gdańsk, 1997.
- [64] P.H. Mayrhofer, C. Mittlere, L. Hulman, H. Clemens, Microstructural design of hard coatings, *Progress in Materials Science* 51 (2006) 1032-1114.
- [65] W. Dobrucki, *Zarys obróbki plastycznej metali*, Wydawnictwo Śląsk, Katowice, 1975.
- [66] M. Morawiecki, L. Sadok, E. Wosiek, *Przeróbka plastyczna. Podstawy teoretyczne*, Wydawnictwo Śląsk, Katowice, 1986.
- [67] S. Muenstermann, R. Telle, Wear and corrosion resistance of alumina dies for isothermal semi-solid processing of steel, *Wear* 267 (2009) 1566-1573.
- [68] I. Nowotyska, S. Kut, Numeryczna analiza wpływu kąta matrycy na deformację narzędzi podczas wyciskania, *Rudy i Metale Nieżelazne* 6 (2010) 337-340.
- [69] L.A. Dobrzański, E. Hajduczek, J. Marciniak, R. Nowosielski, *Obróbka cieplna materiałów narzędziowych*, Wydawnictwo Politechniki Śląskiej, Gliwice, 1990.

- [70] E. Żmihorski, *Stale narzędziowe i obróbka cieplna narzędzi*, Wydawnictwa Naukowo-Techniczne, Warszawa, 1976.
- [71] L.A. Dobrzański, J. Mazurkiewicz, E. Hajduczek, Effect of thermal treatment on structure of newly developer 47CrMoWVTiCeZr16-26-8 hot work tool steel, *Journal of Processing Technology* 157-158 (2004) 472-484.
- [72] S. Syahrullail, B.M. Zubil, C.S.N. Azwadi, M.J.M. Ridzuan, Experimental evaluation of palm oil as lubricant in cold forward extrusion process, *International Journal of Mechanical Sciences* 53 (2011) 549-555.
- [73] S.S. Akhtar, A.F.M. Arif, B.S. Yilbas, Nitriding of aluminum extrusion die: Effect of die geometry, *Journal of Materials Engineering and Performance* 19 (2010) 401-412.
- [74] M. Tercej, A. Smolej, P. Fajfar, R. Turk, Laboratory assessment of wear on nitrided surfaces of dies for hot extrusion of aluminium, *Tribology International* 40 (2007) 374-384.
- [75] T. Bjork, M. Berger, R. Westergard, S. Hogmark, J. Bergstrom, New physical vapour deposition coatings applied to extrusion dies, *Surface and Coatings Technology* 146-147 (2001) 33-41.
- [76] M.B. Karamis, H. Sert, The role of the PVD TiN coating in wear behaviour of aluminium extrusion die, *Wear* 217 (1998) 46-55.
- [77] K. Bobin, N. Bagecivan, P. Immich, C. Warnke, F. Klocke, C. Zeppenfeld, P. Mattfeld, Advancement of a nanolaminated TiHfN/CrN PVD tool coating by a nanostructured CrN top layer in interaction with biodegradable lubricant for green metal forming, *Surface and Coatings Technology* 203 (2009) 3184-3188.
- [78] J. Smolik, Rola warstwy hybrydowej typu warstwa azotowana/powłoka CrN w procesie zwiększania trwałości matryc kuźniczych, *Inżynieria Materiałowa* 29 (2008) 891-894.
- [79] M. Polok-Rubiniac, L.A. Dobrzański, M. Adamiak, Comparison of the PVD coatings deposited onto plasma nitrided steel, *Journal of Achievements in Materials and Manufacturing Engineering* 42 (2010) 172-179.
- [80] J. Smolik, A. Mazurkiewicz, Rozwój hybrydowych technologii powierzchniowych w oparciu o praktyczne zastosowania przemysłowe, *Problemy Eksploatacji* 3 (2010) 105-114.
- [81] R.R. Chromik, C.C. Baker, A.A. Voevodin, K.J. Wahl, In situ tribometry of solid lubricant nanocomposite coatings, *Wear* 262 (2007) 1239-1252.
- [82] R. Rodriguez-Baracaldo, J.A. Benito, E.S. Puchi-Cabrera, M.H. Staia, High temperature wear resistance of (TiAl)N PVD coating on untreated and gas nitrided AISI H13 steel with different heat treatments, *Wear* 262 (2007) 380-389.
- [83] T. Bjork, J. Bergstrom, S. Hogmark, Tribological simulation of aluminium hot extrusion, *Wear* 224 (1999) 216-225.
- [84] T. Bjork, R. Westergard, S. Hogmark, J. Bergstrom, P. Hedenqvist, Physical vapour deposition duplex coatings for aluminium extrusion dies, *Wear* 225-229 (1999) 1123-1130.
- [85] L.A. Dobrzański, K. Lukaszko, A. Kříž, Properties of the multi-layer Ti/CrN and Ti/TiAlN coatings deposited with the PVD technique onto the brass substrate, *Journal of Materials Processing Technology* 143-144 (2003) 832-837.
- [86] B. Tlili, C. Nouveau, M.J. Waloch, M. Nasi, T. Ghrib, Effect of layer thickness on thermal properties of multilayer thin films produced by PVD, *Vacuum* 86 (2012) 1048-1056.
- [87] A. Gilewicz, B. Warcholiński, P. Myśliński, W. Szymański, Anti-wear multilayer coatings based on chromium nitride for wood machining tools, *Wear* 270 (2010) 32-38.
- [88] K. Lukaszko, L.A. Dobrzański, M. Staszuk, M. Pancielejko, Comparison of the PVD gradient coatings deposited onto X40CrMoV5-1 and HS6-5-2 tool steel substrate, *Journal of Achievements in Materials and Manufacturing Engineering* 27/1 (2008) 79-82.
- [89] M. Antonom, I. Hussainova, F. Sergejev, P. Kulu, A. Gregor, Assessment of gradient and nanogradient PVD coatings behaviour under erosive, abrasive and impact wear conditions, *Wear* 267 (2009) 898-906.
- [90] A.A. Voevodin, J.S. Zabinski, Supertough wear-resistant coatings with 'chameleon' surface adaptation, *Thin Solid Films* 370 (2000) 223-231.
- [91] M. Wysiecki, *Nowoczesne materiały narzędziowe*, Wydawnictwa Naukowo-Techniczne, Warszawa, 1997.
- [92] L.A. Dobrzański, K. Lukaszko, A. Zarychta, Mechanical properties of monolayer coatings deposited by PVD techniques, *Journal of Achievements in Materials and Manufacturing Engineering* 20 (2007) 423-426.
- [93] P. Panjan, M. Cekada, R. Kirm, M. Sokolic, Improvement of die-casting tools with duplex treatment, *Surface and Coatings Technology* 180-181 (2004) 561-565.
- [94] M. Sokovic, J. Mikula, L.A. Dobrzański, J. Kopac, L. Kosec, P. Pandan, J. Madejski, A. Piech, Cutting properties of the Al₂O₃+SiC_(w) based tool ceramic reinforced with the PVD and CVD wear resistant coatings, *Journal of Materials Processing Technology* 164-165 (2005) 924-929.
- [95] K. Lukaszko, Review of nanocomposite thin films and coatings deposited by PVD and CVD technology, in: *Nanomaterials*, Mohammed Muzibur Rahman (Ed.), Intech, Rijeka, Croatia, 2011, 145-162.
- [96] C.C. Koch, I.A. Ovid'ko, S. Seal, S. Veprek, *Structural nanocrystalline materials. Fundamentals and applications*, Cambridge University Press, Cambridge, 2007.
- [97] K. Lukaszko, A. Czyżniewski, W. Kwaśny, M. Pancielejko, Structure and mechanical properties of PVD coatings deposited onto the X40CrMoV5-1 hot work tool steel substrate, *Vacuum* 86 (2012) 1186-1194.
- [98] K. Lukaszko, J. Konieczny, Microstructure and mechanical properties of PVD nanocrystalline layers, *Solid State Phenomena* 186 (2012) 230-233.
- [99] K. Lukaszko, J. Sondor, A. Kriz, M. Pancielejko, Structure, mechanical properties and corrosion resistance of nanocomposite coatings deposited by PVD technology onto the X6CrNiMoTi17-12-2 and X40CrMoV5-1 steel substrates, *Journal of Materials Science* 45 (2010) 1629-1637.
- [100] E. Sheinman, Superhard coatings from nanocomposites. Review of foreign publications, *Metal Science and Heat Treatment* 50 (2008) 600-605.
- [101] S. Veprek, R.F. Zhang, M.G.J. Veprek-Heijman, S.H. Sheng, A.S. Argon, Superhard nanocomposites: Origin of hardness enhancement properties and applications, *Surface and Coatings Technology* 2004 (2010) 1898-1906.
- [102] S. Zhang, D. Sun, X.L. Bui, Magnetron Sputtered Hard and Yet Tough Nanocomposite Coatings with Case Studies: Nanocrystalline TiN Embedded in Amorphous SiN_x, in: *Nanocomposite Thin Films and Coatings*, S. Zhang and N. Ali (Eds.), Imperial College Press, London, 2007, 1-110.

- [103] S. Veprek, A. Niederhofer, K. Moto, T. Bolom, H.D. Mannling, P. Nesladek, G. Dollinger, A. Bergmaier, Composition, nanostructure and origin of the ultrahardness in nc-TiN a-Si₃N₄ a- and nc-TiSi₂ nanocomposites with H_v 80 to 105 GPa, *Surface and Coatings Technology* 133-134 (2000) 152-159.
- [104] S. Veprek, H.D. Mannling, P. Karvankova, J. Prochazka, The issue of the reproducibility of deposition of superhard nanocomposites with hardness of ≥ 50 GPa, *Surface and Coatings Technology* 201 (2006) 6064-6070.
- [105] C.W. Zou, H.J. Wang, M. Li, J.F. Yu, C.S. Liu, L.P. Guo, D.J. Fu, Characterization and properties of TiN-containing amorphous Ti-Si-N nanocomposite coatings prepared by arc assisted middle frequency magnetron sputtering, *Vacuum* 84 (2010) 817-822.
- [106] F. Vaz, L. Rebouta, P. Goudeau, J. Pacaud, H. Garem, J.P. Riviere, A. Cavaleiro, E. Alves, Characterisation of Ti_{1-x}Si_xN_y nanocomposite coatings, *Surface and Coatings Technology* 133-134 (2000) 307-313.
- [107] M. Audronis, A. Leyland, P.J. Kelly, A. Mathews, Composition and structure-property relationships of chromium-diboride/molybdenum-disulphide PVD nanocomposite hard coatings deposited by pulsed magnetron sputtering, *Applied Physics A* 91 (2008) 77-86.
- [108] K. Lukaszewicz, L.A. Dobrzański, J. Sondor, Microstructure, mechanical properties and corrosion resistance of nanocomposite coatings deposited by PVD technology, in: *Advances in diverse industrial applications of nanocomposites*, Boreddy S.R. Reddy (Ed.), Intech, Rijeka, Croatia, 2011, 1-16.
- [109] Y.C. Cheng, T. Browne, B. Heckerman, E.I. Meletis, Mechanical and tribological properties of nanocomposite TiSiN coatings, *Surface and Coatings Technology* 204 (2010) 2123-2129.
- [110] K. Polychronopoulou, M.A. Baker, C. Rebolz, J. Neidhardt, M. O'Sullivan, A.E. Reiter, K. Kanakis, A. Leyland, A. Matthews, C. Mitterer, The nanostructure, wear and corrosion performance of arc-evaporated CrB_xN_y nanocomposite coatings, *Surface and Coatings Technology* 204 (2009) 246-255.
- [111] S. Veprek, M. Haussmann, S. Reiprich, L. Shizhi, J. Dian, Novel thermodynamically stable and oxidation resistant superhard coating material, *Surface and Coatings Technology* 86-87 (1996) 394-401.
- [112] S. Veprek, Conventional and new approaches towards the design of novel superhard materials, *Surface and Coatings Technology* 97 (1997) 15-22.
- [113] S. Veprek, Electronic and mechanical properties of nanocrystalline composites when approaching molecular size, *Thin Solid Films* 297 (1997) 145-153.
- [114] S. Veprek, A.S. Argon, Towards the understanding of mechanical properties of super- and ultrahard nanocomposites, *Journal of Vacuum Science and Technology B* 20 (2002) 650-664.
- [115] J. Karch, R. Birringer, H. Gleiter, Ceramics ductile at low temperature, *Nature* 330 (1987) 556-558.
- [116] R.W. Siegel, G.E. Fougere, Grain size dependent mechanical properties in nanophase materials, *Materials Research Society Symposium Proceedings* 362 (2002) 219-229.
- [117] A.A. Voevodin, M.A. Capano, S.J.P. Laube, M.S. Donley, J.S. Zabinski, Design of a Ti/TiC/DLC functionally gradient coating based on studies of structural transitions in Ti-C films, *Thin Solid Films* 298 (1997) 107-115.
- [118] J. Musil, Hard and superhard nanocomposite coatings, *Surface and Coatings Technology* 125 (2000) 322-330.
- [119] C. Mitterer, P.H. Mayhofer, M. Beschliesser, P. Losbichler, P. Warbischler, F. Hofer, P.N. Gibsson, W. Gissler, H. Hrubby, J. Musil, J. Vlcek, Microstructure and properties of nanocomposite Ti-B-N and Ti-B-C coatings, *Surface and Coatings Technology* 120-121 (1999) 405-411.
- [120] S. Veprek, M.G.J. Veprek-Heijman, P. Karvankova, J. Prochazka, Different approaches to superhard coatings and nanocomposites, *Thin Solid Films* 476 (2005) 1-29.
- [121] A.A. Voevodin, J.S. Zabinski, C. Muratore, Recent advances in hard, tough, and low friction nanocomposite coatings, *Tsinghua Science and Technology* 10 (2005) 665-679.
- [122] J.J. Moor, I.W. Park, J. Lin, Nanostructured, multifunctional tribological coatings, in: *Nanocomposite Thin Films and Coatings*, S. Zhang and N. Ali (Eds.), Imperial College Press, London, UK, 329-379.
- [123] J. Robertson, Diamond-like carbon, *Materials Science and Engineering R* 37 (2002) 129-281.
- [124] B.C. Yeldose, B. Ramamoorthy, Characterization of DC magnetron sputtered diamond-like carbon (DLC) nanocoating, *International Journal of Advanced Manufacturing Technology* 38 (2008) 705-717.
- [125] K. Holmberg, H. Ronkainen, A. Laukkanen, K. Wallin, S. Hogmark, S. Jacobson, U. Wiklund, R.M. Souza, P. Stahle, Residual stresses in TiN, DLC and MoS₂ coated surfaces with regard to their tribological fracture behaviour, *Wear* (2009) 2142-2156.
- [126] A. Gilewicz, B. Warcholiński, Twarde powłoki ta-C otrzymane metodą impulsowego katodowego odparowania łukowego, *Inżynieria Materiałowa* 1 (2010) 50-53.
- [127] A. Czyżniewski, W. Gulbiński, M. Pancelejko, G. Radnoczi, M. Szerenci, Mikrostruktura i właściwości cienkich powłok węglowych modyfikowanych wolframem, *Inżynieria Materiałowa* 6 (2009) 529-532.
- [128] R. Galin, M. Larsson, P. Hedenquist, Me-C:H coatings in motor vehicles, *Wear* 249 (2001) 302-309.
- [129] A. Czyżniewski, Wytwarzanie i właściwości cienkich powłok węglowych modyfikowanych wolframem, *Inżynieria Materiałowa* 6 (2008) 772-775.
- [130] H. Ronkainen, J. Likonen, J. Koskinen, S. Varjus, Effect of tribofilm formation on tribological performance of hydrogenated carbon coatings, *Surface and Coatings Technology* 79 (1996) 87-94.
- [131] F. Vaz, L. Rebouta, M. Andritschky, M.F. da Silva, J.C. Soares, The effect of addition of Al and Si on the physical and mechanical properties of titanium nitride, *Journal of Materials Processing Technology* 92-93 (1999) 169-176.
- [132] F. Vaz, L. Rebouta, P. Goudeau, T. Girardeau, J. Pacaud, J.P. Riviere, A. Traverse, Structural transitions in hard Si-based TiN coatings: the effect of bias voltage and temperature, *Surface and Coatings Technology* 146-147 (2001) 274-279.
- [133] D. Rafaja, C. Wustelfeld, M. Dopita, M. Ruzicka, V. Klemm, G. Schreiber, D. Heger, M. Sima, Internal

- structure of clusters of partially coherent nanocrystallites in Cr-Al-N and Cr-Al-Si-N coatings, *Surface and Coatings Technology* 201 (2007) 9476-9484.
- [134] P. Holubar, M. Jilek, M. Sima, Present and possible future applications of superhard nanocomposite coatings, *Surface and Coatings Technology* 133-134 (2000) 145-151.
- [135] J. Kusiński, Inżynieria materiałowa - aktualne i przyszłe kierunki badań, *Inżynieria Materiałowa* 1 (2008) 7-13.
- [136] A. Zieliński, Strategie badań i rozwoju w obszarze inżynierii materiałowej, *Inżynieria Materiałowa* 5 (2008) 514-524.
- [137] A.D. Dobrzańska-Danikiewicz (ed.), *Materials surface engineering development trends*, Open Access Library 6 (2011) 1-549.
- [138] A.D. Dobrzańska-Danikiewicz, Metodologia komputerowo zintegrowanego prognozowania rozwoju inżynierii powierzchni materiałów, *Open Access Library* 1/7 (2012) 1-289.
- [139] S.J. Skrzypek, A. Baczański, E. Kusior, Opracowanie i wdrożenie nowej nieniszczącej metody pomiaru naprężeń własnych opartej na geometrii dyfrakcji promieniowania X przy stałym kącie padania, *Problemy Eksploatacji* 2 (2000) 313-333.
- [140] X. Zheng, J. Li, Y. Zhou, X-ray diffraction measurement of residual stress in PZT thin films prepared by pulsed laser deposition, *Acta Materialia* 52 (2004) 3313-3323.
- [141] P.J. Burnett, D.S. Rickerby, The relationship between hardness and scratch adhesion, *Thin Solid Films* 154 (1987) 403-416.
- [142] K. Laue, H. Stengert, *Extrusion - processes, machinery, tooling*, American Society for Metals, Metals Park, Ohio, 1981.
- [143] T. Sheppard, *Extrusion of aluminium alloys*, Kluwer Academic Publisher, Dordrecht/Boston/London, 1999.
- [144] J. Smolik, Rola warstw hybrydowych typu warstwa azotowana/powłoka PVD w procesie zwiększenia trwałości matryc kuźniczych, *Monograficzna seria wydawnicza Biblioteki Problemów Eksploatacji - Studia i Rozprawy*, Instytut Technologii Eksploatacji - Państwowy Instytut Badawczy, Radom, 2007.
- [145] P. Ostachowski, Analiza mechanizmów odkształcenia w procesie wyciskania z cykliczną zmianą drogi deformacji, *Praca doktorska*, Akademia Górniczo-Hutnicza, Kraków, 2012.
- [146] L. Casarotto, R. Tutsch, R. Ritter, J. Weidenmuller, A. Ziegenbein, F. Klose, H. Neuhauser, Propagation of deformation bands investigated by laser scanning extensometry, *Computational Materials Science* 26 (2003) 210-218.
- [147] W. Ozgovicz, B. Grzegorzczak, Analysis of the Portevin-Le Chatelier effect in tin bronzes at elevated temperatures, *Journal of Achievements in Materials and Manufacturing Engineering* 31/2 (2008) 281-289.
- [148] E. Rizzi, P. Hahner, On the Portevin-Le Chatelier effect: theoretical modelling and numerical results, *International Journal of Plasticity* 20 (2004) 121-165.
- [149] L.A. Dobrzański, T. Tański, J. Trzaska, Modeling of the optimum heat treatment conditions of Mg-Al-Zn magnesium cast alloys, *International Journal of Computational Materials Science and Surface Engineering* 1/5 (2007) 540-554.
- [150] A.D. Dobrzańska-Danikiewicz, a E. Jond, J. Trzaska, A. Jagiełło, K. Labisz, Neural network aided future events scenarios presented on the example of laser surface treatment, *Journal of Achievements in Materials and Manufacturing Engineering* 51/2 (2011) 69-96.
- [151] H.K. Bhadeshia, *Neural Networks in Materials Science*, ISIJ International 39 (1999) 966-1000.
- [152] W. Sitek, Employment of rough data for modeling of materials properties, *Journal of Achievements in Materials and Manufacturing Engineering* 21/2 (2007) 65-68.
- [153] L.A. Dobrzański, M. Sroka, J. Dobrzański, Application of neural networks to classification of internal damages in steels working in creep service, *Journal of Achievements in Materials and Manufacturing Engineering* 20 (2007) 303-306.
- [154] R. Kapoor, D. Pal, J.K. Chakravartty, Use of artificial neural networks to predict the deformation behavior of Zr-2.5Nb-0.5Cu, *Journal of Materials Processing Technology* 169/2 (2005) 199-205.
- [155] S. Delijaicov, A.T. Fleury, F.P.R. Martins, Application of multiple regression and neural networks to synthesize a model for peen forming process planning, *Journal of Achievements in Materials and Manufacturing Engineering* 43/2 (2010) 651-656.
- [156] F. Musharavati, A.S.M. Hamouda, Application of artificial neural networks for modelling correlations in age, hardenable aluminium alloys, *Journal of Achievements in Materials and Manufacturing Engineering* 41 (2010) 140-146.
- [157] J. Trzaska, L.A. Dobrzański, Modelling of CCT diagrams for engineering and constructional steels, *Journal of Materials Processing Technology* 192-193 (2007) 504-510.
- [158] L.A. Dobrzański, R. Maniara, J.H. Sokolowski, M. Krupiński, Modeling of mechanical properties of Al-Si-Cu cast alloys using the neural network, *Journal of Achievements in Materials and Manufacturing Engineering* 20 (2007) 347-350.
- [159] J. Trzaska, W. Sitek, L.A. Dobrzański, Application of neural networks for selection of steel grade with required hardenability, *International Journal of Computational Materials Science and Surface Engineering* 1/3 (2007) 366-382.
- [160] M.E. Haque, K.V. Sudhakar, Prediction of corrosion-fatigue behavior of DP steel through artificial neural network, *International Journal of Fatigue* 23 (2001) 1-4.
- [161] W. Zeng, N. Chen, Artificial neural network method applied to enthalpy of fusion of transition metals, *Journal of Alloys and Compounds* 257 (1997) 266-267.
- [162] Q. Luo, A.H. Jones, High-precision determination of residual stress of polycrystalline coatings using optimised XRD- $\sin^2\psi$ technique, *Surface and Coatings Technology* 205 (2010) 1403-1408.
- [163] R. Machunze, G.C.A.M. Janssen, Stress and strain in titanium nitride thin films, *Thin Solid Films* 517 (2009) 5888-5893.
- [164] S.P. Kim, H.M. Choi, S.K. Choi, A study of the crystallographic orientation with residual stress and electrical property of Al films deposited by sputtering, *Thin Solid Films* 322 (1998) 298-302.
- [165] S. Govindarajan, J.J. Moore, B. Mishra, D.L. Olson, Physical vapor deposition of molybdenum and silicon thin films, *Surface and Coatings Technology* 68/69 (1994) 45-50.

- [166] H.C. Barshilia, A. Ananth, J. Khan, G. Srinivas, Ar+H₂ plasma etching for improved adhesion of PVD coatings on steel substrates, *Vacuum* 86 (2012) 1165-1173.
- [167] A.R. Bushroa, H.H. Masjuki, M.R. Muhamad, B.D. Beake, Optimized scratch adhesion for TiSiN coatings deposited by a combination of DC and RF sputtering, *Surface and Coatings Technology* 206 (2011) 1837-1844.
- [168] J. Gerth, U. Wiklund, The influence of metallic interlayers on the adhesion of PVD TiN coatings on high-speed steel, *Wear* 264 (2008) 885-892.
- [169] R. Escobar Galindo, A. van Veen, H. Schut, G.C.A.M. Janssen, R. Hoy, J.Th.M. de Hosson, Adhesion behaviour of CrN_x coatings on pre-treated metal substrates studied in situ by PBA and ESEM after annealing, *Surface and Coatings Technology* 199 (2005) 57-65.
- [170] A.O. Sergici, N.X. Randall, Scratch testing of coatings, *Advanced Materials and Processes* 4 (2006) 1-3.
- [171] Y. He, I. Apachitei, J. Zhou, T. Walstock, J. Duszczyk, Effect of prior plasma nitriding applied to a hot-work tool steel on the scratch-resistant properties of PACVD TiBN and TiCN coatings, *Surface and Coatings Technology* 201 (2006) 2534-2539.
- [172] K.E. Pappacena, D. Singh, O.O. Ajayi, J.L. Roitbort, O.L. Erilymaz, N.G. Demas, G. Chen, Residual stresses, interfacial adhesion and tribological properties of MoN/Cu composite coatings, *Wear* 278-279 (2012) 62-70.
- [173] S.H. Tamboli, V. Puri, R.K. Puri, Adhesion and stress of magnesium oxide thin films: Effect of thickness, oxidation temperature and duration, *Applied Surface Science* 256 (2010) 4582-4585.
- [174] C.A. Johnson, J.A. Ruud, e R. Bruc, D. Wortman, Relationships between residual stress, microstructure and mechanical properties of electron beam-physical vapor deposition thermal barrier coatings, *Surface and Coatings Technology* 108-109 (1998) 80-85.
- [175] J.A. Thornton, The microstructure of sputter-deposited coatings, *Journal Vacuum Science Technology A* 4 (1986) 3059-3065.
- [176] W. Kwaśny, L.A. Dobrzański, Structure, physical properties and fractal character of surface topography of the Ti+TiC coatings on sintered high speed steel, *Journal of Materials Processing Technology* 164-165 (2005) 1519-1523.
- [177] J.C. Russ, Fractal dimension measurement of engineering surfaces, *International Journal of Machine Tools and Manufacture* 38 (1998) 567-571.
- [178] S. Stach, S. Roskosz, J. Cybo, J. Cwajna, Properties of salon ceramics evaluated by means of multifractal, surface stereometry and quantitative fractography techniques, *Materials Characterization* 60 (2009) 1151-1157.
- [179] G. Meisel, R.B. Heimann, Correlation between surface roughness of plasma-sprayed chromium oxide coatings and powder grain size distribution: a fractal approach, *Surface and Coatings Technology* 185 (2004) 215-221.
- [180] W. Kwaśny, M. Woźniak, J. Miłkuła, L.A. Dobrzański, Structure, physical properties and multifractal characteristics of the PVD and CVD coatings deposition onto the Al₂O₃+TiC ceramics, *Journal of Computational Materials Science and Surface Engineering* 1 (2007) 97-113.
- [181] H. Xie, J.A. Wang, E. Stein, Direct fractal measurement and multifractal properties of fracture surfaces, *Physics Letters A* 242 (1998) 41-50.
- [182] A. J. Perry, The surface topography of titanium nitride made by chemical vapor deposition, *Surface and Coatings Technology* 132 (2000) 21-25.
- [183] W. Kwaśny, Predicting properties of PVD and CVD coatings based on fractal quantities describing their surface, *Journal of Achievements in Materials and Manufacturing Engineering* 37/2 (2009) 125-192.
- [184] A. Kocańda, W. Presz, G. Adamczyk, Doświadczalne wyznaczenie rozkładu nacisków na powierzchni narzędzia, *Obróbka Plastyczna Metali* 2/3 (1995) 57-60.
- [185] M. Lacki, Numeryczna analiza obciążenia narzędzia do wyciskania współbieżnego, *Rudy Metale* 11 (2001) 574-578.
- [186] I. Nowotyńska, S. Kut, Numeryczna i eksperymentalna analiza wpływu geometrii matrycy na rozkład naprężeń i odkształceń podczas wyciskania materiałów złożonych, *Rudy Metale* 10 (2009) 604-608.
- [187] F. Stalony-Dobrzański, W. Bochniak, P. Ostachowski, Rola temperatury w procesie wyciskania metali na prasie z rewersyjnie skręcaną matrycą w świetle testu teksturowego, *Inżynieria Materiałowa* 6 (2007) 902-906.
- [188] X.J. Wang, K.B. Nie, X.S. Hu, Y.Q. Wang, X.J. Sa, K. Wu, Effect of extrusion temperatures on microstructure and mechanical properties of SiCp/Mg-Zn-Ca composite, *Journal of Alloys and Compounds* 532 (2012) 78-85.
- [189] P. Dou, A. Kimura, T. Okuda, M. Inoue, S. Ukai, S. Ohnuki, T. Fujisawa, F. Abe, Effects of extrusion temperature on the nano-mesoscopic structure and mechanical properties of an Al-alloyed high-Cr ODS ferritic steel, *Journal of Nuclear Materials* 417 (2011) 166-1701.
- [190] A. Korbel, W. Bochniak, P. Ostachowski, M. Łagoda, Praca niepublikowana, Akademia Górniczo-Hutnicza, Kraków, 2011.
- [191] J. Lauridsen, N. Nedfors, U. Jansson, J. Jensen, P. Eklund, L. Hultman, Ti-B-C nanocomposite coatings deposited by magnetron sputtering, *Applied Surface Science* 258 (2012) 9907-9912.
- [192] A.P. Carapeto, A.P. Serro, B.M.F. Nunes, M.C.L. Martins, S. Todorovic, M.T. Duarte, V. Andre, R. Colaco, B. Saramago, Characterization of two DLC coatings for joint prothesis: The role of albumin on the tribological behavior, *Surface and Coatings Technology* 204 (2010) 3451-3458.
- [193] D.K. Lee, D.S. Kang, J.H. Suh, C.G. Park, K.H. Kim, Synthesis and mechanical evaluation of quaternary Ti-Cr-Si-N coatings deposited by a hybrid method of arc and sputtering techniques, *Surface and Coatings Technology* 200 (2005) 1489-1494.
- [194] H.W. Chen, Y.C. Chan, J.W. Lee, J.G. Duh, Oxidation behavior of Si-doped nanocomposite CrAlSiN coatings, *Surface and Coatings Technology* 205 (2010) 1189-1194.
- [195] M.H. Ahmed, J.A. Byrne, Effect of surface structure and wettability of DLC and N-DLC thin films on adsorption glycine, *Applied Surface Science* 258 (2012) 5166-5174.
- [196] C. Srisang, P. Asanithi, K. Siangchaew, A. Pokaipisit, P. Limswan, Characterization of SiC in DLC/a-Si films prepared by pulsed filtered cathodic arc using Raman spectroscopy and XPS, *Applied Surface Science* 258 (2012) 5605-5609.
- [197] P.L. Wong, F. He, X. Zhou, Interpretation of the hardness of worn DLC particles using micro-Raman spectroscopy, *Tribology International* 43 (2010) 1806-1810.

- [198]P.A. Steinmann, Adhesion of TiC and Ti(C,N) coatings on steel, *Journal of Vacuum Science and Technology A: Vacuum, Surfaces, and Films* 3 (1985) 2394-2400.
- [199]F. Ashrafizadeh, Adhesion evaluation of PVD coatings to aluminium substrate, *Surface and Coatings Technology* 130 (2000) 186-194.
- [200]I. Lhermitte-Sebire, R. Colmet, R. Naslain, The adhesion between physically vapour-deposited or chemically vapour-deposition alumina and TiC-coated cemented carbides as characterized by Auger electron spectroscopy and scratch testing, *Thin Solid Films* 138 (1986) 221-233.
- [201]K. Koski, J. Hosla, J. Ernoult, A. Rouzaud, The connection between sputter cleaning and adhesion of thin solid films, *Surface and Coatings Technology* 80 (1996) 195-199.
- [202]T. Burakowski, *Rozważania o synergizmie w inżynierii materiałowej*, Wydawnictwo Politechniki Radomskiej, Radom, 2004.
- [203]M.M. Morshed, B.P. McNamara, D.C. Cameron, M.S.J. Hashmi, Stress and adhesion in DLC coatings on 316L stainless steel deposited by a neutral beam source, *Journal of Materials Processing Technology* 143-144 (2003) 922-926.